MICROSCALE PATTERNING OF OSTEOGENIC RESPONSE AND MINERALIZATION ON PEGDA HYDROGELS

BY

KRISTOPHER A. WHITE

A dissertation submitted to the

School of Graduate Studies

Rutgers, The State University of New Jersey

In partial fulfillment of the requirements

For the degree of

Doctor of Philosophy

Graduate Program in Chemical and Biochemical Engineering

Written under the direction of

Ronke M. Olabisi

And approved by

_____

_____

_____

_____

New Brunswick, New Jersey

May, 2019

ABSTRACT OF DISSERTATION

Microscale Patterning of Osteogenic Response and Mineralization on PEGDA Hydrogels

by KRISTOPHER WHITE

Dissertation Director:
Ronke M. Olabisi

Global increases in life expectancy are accompanied by an increasing need for bone tissue regeneration. The gold standard for bone repair is the autologous graft (autograft), which enjoys excellent clinical outcomes. However, the autograft suffers from significant drawbacks including donor site morbidity and limited availability. Although collagen sponges delivered with bone morphogenetic protein, type 2 (BMP-2) are a common alternative or supplement to grafts, they do not efficiently retain BMP-2, necessitating extremely high doses to elicit bone formation. As a result, reports of BMP-2 complications are on the rise, including the promotion of cancer and ectopic bone formation, the latter of which induces complications such as breathing difficulties and neurologic impairments. Therefore, efforts to exert spatial control over bone formation are of particular interest. Using the tissue engineering paradigm of scaffolds, biological factors, and cells, several studies have demonstrated the potential of this approach to elicit targeted and controlled bone formation. These approaches include biomaterial

scaffolds derived from synthetic sources such as calcium phosphates or polymers, natural sources such as bone or seashell, and biofactors such as BMP-2 that are immobilized within the scaffolds. Although BMP-2 is the only protein clinically approved for use in a surgical device, there are several proteins, small molecules, and naturally derived osteogenic growth factors that show promise in tissue engineering applications. This dissertation presents research directed at achieving control over the location and onset of bone formation (spatiotemporal control) for tissue engineered bone towards avoiding the current complications associated with BMP-2.

Spatiotemporal control over tissue formation is relatively unreported in literature, particularly microspatial control. The first aim of this work seeks elucidate the mineralization capacity of osteogenic growth factors covalently tethered to a substrate via a poly(ethylene glycol) (PEG) linker. This was accomplished by PEGylating growth factors and covalently tethering them to acrylated glass substrates. The results of this study indicated that PEGylated WSM can induce mineralization in acellular solution. Further, the results reveal the presence of sub-micron features within the mineralized matrix. Further work in this dissertation sought elucidate the relationship between cellular and acellular osteogenesis and mineralization induced by osteogenic growth factors. The initial hypothesis was

that growth factors capable of directing acellular nucleation would demonstrate the ability to microspatially direct cell-mediated osteogenesis and mineralization. The results revealed that both PEGylated BMP-2 and nacre WSM show some ability to direct osteogenesis when patterned onto PEGDA hydrogel substrates. These findings have broad implications on the design and development of orthopaedic interventions and drug delivery.

DEDICATIONS

To my mother, Treasa White – Thank you for holding the light against ever present uncertainty, for showing me that there is a life beyond our beginnings and for dragging me toward it, often kicking and screaming.

To my brother, Joseph Merchant – For always pushing your big brother into the world and occasionally proving me wrong.

And, finally, to Bill Worley, my Dad – Thank you for sharing your life and love with my brother and me and for never telling me to "get a real job."

ACKNOWLEDGEMENTS

This dissertation is the culmination of a lifetime of work. While I am extremely proud of the time, effort, and tears I have poured into it, I cannot claim to have gotten to this point by myself.

First and foremost, my eternal gratitude is owed to my advisor, Dr. Ronke Olabisi. Thank you for taking a chance – for giving me a real chance. My thanks also go out to my other committee members, Dr. Charles Roth, Dr. David Shreiber, and Dr. J. Christopher Fritton.

Several members of the broader Rutgers community have played a significant role in my development. First, I would like to acknowledge Assistant Dean Teresa Delcorso for providing an immeasurable degree of moral, financial, and practical support during my time at Rutgers. I also owe a great deal of gratitude to the departmental staff members in Chemical and Biochemical Engineering and Biomedical Engineering. I would like to especially thank Robin Yarborough and Larry Stromberg in the BME department for always taking my unconventional situation in stride.

I am also grateful for the various sources of funding and support given to me by my department. I would especially like to thank the CBE department for supporting me through a difficult transition early in my doctoral studies. The support offered to me went above and beyond expectation. I extend my sincerest gratitude to the BME department for accommodating me even when they had no obligation to do so.

This work was started in a new lab, requiring me to develop my own protocols and borrow knowledge and experience from my peers in my own lab and in more established labs. I'd like to particularly thank former members of the Olabisi Lab, Dr. Ayesha Aijaz and Dr. Corina White for all their assistance and troubleshooting during the early stages of this work. Many of my protocols have been designed and improved with their input and collaboration. A special thanks goes out to Vincent Cali for exceeding any and all expectation I placed on him over the summer of 2017.

Beyond academic support, my fellow students provided me with friendship and moral support, even if I failed to reciprocate at times. Thank you to John Mattick and Fabian Casteblanco for the early pep talks and helping me acclimate to the doctoral student experience. Thank you to my colleagues and friends at

GradFund. Your advice and our shared experiences across disciplines have been most enlightening and encouraging. You are all rock stars.

Finally, this thesis would not have been accomplished without the support of my family and friends. The love and appreciation I have for my parents and siblings as well as my extended family is immeasurable. My mother and my brother haver offered nothing but love and support throughout this process. I have also been blessed to call Bill Worley my Dad since I was 8 years old. Thank you for your unquestioning support and pride in my accomplishments through the years. I will forever miss your laugh.

PUBLICATIONS AND PRESENTATION

Several sections of this dissertation and related research have been published in peer-reviewed journals and/or presented at scientific conferences.

Peer- reviewed journal publications:

K White, R Olabisi. Spatiotemporal Control Strategies for Bone Formation through Tissue Engineering and Regenerative Medicine Approaches. *Adv. Healthcare Mater.*. 2019:8

D Browe, C Wood, M Sze, K White, T Scott, R Olabisi, J Freeman. Characterization and optimization of actuating poly(ethylene glycol) diacrylate/acrylic acid hydrogels as artificial muscles. *Polymer*. 2017:117

D Perera, M Medini, D Seethamraju, R Falkowski, K White, R Olabisi. The effect of polymer molecular weight and cell seeding density on viability of cells entrapped within PEGDA hydrogel microspheres. *Journal of Microencapsulation*. 2018:35

K White, N Lorenz, T Potts, W Penney, R Babcock, A Hardison, E Canuel, J Hestekin. Production of biodiesel fuel from tall oil fatty acids via high temperature methanol reaction. *Fuel*. 2011:90

Conference presentations:

K White, R Olabisi, "PEG-Protein Hydrogels Enhance In Vitro Osteogenic Mineralization in MC3T3 Preosteoblast Cells," Biomedical Engineering Society Annual Meeting, Atlanta GA (2018)

Conference posters:

K White, R Olabisi, "Microspatial Control of Mineralization via Covalent Immobilization of Nacre Proteins onto Poly(ethylene glycol) Hydrogels," Laboratory for Surface Modification Symposium, Piscataway NJ (2016)

K White, R Olabisi, "Covalently Immobilized Nacre Proteins Induce Osteogenesis in Mesenchymal Stem Cells and Osteoblasts," Orthopaedic Research Society, Las Vegas NV (2015)

K White, R Olabisi, "Directing Osteoblast Differentiation and Mineralization Using PEG-conjugated Proteins Derived from Seashell and Bone," Biomedical Engineering Society Annual Meeting, Tampa FL (2015)

K White, R Olabisi, "Patterning Bone Formation Using Proteins Derived from Seashell and Bone," Society for Biomaterials Annual Meeting, Charlotte NC (2015)

K White, C Franco, J West, R Olabisi, "Patterning Bone Formation Using Nacre Proteins Patterned on Poly(ethylene glycol) Substrates," Biomedical Engineering Society Annual Meeting, San Antonio TX (2014)

TABLE OF CONTENTS

TABLE OF FIGURES

CHAPTER 1 : BACKGROUND AND INTRODUCTION

Sections of this chapter are reproduced from the following citation:

K White, R Olabisi. Spatiotemporal Control Strategies for Bone Formation through Tissue Engineering and Regenerative Medicine Approaches. Adv. Healthcare Mater. 2019:8.

1.1 Bone Tissue Engineering

The autologous bone graft (autograft), in which tissue is harvested and transplanted within the same patient, is the current gold standard in clinical practice for the repair of skeletal trauma.[1, 2] This can be attributed to the osteogenic properties of osteoprogenitor cells within the grafts and the fact that these grafts do not elicit an immune response in the patient. However, the autograft's drawbacks are donor site morbidity, limited supply, and increased risk of infection due to the multiple surgical sites required.[2, 3] In contrast, allogeneic graft materials are widely available, but they increase the risk of disease transmission and graft rejection.[4] Also, allogeneic grafts generally have reduced osteogenic activity due to storage and processing that destroys osteoprogenitors.[5] In order to address this shortcoming, they are codelivered with recombinant human bone morphogenetic protein, type 2 (rhBMP2), an FDA-

approved growth factor that has been shown to induce bone formation in vitro, in vivo, in clinical trials, and in clinical practice.[6]

Bone morphogenetic protein, type 2 (BMP2), while FDA-approved for very specific spinal fusion techniques,[7] reportedly increases the proliferation of cancer cells and is thus ill-suited for use in patients with a history of cancer.[8, 9] It may also present life-threatening complications even in otherwise healthy patients, especially when used off-label.[1] Reports of these complications are increasing as off-label BMP2-based therapies increase in use. Obstruction of the airway and neural pathways due to swelling in the neck and throat have been reported, with some cases requiring emergency tracheotomies or even feeding tube insertion.[1, 10] Other reported complications involve delayed ectopic bone growth requiring a second operation to decompress spinal nerves (Figure 1.1).[7, 11] Another study reported that 43% of patients who had BMP2-augmented spinal fusion experienced in-hospital complications compared to a 3.5% complication rate of patients receiving autograft spinal fusions.[12]

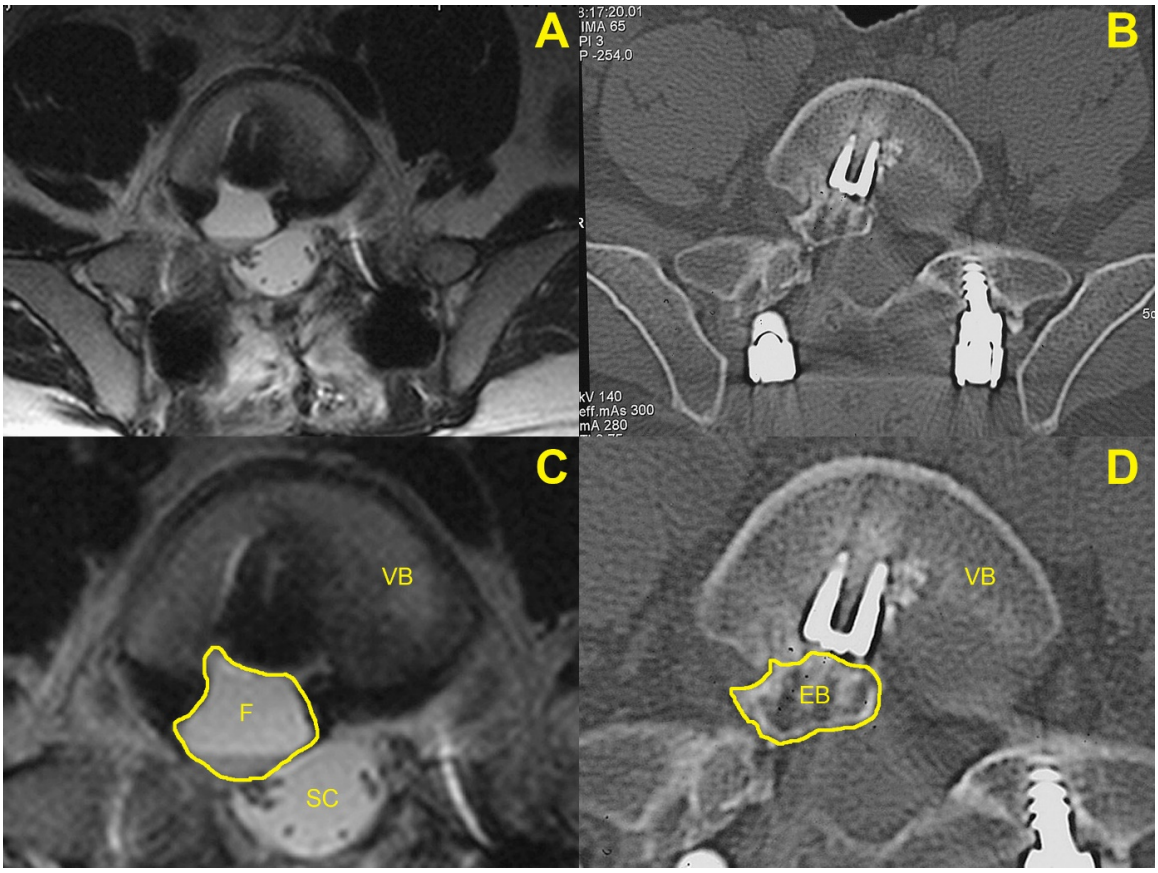

Figure 1.1: Axial magnetic resonance and computed tomography imaging at the L5-S1 vertebrae. A, C. Postoperative (2.5 months) magnetic resonance imaging scan showing fluid collection (F) in the surgical area, posterior to the vertebral body (VB) and anterior to the spinal cord (SC). B, D. Computed tomography scan 9 months following original surgery (6 months following fluid drainage) shows ectopic bone (EB) formation adjacent to the transforaminal lumbar interbody fusion entry site and extending posterior into the spinal canal. The bone mass has a well corticated exterior shell. Adapted with permission[11] *2007, Elsevier.*

Many of these complications are thought to be due to the BMP2 dosing (on the

order of milligrams) required to reach therapeutic levels at the site of repair.[13] This amount is more than one thousand times higher than what is naturally present within the human body.[14] Because of a generally poor affinity to current delivery scaffolds, BMP2 must be delivered in these high dosages so that enough growth factor remains to retain long-term therapeutic localization. Current allogeneic and synthetic graft materials absorb BMP2 into a polymer scaffold, such as collagen, and then release the drug at or near the site of injury.[7] However, over 90 percent of their content may be released within 24 hours, causing a systemic spike in BMP2.[15]

To address these issues, there has been a concerted effort to develop synthetic scaffolds with more stable presentations of growth factors. Increasingly investigated are scaffold design approaches to control bone formation, particularly the precise location and onset of osteogenesis, termed spatiotemporal control. Towards that goal, scaffolds bearing factors such as bone morphogenetic proteins, dentin matrix proteins, proteins isolated from seashell, insulin-like growth factors, small molecules such as N-acetyl cysteine, and a variety of other biofactors have been used to effectively control bone formation.[16-19] Furthermore, within the literature are effective strategies for healing without spatiotemporal strategies in mind that nevertheless have key elements with the potential to optimize the

spatiotemporal control of new bone formation.

Although spatiotemporal control strategies are more straightforward with strategies that directly apply the therapeutic to the desired site of bone formation, systemic strategies to control bone formation have achieved some success. Metabolic bone diseases, such as osteoporosis or Paget's disease, drive such efforts. In these diseases, the resorption of bone by osteoclasts outpaces the deposition of bone by osteoblasts. These diseases leave many microscopic pits and pores within the bone, resulting in a significantly weaker bone structure.[20] Efforts to reverse or halt the disease progression are driven by a goal of mitigating fracture risk. Once such bone is fractured, there are additional challenges associated with treating the resulting types of pathological fractures. Because these injuries are likely to never heal properly, re-injury and mortality rates increase dramatically.[20-22]

Most clinical therapies to treat osteoporosis are antiresorptive agents, focusing on slowing down the rate at which osteoclasts resorb bone, such as estrogen, bisphosphonates, raloxifene, and calcitonin.[23] Bisphosphonates, for example, trigger the apoptosis of osteoclasts, thus slowing overall osteoclast activity and resulting in a kind of temporal control over bone loss. However, by slowing

osteoclast activity, bisphosphonates and their adjuvant treatments may result in a skeletal "freezing" in which bone tissue is not remodeled at all.[24-26] When remodeling is slowed or stopped, the skeletal tissue may accumulate multiple fatigue fractures over time, leading to atypical severe fractures in the mid-shaft of the femur rather than the typical osteoporotic fractures in the hip.[26-28] Although currently accounting for only a small amount of osteoporosis-related fractures among those receiving bisphosphonate treatments, this type of mid-shaft femoral fracture is increasing.[27] What is most disturbing about these injuries is the relatively mild physical activities that lead to them; fractures occur during normal tasks with no falls or excessive trauma.[28] These types of fractures require invasive surgical interventions, are slow to heal even in healthy individuals, and are likely to never properly heal in osteoporotic bone.

In stark contrast to the bevy of antiresorptive agents available, anabolic osteoporosis treatments are lacking. While calcium mimetics, such as strontium ranelate, may hold anabolic properties, human parathyroid hormone is the only anabolic medication currently marketed to treat osteoporosis.[29] Thus, there is a need to develop anabolic therapeutic delivery systems capable of promoting bone formation, both systemically and focally, on the microscopic-scale, rather than simply arresting bone resorption altogether. The ability to precisely control the

location of tissue formation can be critical for a variety of tissues, particularly bone. Spatial control of bone formation prevents the problems associated with ectopic bone growth, thereby minimizing clinical complications. This review aims to organize and present the current state of osteogenic therapeutics and various delivery strategies to exert spatiotemporal control over osteogenesis for applications in bone tissue engineering and regenerative medicine.

1.2 Osteogenic Growth Factors

1.2.1 Bone Morphogenetic Proteins

One approach to increasing spatiotemporal control of delivered BMPs is by reducing the effective dose, thereby reducing the likelihood of ectopic bone formation from BMP that has diffused from the site of application. Several groups have explored this strategy by combining BMPs. BMPs commonly operate as dimers. BMP2, for instance, forms a natural homodimer. Following this understanding, several studies have incorporated other BMPs with BMP2 to form heterodimers. Karfeld-Sulzer et al. explored the use of BMP2 and BMP7 heterodimers in their work. They show that BMP2/BMP7 heterodimers are more effective than the BMP2 homodimer. This combination is further supported in recent literature. Zhu et al. has shown that BMP2/BMP7 heterodimers are less affected by Noggin, a soluble BMP antagonist, than either BMP2 or BMP7

homodimers.[30] Sun et al. demonstrated an increased osteogenic potency when using a BMP2/BMP7 heterodimer in peri-implant bone defects.[31] Heterodimers with BMP6 show similar gains. Valera et al. demonstrated increased osteodifferentiation of stem cells exposed to BMP2/BMP6 heterodimers over homodimers of either protein.[32] These strategies hold the potential to reduce the risk of ectopic bone formation by lowering the effective dosage threshold by increasing BMP efficacy.[33, 34] However, the level of BMP heterodimer delivered is still relatively high, and there still exists the possibility of ectopic bone formation, cancer promotion, or adverse immunological reaction even at a lower dosage.[33, 34]

1.2.2 Temporal Control

1.2.2.1 Affinity-based delivery systems

Growth factors on their own have an incredibly short half-life in vivo, and require high dosages that are often incompatible with human physiology.[35, 36] Attaching these growth factors to substrates can significantly prolong their bioavailability. Thus, it can be argued that the most important work currently focuses on therapeutic delivery systems that mate growth factor to substrate through various methods.

Traditionally, delivery systems have relied on non-specific interactions between the target therapeutic and the carrier substrate. For instance, this is true of the Infuse™ BMP2-loaded bone graft system developed and marketed by Medtronic.[33, 37] To alleviate the problems associated with non-specific adsorption, researchers have modified substrates and growth factors with various motifs designed to increase the affinity or retention between substrate and growth factor. Poynton and Lane reported that the half-life of rhBMP2 can range from a matter of minutes when the growth factor is unprotected to over a week when incorporated into a collagen sponge.[36] However, these passive systems do not sufficiently address the problems associated with high dosage.[38]

One strategy to reduce the required dose is to physically entrap or encapsulate growth factors to increase their retention. Because bone tissue is highly vascularized, VEGF has been used within co-delivery systems to promote vascularization simultaneously with mineralization.[39-43] Patel et al. developed a dual encapsulation technique for the delivery of vascular endothelial growth factor (VEGF) and BMP2.[41, 43, 44] In these studies, a composite substrate consisting of biodegradable gelatin microparticles constrained within a porous poly(propylene fumarate) (PPF) scaffold was used to control the release kinetics of VEGF and BMP2. The gelatin was used as a binding substrate for the respective

growth factors while the PPF scaffold was used to localize delivery and maintain structural integrity. When placed into rat critical size cranial defects, the scaffolds induced vascularized fibrous tissue and bone at 4 weeks and by 12 weeks the fibrous tissue was replaced with bone.[40, 41] At the 12 week time point, scaffolds containing only BMP2 or the combination of VEGF and BMP2 showed bony ingrowth within the scaffold pores and along the outer surfaces of the scaffold. This bone formation was localized to the scaffold interface and was significantly greater in the dual release hydrogels. They concluded that the codelivery of VEGF and BMP2 resulted in a synergistic effect, which has the potential to reduce the risk of ectopic bone formation by reducing the dose of BMP2 necessary. These results demonstrate a level of spatial control over bone formation, with the bone formed at the bone-scaffold interface.

Other strategies to retain growth factors rely on how proteins will adsorb to certain substances. For instance, in scaffolds like collagen or alginate, proteins simply adsorb to the surface of the substrate due to non-specific interactions. To increase overall affinity to proteins, substrates can be chemically modified to include copolymers or other compounds that show high affinity for proteins.[45-48] Studies have indicated that integrin-binding motifs such as Arginine-Glycine-Aspartic acid (RGD) show a high affinity for many proteins, including BMPs.[48,

49] Cyclodextrin pendant groups have been covalently incorporated into poly(ethylene glycol) (PEG) hydrogel networks to increase the hydrogel affinity for hydrophobic small molecules.[50] Heparin, which shows a high affinity for multiple growth factors and proteins, has also been incorporated into PEG hydrogels and has been used to bind and release bioactive BMP2 in a temporally controlled manner.[51-53]

More recently, Kolambkar et al. have developed a dual system comprised of an alginate hydrogel encapsulated within a nanofiber mesh tube for implantation into a rat critical size femoral defect model.[54] The alginate gels incorporated RGD peptides to increase their affinity to rhBMP2 while the nanofibers were intended to provide structural support in vivo. The alginate gels exhibited the familiar burst release kinetics, with 98.6% of the total release observed in the first 7 days. However, the study also presented data indicating that approximately 9% of the total loaded rhBMP2 remained unreleased and was still contained inside the gel after 21 days. Thus, the scaffold affinity for rhBMP2 was too low to deliver it in a non-burst fashion, but too high to release all of the loaded protein. The in vivo efficacy of this system appeared to have effected fracture repair as indicated by the post-healing mechanical testing of the repaired bone, which approximated that of age-adjusted mature bone. These systems, however, do not

completely circumvent the innate problems associated with encapsulation and affinity-based therapies. Though long-term therapeutic retention, and thus temporal control, is improved, the lack of spatial control risks the complications associated with initial burst release kinetics.[49, 54, 55]

1.2.2.2 Covalent Immobilization

A more recent solution towards preventing burst kinetics is to covalently incorporate, or tether, the bioactive compound to the substrate. Covalently bound bioactive compounds are effectively immobilized and therefore localized to the site of the gel. N-hydroxysuccinimide (NHS) ester-based linkers, such as succinimidyl valerate, are widely used to tether PEG to proteins via carboxamide coupling with primary amines. Heterobifunctional PEG molecules incorporating an NHS ester at one end and a different reactive group, such as an acrylate group, at the other end have been used to covalently link proteins to substrates.[56-59] Degradable enzyme-based linkers have been used to tether VEGF into PEG-based hydrogels.[60] It is also common practice to covalently incorporate integrin-binding peptides into substrates to facilitate cell-adhesion.[48, 56, 61]

While covalent modification can prolong the systemic residence time and localization of bioactive compounds, there are potential drawbacks to polymer

conjugation, especially when the bioactive compound is a fragile protein or growth factor. The conjugation may decrease the bioactivity of the compound.[62] However, this observation is highly variable between studies and seems to depend on the tethering technique and the target protein. BMP2, for example, has been shown to retain some bioactivity when conjugated to polymers and substrates.[63, 64]

Though there are examples of covalently tethered protein-substrate complexes in literature, the application to bone tissue engineering has thus far been limited. An early in vivo study by Suzuki et al. demonstrated that a BMP2-derived oligopeptide can be tethered to alginate hydrogels via surface activation with NHS ester.[65] When these hydrogels were implanted into the calf muscles of Wistar rats, they stimulated bone growth while no bone formation was observed in alginate controls containing adsorbed BMP2. The observed osteogenesis supports the conclusion that long-term presentation of osteogenic factors via covalent immobilization can positively affect osteogenic mineralization and provide some temporal control over the presentation of the BMP2 and the subsequent bone formation.

In a 2007 study reported by Liu et al., a bioactive poly(lactide-co-glycolide) (PLG)

scaffold was synthesized by incorporating BMP2 via a heterobifunctional PEG tether.[64] Through this technique, PEG was conjugated to BMP2 via NHS-ester coupling on one end of a PEG chain followed by acrylate coupling to PLG on the other end. This resulted in a synthetic polymer scaffold that presented osteogenic growth factors to mesenchymal stem cells (MSCs). The tethered BMP2 retained a dose-dependent bioactivity, indicating that this motif is suitable for incorporating BMP2 into polymer substrates. Their in vivo rabbit models of critical-sized cranial defects also demonstrated improved healing efficacy, especially when pre-seeded with MSCs prior to implantation.

Shiels et al. incorporated BMP2 onto a hydroxyapatite substrate via a combination of two polymer tethers: polyethyleneimine (PEI) and PEG.[63] The tubes were first coated with branched PEI followed by subsequent attachment of heterobifunctional PEG (maleimide-PEG-succinimide) via maleimide conjugation to PEI. Finally, BMP2 was conjugated to the surface via succinimide coupling to the free end. This covalent coupling motif greatly reduced the burst-release associated with affinity-based substrates, with only a 14.5% release after 24 hours compared to 43% in adsorbed controls. The presence of covalently bound BMP2 also resulted in a 10-fold increase in cell attachment after 2 hours, and a significant increase in cell attachment was observed after 8 hours. Cell morphology was also

improved on the tethered BMP2 substrates after 8 hours. Taken together, these results indicate that BMP2 can be effectively tethered to osteogenic substrates and retain suitable bioactivity, at least in vitro, via NHS coupling to free amines within the protein sequence. Though this tethering resulted in a level of temporal control over the presentation of BMP2, it is not clear whether this translated to an increased spatial or temporal control over bone formation.

Using similar techniques, there are several promising bone tissue engineering strategies currently being explored. Covalently tethering growth factors to polymer substrates may provide a more stable temporal presentation of those factors. Indeed, Peeters et al. showed that BMP release rates were reduced by a factor of 4 when tethered to a degradable fibrin substrate, indicating a higher potential for controlled release.[66] However, this study did not indicate whether the BMP heterodimers retained bioactivity in vivo. As such, there is a push to develop tethering motifs which do not adversely affect the bioactivity of the bound osteogenic growth factors.

Another promising strategy to exert temporal control of bone formation involves exerting temporal control over the degradation and thus release of bound substrates. This can be achieved using degradable substrates or degradable

chemical tethers. These approaches allow researchers to tightly control temporal release kinetics simply by increasing or decreasing the concentration of the cleavable element. Karfeld-Sulzer et al. modified BMP2 and BMP7 dimers with plasmin-degradable linkers, a type of active degradation strategy that requires biochemical processes, such as an enzyme, to cleave the chemical bonds constraining the growth factor.[67] Other strategies involve a passive degradation that simply relies on non-biological cues, such as pH, to degrade the substrate.[68]

1.2.3 Spatial Control

Poly(ethylene glycol) PEG has been investigated for numerous tissue engineering applications, most notably in the form of highly crosslinked hydrogel networks, created by modifying the hydroxyl endgroups of PEG and incorporating crosslinkable functional groups such as acrylate derivatives.[62, 69] Due to its resistance to cell adhesion and protein adsorption as well as its non-immunogenicity, PEG can be used to encapsulate and protect cells from attack by the immune system while its tunable mesh size allows the transport of wastes/nutrients and growth factors to and from the encapsulated cells.[62] For example, PEG hydrogels have been used to immunoisolate implanted cells that produce BMP2 as a localized delivery vector.[70] MC3T3 cells were transduced to express BMP2, then injected into mouse hindlimbs with or without prior

encapsulation into PEG hydrogel microspheres. This delivery system greatly increased heterotopic bone formation over non-encapsulated cells when injected intramuscularly into the hindlimbs of mice (Figure 1.2). The transduced cells released sustained physiologic levels of BMP2, thus, aside from the injection site, no ectopic bone formation was observed. Histological results demonstrated that all bone formation was directly adjacent to the PEG microspheres. The system showed high spatial control of bone formation, and by using a tetracycline regulated gene expression system (Tet-On system), it is very likely that this system could also display temporal control of bone formation.

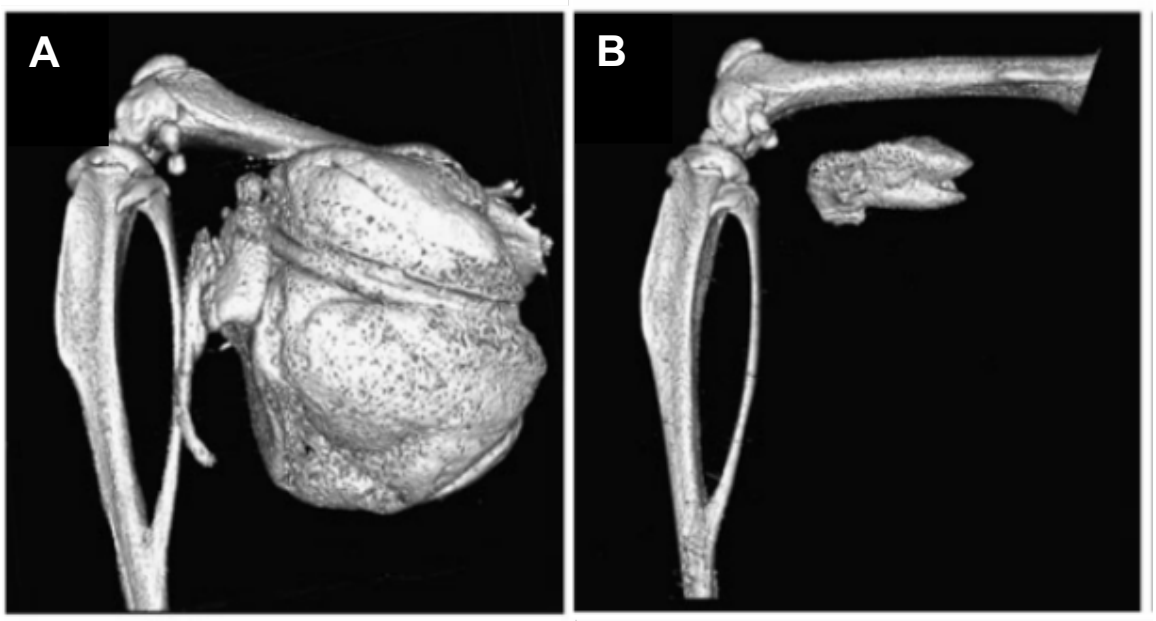

Figure 1.2: Micro computed tomography rendering of heterotopic bone formation after injection of adBMP2 transfected cells. (A) Cells encapsulated in PEGDA microspheres. (B) Non-encapsulated Cells. Adapted images reproduced with

permission[70] 2010, Mary Ann Liebert.

Bone tissue engineering has addressed the limitations of BMP2-based therapies to circumvent ectopic bone growth and new approaches to achieve spatial control over bone formation have been developed. One of the most promising aspects of protein-substrate conjugation is the promise of exact spatial control over tissue formation. Proteins conjugated to PEG (PEGylated) and other covalently immobilized proteins can be patterned into hydrogels via several methods. Some groups directly pattern BMP2 into their substrates. In a series of studies, Perikamana et al. demonstrated that covalently immobilized BMP2 enhanced in vitro differentiation of human mesenchymal stem cells (hMSCs) and in vivo remodeling in a rat calvarial defect.[71, 72] The same group also showed that the alignment of the fibers in poly(l-lactic acid) (PLLA) scaffolds influences the directionality of collagen fiber formation in vivo.[71] Other groups pattern attachment sites into their substrates.[61] Thus cells are only attached within the patterns and thus mineralization only occurs within these patterns. While these approaches show success in vitro, tissues present infinite attachment sites in vivo, and inhibiting cell attachment to specified sites on BMP2 loaded scaffolds are not likely to prevent ectopic bone formation in host tissues.

Still, other groups have achieved patterned mineralization by promoting bone formation in selected areas while inhibiting it in other areas (Figure 1.3).[73] The right half of human allograft scaffold disks were inkjet printed with three-dimensional patterns of BMP2 with and without its inhibitors on the left half. Scaffolds were seeded with C2C12 cells and stained for alkaline phosphatase activity. At lower doses, the scaffolds achieved spatial control of osteoblastic differentiation. As BMP2 concentration increased, the spatial control decreased. It was thought that the loss of spatial control was due to desorption of BMP2 at high doses and re-adsorption elsewhere on the discs. Noggin inhibited off-pattern osteoblastic differentiation.

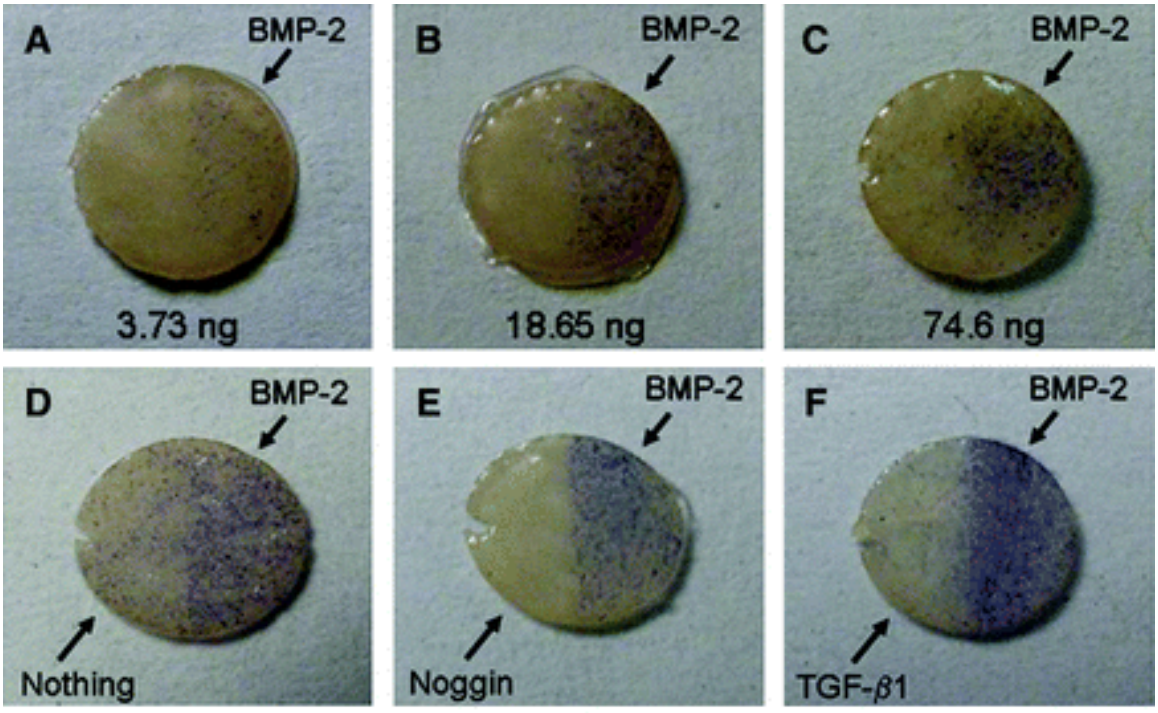

Figure 1.3: Spatial patterning of osteoblast differentiation was achieved using

Inkjet-printed BMP2 and its inhibitors in a dose-dependent manner in C2C12 cells. Reproduced with permission[73] 2010, Mary Ann Liebert.

Inhibiting osteogenesis in specified areas on BMP2-loaded scaffolds may prevent osteogenesis in those areas, but may not prevent ectopic bone formation, particularly if bioactive BMP2 is desorbing from the scaffold. To establish whether these methods were also capable of achieving spatial control over osteogenesis in vivo, the ink-jet printed disks were used to treat critical-size calvarial defects in mice (Figure 1.4).[74] Patterning BMP2 with a cofactor, stromal cell-derived factor-1β, induced bone growth with an effective BMP2 dosage reduced by several orders of magnitude below current clinical standards.[73]

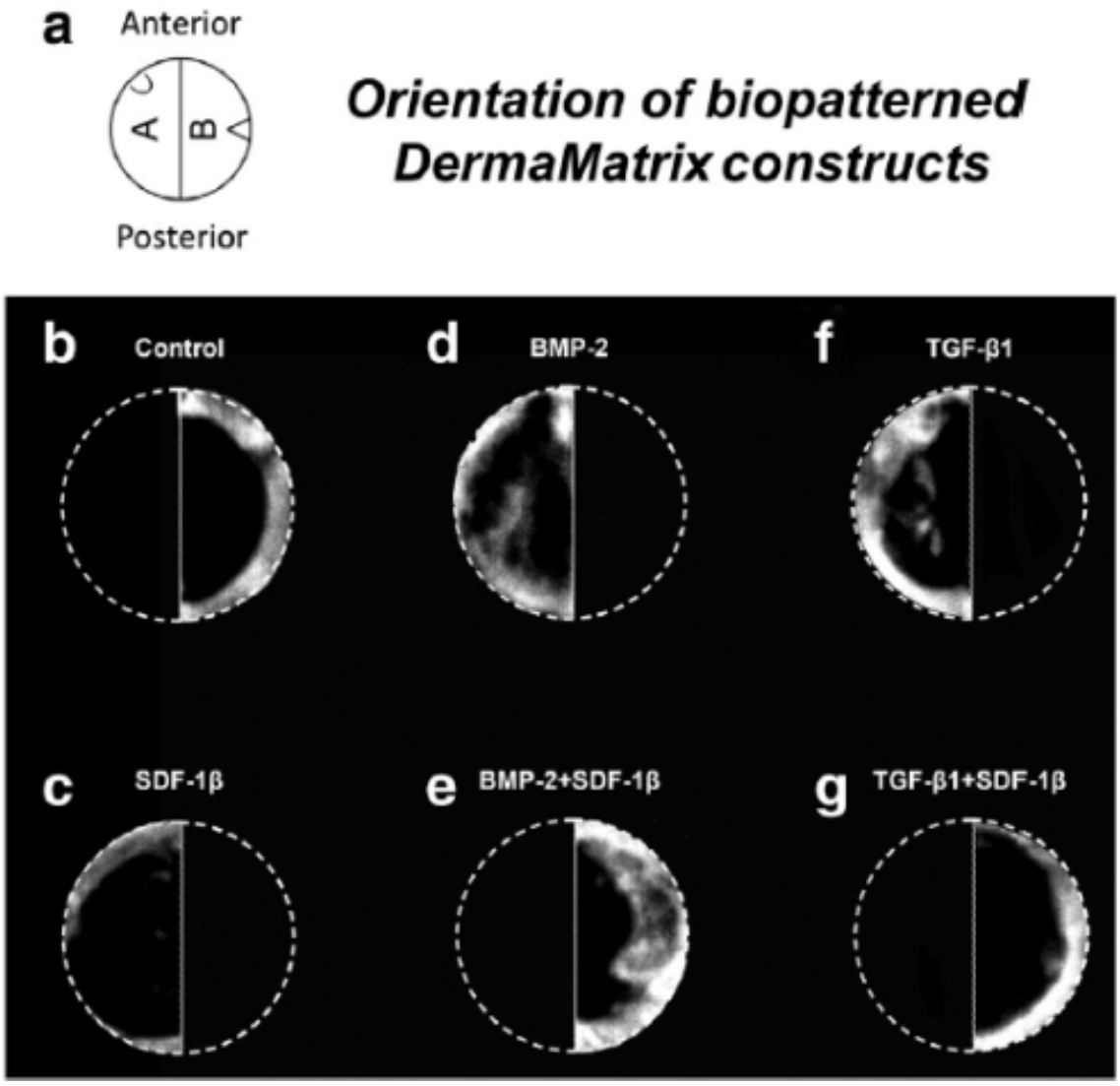

Figure 1.4: Radiographs of mouse critical-size calvarial defect treated with inkjet-patterned BMP2 and cofactors. Circles represent implanted discs; semicircles show the blank side (black) and the side bioprinted with growth factors. Reproduced with permission[74] 2014, Elsevier.

Such successes drive investigations into a variety of spatial presentations of growth factors in scaffolds. Mechanical and chemical gradients have also been

employed to control osteogenic differentiation and mineralization. A microfluidic device was used to create a BMP2 gradient in a polymer film. The resulting gradient showed a dose-dependent response when exposed to mesenchymal stem cells.[75] Liu et al. recently demonstrated spatial control of osteogenic differentiation on woven poly(lactic-co-glycolic acid) (PLGA) nanofibers by applying a mineral gradient across the scaffold.[76] Gradients in pore size in poly(caprolactone) and poly(ethylene oxide therphtalate) and poly(butylene therephtalate) also demonstrate spatial control over the early stages of osteogenesis and mineralization.[77]

1.3 Non-BMP Proteins

In addition to BMPs, several other proteins have exhibited osteogenic potential and have been incorporated into tissue engineering applications. Dentin matrix protein 1 (DMP1) has been shown to enhance the differentiation of rat bone marrow stromal cells.[78] Past studies have also shown that DMP1 facilitates the acellular deposition of apatite and hydroxyapatite when adsorbed to glass substrates, indicating promise for spatial control applications.[79, 80] It is thought that DMP1 nucleates mineral formation in specific sites on collagen (the N-terminal end), and that this spatial control can be harnessed for tissue engineering purposes.[17, 81] Lin et. al recently incorporated DMP1 into a hydrogel

network.[82] The incorporation of DMP1 led to increased differentiation of primary rat bone marrow stromal cells as well as increased mineralization, further establishing its potential for spatial control.

Recent developments suggest that insulin-like growth factors (IGFs) may also be beneficial in osteogenic tissue engineering systems.[19, 83-85] Wang et al. have shown that IGF1 promotes osteogenic differentiation in stem cells from apical papilla.[83] Reible et al. found that IGF1 induces osteogenic differentiation of hMSCs in a manner comparable to BMP7.[84] Kang et al. have shown that IGF2 may enhance the osteogenic differentiation potential of parthenogenetic murine embryonic stem cells, which are inherently deficient in IGF.[19] In addition to using IGFs as osteoinducers, inhibiting their expression has been shown to reduce osteogenic differentiation. Ochial et al. have even shown that the introduction of TGF-β1 suppresses osteoblast differentiation in MC3T3-E1 cells by inhibiting IGF1 production.[85] A scaffold incorporating TGF-β1 in areas where bone formation is not desired and IGFs in areas where it is desired may be able to harness these osteogenic induction and suppression properties to achieve spatial control of bone formation.

1.3.1 Temporal Control

Kempen et. al showed the potential of temporal control over BMP2 and VEGF delivery to increase bone formation in a rat model. PLGA microspheres loaded with BMP2 were embedded in a gelatin hydrogel loaded with VEGF to facilitate the sequential release of the growth factors. These scaffolds were evaluated for their ability to induce both ectopic and orthotopic bone formation. The scaffolds were implanted for 56 days into femoral defects and subcutaneous implants into contralateral lower limbs and the dorsa. Temporal control over the release of the growth factors was successful, with VEGF released in a burst over the first 3 days and BMP2 released in a sustained manner over the 56-day duration. While this method significantly increased heterotopic bone formation, no significant increase in orthotopic bone formation was observed in the segmented femur defect.[42] These results both show the potential of temporal delivery of growth factors, and that further work is needed.

1.3.2 Spatial Control

Tethered proteins have been investigated for bone tissue engineering to directly promote bone formation or auxiliary function, such as the delivery of anti-inflammatory agents to aid in osteoblast function during wound healing. A 2012 study by Rodrigues et al. reported that surface tethered endothelial growth factor

served to protect MSC-differentiated preosteoblasts from cytotoxic inflammatory cytokines that would be present during wound healing.[86] Sofia et al. tethered RGD, parathyroid hormone, and a modified parathyroid hormone peptide onto a silk-based scaffold.[56] They observed elevated levels of cell adhesion, osteogenic markers, and mineralization in human osteoblast-like cells. This study also indicated that RGD had the greatest impact on osteogenesis in this model. However, RGD is the primary facilitator of cell adhesion in in vitro models, so it is possible that increased cell attachment could be the primary driver of these particular results. Bentz et al. tethered transforming growth factor-β (TGF- β) into a collagen network via a heterobifunctional PEG tether.[87] The covalently tethered TGF-β was stable in PBS and fully retained bioactivity throughout the four-week study. Conversely, unmodified TGF-β lost activity after one week of incubation. Thus, their results were promising for potentially using their method to also tether BMP2 since BMP2 is a member of the TGF-β family and has also been shown to retain bioactivity when conjugated to polymers and substrates.[63, 64]

Though few studies have demonstrated microscale patterned bone formation, promising work has been conducted with other tissues, including those important in bone formation. A study conducted by Leslie-Barbick et al. induced microscale cellular angiogenic activity on PEG hydrogels via VEGF surface patterning.[60]

Human umbilical vascular endothelial cells showed significantly increased tubule formation when cultured on these VEGF-patterned PEG hydrogels (Figure 1.5). Combining this approach with BMP2 may result in microscale spatial control of bone formation, particularly considering the combined role BMP2 and VEGF plays in bone tissue formation.[39-43]

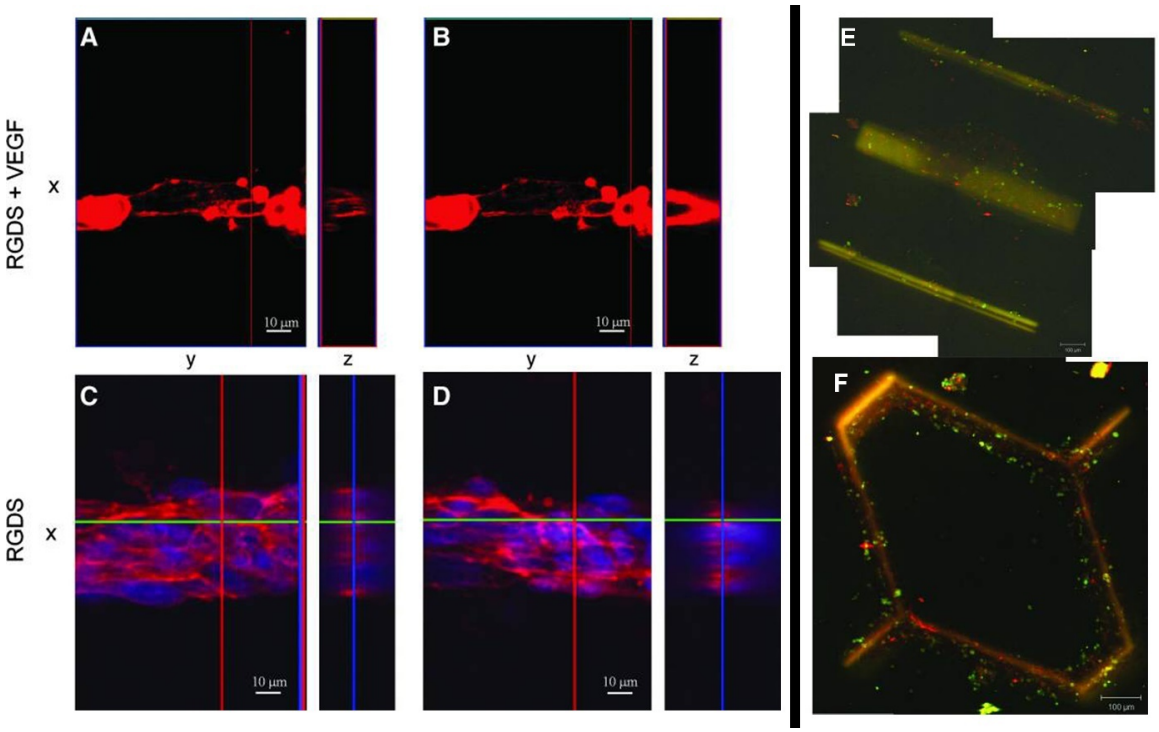

Figure 1.5: Patterned angiogenesis on PEGDA substrates containing covalently conjugated VEGF. (A, B) Tubule formation and cross-section on VEGF-patterned PEGDA hydrogels. (C, D) Cells cultured on non-VEGF-patterned hydrogels display no tubule formation. (E, F) Fluorescent VEGF pattern visualization. Adapted images reproduced with permission[60] 2011, Mary Ann Liebert.

1.4 Small Molecules

Small molecules and compounds have also garnered interest in drug delivery, regenerative medicine, and tissue engineering.[88] They are attractive targets for bone tissue engineering because their low molecular weight is often too small to induce the immune responses observed with larger proteins, and unlike proteins, they do not require structural integrity to retain bioactivity.[88-92] This makes them ideal candidates to covalently incorporate into scaffolds.

Locally delivered bisphosphonate has been used to prevent the loosening of orthopaedic implants in an osteoporotic sheep model.[93] When ovariectomized sheep had bisphosphonate coated implants inserted into their femoral condyles, bone at the implant site was 50% higher than controls, demonstrating high spatial control. Sphingosine 1-phosphate and a synthetic analog, FTY720, have been shown to promote the incorporation of bone allografts in rat critically sized tibial defect models.[94] When bone allografts were coated with FTY720, significantly more bone formed at the allograft-host bone interface, demonstrating high spatial control. N-acetyl cysteine (NAC) has been shown to upregulate bone-related gene expression and mineralization in primary rat bone marrow stromal cells.[95] Additionally, NAC-infused collagen sponge implants enhanced trabecular bone formation in a critical-size femoral cortical bone defect model in rats. All bone

formation occurred at the site of the sponges, thus demonstrating high spatial control.

Statins, commonly used to treat high-cholesterol, when delivered systemically or locally promote bone formation by stimulating BMP2 gene expression, inhibiting osteoblast apoptosis, and inhibiting osteoclast differentiation.[96] Though there are conflicting reports of success using statins, many of the variables can be traced to the differing routes of administration, doses, and statin type.[96] Simvastatin, Lovastatin, Rosuvastatin, and Fluvastatin have been all delivered to defect models in rabbits, rats, and mice, using scaffolds comprised of collagen sponges, hydroxyapatite fibers, poly(D,L-lactide) (PDLLA), hyaluronic acid hydrogels, calcium sulfate, polyurethane, methylcellulose/polylactide, propylene glycol alginate, and gelatin.[97-110] In each of these studies, the statin enhanced bone formation or otherwise induced osteogenesis at the defect site, with the exception of PDLLA, which had conflicting results. In one study using PDLLA as a scaffold carrier of simvastatin, the higher dose had catabolic effects on bone compared to the lower dose, while another study by the same group using PDLLA as a coating carrier of simvastatin, the local delivery of simvastatin improved fracture healing in a dose-dependent manner.[105, 106] In each of these results the bone formed was localized to the scaffold, with no reports of ectopic bone formation. Thus,

small molecules have demonstrated a strong potential for spatial control in bone tissue engineering.

1.5 Bone Tissue Engineering Substrates

While incorporating proteins, growth factors, and small molecules into scaffold substrates is a main approach in achieving spatiotemporal control over bone formation, another approach is using substrates and scaffolds that are themselves osteogenic.

1.5.1 Substrates Derived from Bone

In addition to being osteogenic, the substrate must be suitable for tissue engineering purposes. Ideal substrates should be biocompatible and non-toxic, mimic the mechanical and biochemical properties of natural bone, prevent soft or foreign tissue invasion, and be resorbed or replaced once they are no longer needed to facilitate osteogenesis. To this end, natural substrates often exhibit a more complete mimetic profile, and therefore they tend to begin closer to this ideal. Aside from the use of raw bone, either as an autograft, allograft, or xenograft, the most obvious solution is to produce or derive the substrate directly from bone. Most research into bone-derived scaffolds investigates decellularized bone, collagen, or demineralized bone matrix (DBM) and much of the work on the latter

two dates back decades.

Decellularizing tissues is a relatively new method that results in natural scaffolds for tissue engineering purposes. Decellularized tissues are gaining popularity in the field because they possess microarchitectural cues, intact bioactive molecules such as growth factors, chemokines, and cytokines, and are capable of directing MSCs to differentiate towards the tissue of origin.[111] Immune responses are avoided by removing the cells, and thus DNA, from the tissue. Successful decellularization has been reported for a variety of organs and soft tissues, but there are fewer reports of decellularized hard tissues, such as bone. Lee et al. investigated the osteogenic capacity of decellularized bone matrix both *in vitro* and *in vivo*.[112] When rat MSCs were incubated with decellularized bone particles, the osteogenic gene expression of the MSCs were significantly higher in bone sialoprotein and alkaline phosphatase activity than control MSCs without the particles. In addition, the MSCs with the decellularized bone particles exhibited significantly greater mineralization than controls. When implanted into calvarial defects, decellularized bone grafts alone stimulated bony ingrowth into the graft. When combined with MSCs, the response was even greater. New bone formation was significantly higher than controls, but without MSCs, bone only formed at the interface of the decellularized bone graft and the host bone. Thus, decellularized

bone is a strong candidate for achieving spatial control of bone formation.

When human decellularized bone grafts from healthy young and osteoporotic aged donors were exposed to MSCs from old and young donors, the aged bone grafts increased the osteogenic activity of MSCs significantly more than the young decellularized bone.[113] In both old and young MSCs, alkaline phosphatase activity, the osteogenic markers RUNX2, and osteopontin, were significantly increased over day 0 controls. The osteogenic marker osteocalcin was only increased in young MSCs. The researchers demonstrated that the concentration of IGF binding protein 1 (IGFBP1) was significantly higher in young decellularized bone matrix, and postulated that the combination of reduced IGFBP1 availability and increased porosity resulted in the significantly greater osteogenic differentiation induced by the older bone, and further suggested that this explained the excellent clinical results observed with aged allograft. These results show the potential of decellularized bone, particularly derived from aged bone, combined with the patient's own MSCs to form bone with high spatial precision.

While decellularized bone matrices contain the mineral content of the bone, demineralized bone matrices lack it. Demineralized bone matrix is human-derived allograft bone that has had the inorganic, or mineral, components removed,

leaving a mostly collagenous matrix that can be modified or implanted as-is.[114] It is commercially available and clinically approved. Demineralized bone matrix-based devices, in fact, account for approximately twenty percent of the $1 billion per year bone grafting market.[115] Its properties as a substrate, however, vary greatly depending on the source of the bone, the demineralization method, and any post demineralization processing.[116, 117] Pietrzak compared twenty available demineralized bone matrix formulations and found that the protein content of several bone morphogenetic proteins correlated to donor gender, but varied independent of donor age and other factors.[117] Despite these drawbacks, however, there are notable advantages compared to other therapies. Demineralized bone matrix has a much higher concentration of osteogenic factors than raw bone or hydroxyapatite-derived materials and contains collagen, which may significantly contribute to mineralization.[81] Demineralized bone matrix can also be extensively modified and or incorporated with other therapies, such as for use with BMP2. Francis et al. reported that incorporating rhBMP2 into demineralized bone matrix served as a viable alternative to autograft in alveolar cleft reconstruction with a 94.4 percent clinical success rate.[118] Of note, the demineralized bone matrix treatment group consisted of ten subjects who had previously undergone failed autograft treatments. Within this group 9 out of 10 were deemed clinically successful. While demineralized bone matrix alone does

not result in ectopic bone formation and in that sense offers relatively high spatial control, when BMP2 is incorporated into it, the same risks of ectopic bone formation are associated with it.

1.5.2 Substrates Derived from Non-bone Biominerals

Certain species of coral are structurally and mechanically similar to trabecular bone. Coral has been researched for over 45 years in vitro and in vivo, in humans and in animals.[2] It is currently used as a bone graft in a variety of surgical specialties: orthopedic, cranial, maxillofacial, periodontal and plastic.[119-123] Coralline hydroxyapatite is derived from sea coral, and can occur naturally, can be converted from calcium carbonate to hydroxyapatite by exchanging the carbonate of coral with phosphate to form coralline hydroxyapatite, or it can be coated with hydroxyapatite. With the exception of naturally occurring coralline hydroxyapatite, most coral is over 97% calcium carbonate. When implanted in vivo, coral has neither induced an inflammatory nor an immune response.[119, 124-128] By itself, coral is osteoconductive, but not osteoinductive.[119] However, it can be treated so that it is osteoinductive. When coral blocks were coated with nano-hydroxyapatite and VEGF, they induced osteogenesis in a canine mandibular defect model.[129] The bone formation was localized to the coating of the nano-hydroxyapatite, thus exhibiting spatial control.

Conversely, mother of pearl is both osteoconductive and osteoinductive. Also known as nacre, it is another marine biomineral that has been heavily investigated. In the same way that bone and some of its extracted proteins (e.g., BMPs) are powerful osteogenic agents, nacre and its extracted proteins are proving to be as well. A primary difference is that nacre does not lose its osteogenic capabilities when subjected to processing. Archeological discoveries suggest that the Mayans performed the world's earliest known endosseous implant in the seventh century using nacre, as evidenced by a human skull containing nacre teeth implants that had fused with the underlying bone of the jaw.[130] More recent research over the last two decades has demonstrated that nacre is highly osteogenic, osteoclast-degradable, and does not elicit an immune response. Since its promise as an "implantation material of unparalleled virtues," it has been studied extensively to harness its osteogenic properties.[130]

Following the rediscovery of nacre, both whole nacre and its extracted proteins have been investigated through in vitro and in vivo studies. When bone chips and nacre chips were separated by a millimeter and placed on mammalian osteoblasts, highly ordered bone formed between the two chips, and not elsewhere.[131] Using nacre as a subchondral implant in sheep knees, analysis of the interface between

nacre and bone showed in-growth of bone into the nacre material with erosion present on the nacre surface, indicating that nacre can be resorbed by osteoclasts to some extent.[132-134] Further studies that exposed nacre to osteoclasts showed osteoclast pits on nacre were fewer than those on bone.[135] The authors established that nacre inhibited osteoclast activity. Although these studies demonstrate that nacre itself may serve as an implant scaffold, unprocessed nacre is limited by the geometry of its source (e.g. seashell) because it is too thin to fill in larger defects. To circumvent this limitation, nacre has been ground into a powder and implanted as a moldable paste in both humans and animals. These nacre powder implants have shown both osteogenic and chondrogenic activity.[136, 137] Nacre powders injected into the vertebral cavities of sheep showed slow degradation and demonstrated a lining of osteoid containing active osteoblasts in contact with the nacre.[137] These findings suggest that nacre was inducing the formation of bone along the interface. Additionally, nacre powders implanted into human maxillary defects showed no immunogenic response and no resulting toxicity after osteoclast resorption.[136] These powders, however, drifted in vivo, resulting in malformed bone.[136]

Incorporating powdered nacre or bioactive nacre extracts into a polymer network has the potential to eliminate powder drift and malformed bone. When powdered

nacre was encapsulated with hMSCs in an alginate hydrogel, a significant increase in collagen matrix and hydroxyapatite deposition was observed over hMSCs encapsulated in alginate with no nacre.[138] Powdered nacre encapsulated with MC3T3-E1 cells in a PLGA hydrogel showed increased osteogenesis-relevant markers of collagen I, osteopontin, and osteocalcin over control.[139] When MSCs were seeded on PLGA scaffolds incorporating pearl nacre or tricalcium phosphate, the scaffolds containing nacre exhibited greater biocompatibility and osteoconductivity, as determined by alkaline phosphatase activity and real time reverse transcription polymerase chain reaction (RT-PCR).[140]

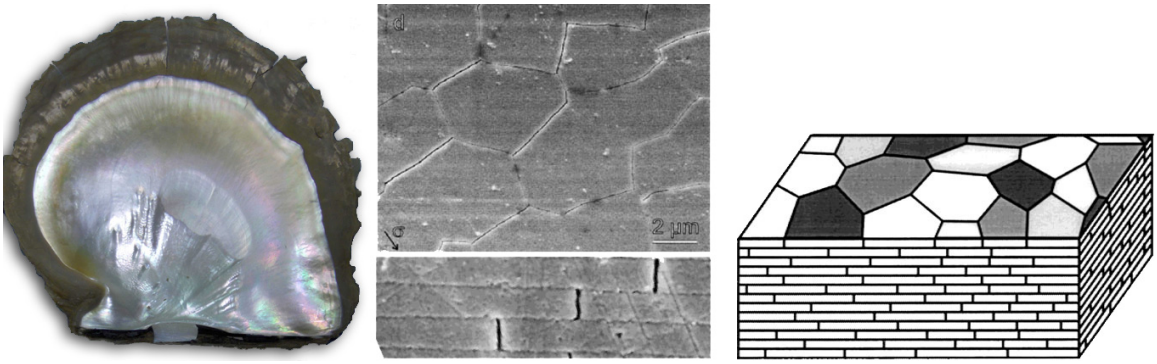

Figure 1.6: The lamellar brick and mortar structural organization of nacre. Adapted images reproduced with permission[141] 2001, Materials Research Society.

Although the powders are easier to incorporate into hydrogels, extracted nacre

proteins are also known to direct the molecular orientation of the different polymorphs of calcium carbonate crystals that comprise mollusk shells, controlling the formation of aragonite (nacre) and calcite (the outer layer) (Figure 1.6).[141-143] This protein-nucleated aragonite has a fracture resistance approximately 3,000 times that of its geological counterpart due to its protein-controlled interdigitating structure.[144] Since nacre and its proteins are capable of controlling both de novo mineralization and osteoblast-mediated bone formation, it is thought that nacre's high control over calcium mineralization (Figure 1.7) may provide insight into spatially controlling the formation of bone tissue using orthopaedic biomaterials, tissue engineering, and regenerative medicine.

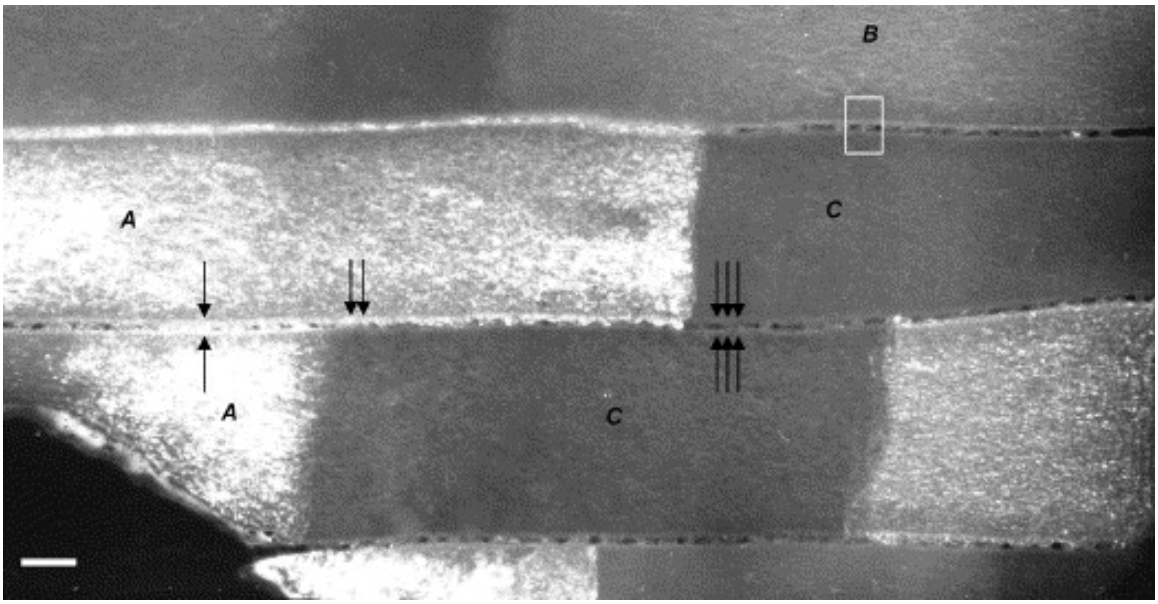

Figure 1.7: Proteins spatially direct the lamellar brick-and-mortar structure of nacre. Arrows indicate the organic layer between mineral crystals. Reproduced

with permission[144] 2005, Elsevier.

The water-soluble portion of nacre protein extracts have shown the capability to induce osteogenesis in mouse pre-osteoblasts, rat bone marrow tissue, and human mesenchymal stem cells in vitro.[145] Although BMP2 is present in nacre and highly conserved between mollusks and humans, several non-BMP2 proteins within nacre have demonstrated the ability to nucleate aragonite from solution and to induce osteogenesis in mammalian cells.[145-147] Though several proteins and peptides capable of nucleating aragonite have been isolated from nacre, only three have been shown to induce osteogenesis in vitro.[147-149] Many of the pathways for non-BMP2 nacre osteogenesis are unknown. Thus, the exact mechanisms by which nacre proteins initiate and seemingly augment osteogenesis is poorly understood. Despite this poor understanding, the collective conclusion from these studies is that nacre appears to have all the osteogenic benefits of BMP2 with none of the immunogenic or uncontrolled growth side effects. Hence, there is strong motivation to develop a delivery system capable of presenting nacre or its proteins in the desired geometry while preventing its migration.

In a preliminary investigation, Olabisi et al. explored the potential of PEGylated nacre proteins to exert microscopic spatial control of bone mineralization.[18]

After incorporating pegylated fibronectin into bulk hydrogel sheets to provide attachment ligands, PEGylated proteins isolated from the water soluble matrix of oyster nacre were photopatterned onto PEG hydrogel surfaces. Prior to photopatterning, nacre proteins were combined with an acrylated fluorescent marker to enable visualization. Prepared hydrogel surfaces were seeded with MC3T3-E1 osteoblasts and hydrogels were stained on day 12 using the von Kossa silver staining method for calcium. Mineralization was concentrated within patterned regions (Figure 1.8).

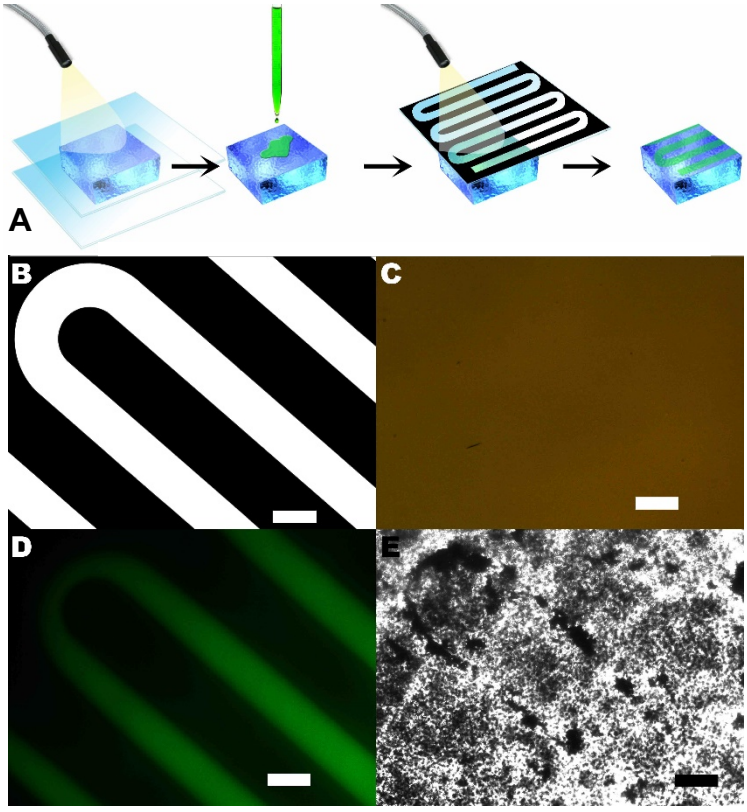

Figure 1.8: Micropatterning osteoblast-mediated mineralization using nacre proteins photopatterned on PEGDA. (A) Hydrogel sheets are photopolymerized

then pegylated nacre proteins are added to surfaces and covalently bound in place using photolithography. (B) Photomask used. (C) Color image of hydrogel surface. (D) Fluorescent image of hydrogel surface. (E) Hydrogel surface following von Kossa staining 12 days after seeding with MC3T3-E1 osteoblasts. Scale bars are 200 μm. Adapted images reproduced with permission[18] 2011, Biomedical Engineering Society.

1.5.3 Synthetic Substrates

Although some studies have presented compelling evidence that bone mineral is composed of mostly carbonated apatite, hydroxyapatite has generally been recognized as the primary mineral component of teeth and bones.[150, 151] As such, hydroxyapatite has been the primary mineral substrate in orthopaedic studies. It is biocompatible, immunologically inert, and is resorbable in vivo.[152-154] Recently, Woodard et al. demonstrated that implanted microporous hydroxyapatite scaffolds may approximate the mechanical properties of trabecular bone.[155] These substrates show high spatial control as the substrate itself induces osteogenesis. Studies using hydroxyapatite do not report ectopic bone formation as do those using BMP2.

Chemically synthesized or geologic hydroxyapatite with smooth surfaces suffer

from a relatively poor binding affinity to bone, and such hydroxyapatite ceramics by themselves do not induce osteogenesis without the presence of progenitor cells.[156, 157] When nanoscale features are introduced to hydroxyapatite surfaces, the binding affinity and osteogenic properties are improved. Apatite from human bone was discovered to be comprised of nanoscale calcium phosphate crystals and that nanoscale hydroxyapatite resembles the inorganic component of human bone.[158-160] Nanostructured hydroxyapatite surfaces promote the adhesion, proliferation, and osteogenic differentiation of MSCs and osteoprogenitors, and increase mineral deposition[161-166] while improving the biocompatibility, biological activity, and bony integration of any material coated by it.[159, 161, 166] Hydroxyapatite is often used as a coating of another material rather than as the implant material itself because its brittleness and poor mechanical stability limit its use.[167] Thus, other ceramics and polymers are coated with hydroxyapatite. Calcium carbonate and calcium phosphate ceramics demonstrate high biocompatibility and osteoconduction, though they are not inherently osteoinductive and often require supplementation with BMPs. When combined or coated with hydroxyapatite, the suitability of these ceramics for bone tissue engineering is improved. Biphasic calcium phosphate is comprised of hydroxyapatite and beta-tricalcium phosphate (β-TCP). The degradation and bioactivity of biphasic calcium phosphate can be adjusted by adjusting the ratio of

hydroxyapatite and β-TCP.[168, 169] Nevertheless, traditional biphasic calcium phosphate is not osteoinductive. Hu et al. coated biphasic calcium phosphate with nano-hydroxyapatite then seeded MSCs onto them. Several osteogenic markers of differentiation, alkaline phosphatase activity, collagen I production, and osteocalcin expression were significantly greater on coated biphasic calcium phosphate scaffolds than on the uncoated scaffolds.

Spence et al. investigated the incorporation of calcium carbonate into an hydroxyapatite scaffold, resulting in improved osteoclast resorption and bonding to bone.[170] Calcium carbonate is more soluble in aqueous solution, particularly under acidic condition created by osteoclast secretions, than hydroxyapatite and may therefore be more readily resorbed by osteoclasts.[171, 172] Both synthesized and biologically derived calcium carbonate are osteoclast-degradable.[135] Osteoclast involvement in bone formation is important; during remodeling, osteoclast and osteoblast activity is coupled, thus osteoclasts play an important role in the recruitment and activity of osteoblast progenitor cells during osteogenesis.[170, 173] Thus an implant that stimulates osteoclast resorption may ultimately recruit osteoblast activity.

Though polymers have been successful for use in soft tissue engineering

applications, they have poor mechanical properties compared to bone. Since bone itself is a composite of a brittle substance (apatite) and a compliant one (collagen), a logical approach has been to form polymer/ceramic composite materials. Such composites have been formed using hydroxyapatite and polymers such as PLLA, chitosan, poly(lactic acid), and poly(3-hydroxybutyrate). Wang et al. coated PLLA with nano-hydroxyapatite and found increased alkaline phosphatase activity and collagen I production in rabbit MSCs.[167] When the composite hydroxyapatite/PLLA scaffold was inserted into rabbit mandibular critical sized defects, scaffolds were completely integrated into the host bone. The authors reported that the interface of the scaffolds and the host bone was indistinguishable, and the location of bone formation was highly specific to the implant. Further, the authors reported that the process was accelerated from 16 weeks to 12 weeks with the incorporation of MSCs. Thus, their system demonstrated spatial control over bone formation, and through a dose response with MSCs has the potential to also exhibit temporal control.

1.6 Summary

While several approaches to promote bone formation exhibited successful temporal control by design, the majority of systems demonstrating high spatial control over bone formation do so by happenstance rather than intent. In these

systems, bone formation occurred at the interface of an implant and the host bone. While materials that can cause osseous integration directly into the surface of biomaterial are promising, the ultimate goal is to achieve bony growth throughout the biomaterial, culminating in its replacement. Currently, bone formation did not proceed beyond the biomaterial/bone interface in the majority of systems, with the exception of nacre and decellularized bone matrix. Both nacre and decellularized bone matrix are intact biominerals that are devoid of cells. Accordingly, both nacre and decellularized bone matrix demonstrated the spatial control and presentation necessary to achieve microscale control of bone formation. Further, nacre proteins patterned into a synthetic hydrogel were able to exert spatiotemporal control over the resulting mineralization. Though covalently bound BMP2 was unable to exert patterned spatiotemporal control, adhered BMP2 could at low doses. Such results are promising towards the application of tissue engineering and regenerative medicine approaches to bone formation that avoid producing ectopic bone. The application of spatiotemporal control strategies in bone tissue mineralization should be further explored.

1.7 References

[1] E.J. Carragee, E.L. Hurwitz, B.K. Weiner, A critical review of recombinant human bone morphogenetic protein-2 trials in spinal surgery: emerging safety concerns and lessons learned, The spine journal : official journal of the North

American Spine Society 11(6) (2011) 471-491.
[2] P.V. Giannoudis, H. Dinopoulos, E. Tsiridis, Bone substitutes: an update, Injury 36 Suppl 3 (2005) 20.
[3] J.T. Marino, B.H. Ziran, Use of solid and cancellous autologous bone graft for fractures and nonunions, The Orthopedic clinics of North America 41(1) (2010) 26.
[4] B.L. Taylor, T. Andric, J.W. Freeman, Recent advances in bone graft technologies, Recent Patents on Biomedical Engineering 6(1) (2013) 40-46.
[5] V.V. Valimaki, H.T. Aro, Molecular basis for action of bioactive glasses as bone graft substitute, Scandinavian journal of surgery : SJS : official organ for the Finnish Surgical Society and the Scandinavian Surgical Society 95(2) (2006) 95-102.
[6] A.L. Jones, R.W. Bucholz, M.J. Bosse, S.K. Mirza, T.R. Lyon, L.X. Webb, A.N. Pollak, J.D. Golden, A. Valentin-Opran, Recombinant human BMP-2 and allograft compared with autogenous bone graft for reconstruction of diaphyseal tibial fractures with cortical defects. A randomized, controlled trial, The Journal of bone and joint surgery: American volume 88(7) (2006) 1431-1441.
[7] N.-F. Chen, Z.A. Smith, E. Stiner, S. Armin, H. Sheikh, L.T. Khoo, Symptomatic ectopic bone formation after off-label use of recombinant human bone morphogenetic protein-2 in transforaminal lumbar interbody fusion, Journal of neurosurgery: Spine 12(1) (2010) 40-46.
[8] M.H. Kang, J.S. Kim, J.E. Seo, S.C. Oh, Y.A. Yoo, BMP2 accelerates the motility and invasiveness of gastric cancer cells via activation of the phosphatidylinositol 3-kinase (PI3K)/Akt pathway, Experimental cell research 316(1) (2010) 24-37.
[9] T.-H. Lai, Y.-C. Fong, W.-M. Fu, R.-S. Yang, C.-H. Tang, Osteoblasts-derived BMP-2 enhances the motility of prostate cancer cells via activation of integrins, The Prostate 68(12) (2008) 1341-1353.
[10] B. Perri, M. Cooper, C. Lauryssen, N. Anand, Adverse swelling associated with use of rh-BMP-2 in anterior cervical discectomy and fusion: a case study, The spine journal : official journal of the North American Spine Society 7(2) (2007) 235-239.
[11] D.A. Wong, A. Kumar, S. Jatana, G. Ghiselli, K. Wong, Neurologic impairment from ectopic bone in the lumbar canal: a potential complication of off-label PLIF/TLIF use of bone morphogenetic protein-2 (BMP-2), The spine journal : official journal of the North American Spine Society 8(6) (2008) 1011-1018.
[12] K.S. Cahill, J.H. Chi, A. Day, E.B. Claus, Prevalence, complications, and hospital charges associated with use of bone-morphogenetic proteins in spinal fusion procedures, JAMA, the Journal of the American Medical Association 302(1) (2009) 58-66.
[13] A. Mesfin, J.M. Buchowski, L.P. Zebala, W.R. Bakhsh, A.B. Aronson, J.L. Fogelson, S. Hershman, H.J. Kim, A. Ahmad, K.H. Bridwell, High-dose rhBMP-2 for adults: major and minor complications: a study of 502 spine cases, The Journal

of bone and joint surgery: American volume 95(17) (2013) 1546-1553.
[14] G.M. Calori, D. Donati, B.C. Di, L. Tagliabue, Bone morphogenetic proteins and tissue engineering: future directions, Injury 40 Suppl 3 (2009) 67.
[15] H. Uludag, D. D'Augusta, R. Palmer, G. Timony, J. Wozney, Characterization of rhBMP-2 pharmacokinetics implanted with biomaterial carriers in the rat ectopic model, Journal of Biomedical Materials Research 46(2) (1999) 193-202.
[16] Y. Cai, X. Wang, C.K. Poh, H.C. Tan, M.T. Soe, S. Zhang, W. Wang, Accelerated bone growth in vitro by the conjugation of BMP2 peptide with hydroxyapatite on titanium alloy, Colloids and Surfaces B: Biointerfaces 116 (2014) 681-686.
[17] G. He, A. George, Dentin matrix protein 1 immobilized on type I collagen fibrils facilitates apatite deposition in vitro, J Biol Chem 279(12) (2004) 11649-56.
[18] M.R. R. M. Olabisi, C. L. Franco, J. Hoffmann, J. L. West, Patterning Bone Formation with Mother of Pearl, Biomedical Engineering Society Annual Meeting, Hartford, CT, 2011.
[19] H. Kang, J. Sung, H.M. Jung, K.M. Woo, S.D. Hong, S. Roh, Insulin-like growth factor 2 promotes osteogenic cell differentiation in the parthenogenetic murine embryonic stem cells, Tissue Eng Part A 18(3-4) (2012) 331-41.
[20] J.T. Lin, J.M. Lane, Osteoporosis: a review, Clinical orthopaedics and related research (425) (2004) 126-134.
[21] M.J. Gardner, D. Demetrakopoulos, M.K. Shindle, M.H. Griffith, J.M. Lane, Osteoporosis and skeletal fractures, HSS journal : the musculoskeletal journal of Hospital for Special Surgery 2(1) (2006) 62-69.
[22] The Surgeon General's Report on Bone Health and Osteoporosis: What it Means to You, National Institutes of Health, Washington DC, 2012.
[23] R. Eastell, Management of bone health in postmenopausal women, Hormone research 64 Suppl 2 (2005) 76-80.
[24] P. Franceschetti, M. Bondanelli, G. Caruso, M.R. Ambrosio, V. Lorusso, M.C. Zatelli, L. Massari, E.C. degli Uberti, Risk factors for development of atypical femoral fractures in patients on long-term oral bisphosphonate therapy, Bone (New York, NY, United States) 56(2) (2013) 426-431.
[25] C.V. Odvina, J.E. Zerwekh, D.S. Rao, N. Maalouf, F.A. Gottschalk, C.Y.C. Pak, Severely suppressed bone turnover: a potential complication of alendronate therapy, Journal of Clinical Endocrinology and Metabolism 90(3) (2005) 1294-1301.
[26] J. Schilcher, K. Michaelsson, P. Aspenberg, Bisphosphonate use and atypical fractures of the femoral shaft, New England Journal of Medicine 364(18) (2011) 1728-1737.
[27] L. Gedmintas, D.H. Solomon, S.C. Kim, Bisphosphonates and risk of subtrochanteric, femoral shaft, and atypical femur fracture: A systematic review and meta-analysis, Journal of Bone and Mineral Research 28(8) (2013) 1729-1737.
[28] R.M. Dell, A.L. Adams, D.F. Greene, T.T. Funahashi, S.L. Silverman, E.O.

Eisemon, H. Zhou, R.J. Burchette, S.M. Ott, Incidence of atypical nontraumatic diaphyseal fractures of the femur, Journal of bone and mineral research : the official journal of the American Society for Bone and Mineral Research 27(12) (2012) 2544-2550.
[29] J.T. Potts, Parathyroid hormone: past and present, The Journal of endocrinology 187(3) (2005) 311-325.
[30] W. Zhu, J. Kim, C. Cheng, B.A. Rawlins, O. Boachie-Adjei, R.G. Crystal, C. Hidaka, Noggin regulation of bone morphogenetic protein (BMP) 2/7 heterodimer activity in vitro, Bone 39(1) (2006) 61-71.
[31] P. Sun, J. Wang, Y. Zheng, Y. Fan, Z. Gu, BMP2/7 heterodimer is a stronger inducer of bone regeneration in peri-implant bone defects model than BMP2 or BMP7 homodimer, Dental Materials Journal 31(2) (2012) 239-248.
[32] E. Valera, M.J. Isaacs, Y. Kawakami, J.C. Izpisúa Belmonte, S. Choe, BMP-2/6 heterodimer is more effective than BMP-2 or BMP-6 homodimers as inductor of differentiation of human embryonic stem cells, PloS one 5(6) (2010) e11167.
[33] S.D. Glassman, L.Y. Carreon, M.J. Campbell, J.R. Johnson, R.M. Puno, M. Djurasovic, J.R. Dimar, The perioperative cost of Infuse bone graft in posterolateral lumbar spine fusion, The Spine Journal 8(3) (2008) 443-448.
[34] B.E. Shields Lisa, G.H. Raque, S.D. Glassman, M. Campbell, T. Vitaz, J. Harpring, C.B. Shields, Adverse effects associated with high-dose recombinant human bone morphogenetic protein-2 use in anterior cervical spine fusion, Spine 31(5) (2006) 542-547.
[35] F. Wegman, A. Bijenhof, L. Schuijff, F.C. Oner, W.J.A. Dhert, J. Alblas, Osteogenic differentiation as a result of BMP-2 plasmid DNA based gene therapy in vitro and in vivo, European Cells & Materials 21 (2011) 242; discussion 242.
[36] A.R. Poynton, J.M. Lane, Safety profile for the clinical use of bone morphogenetic proteins in the spine, Spine 27(16 Suppl 1) (2002) 40.
[37] W.F. McKay, S.M. Peckham, J.M. Badura, A comprehensive clinical review of recombinant human bone morphogenetic protein-2 Bone Graft, International Orthopaedics 31(6) (2007) 729.
[38] A.L. Shimer, F.C. Oner, A.R. Vaccaro, Spinal reconstruction and bone morphogenetic proteins: open questions, Injury 40 Suppl 3 (2009) 32.
[39] E.A. Kruger, D.D. Im, D.S. Bischoff, C.T. Pereira, W. Huang, G.H. Rudkin, D.T. Yamaguchi, T.A. Miller, In Vitro Mineralization of Human Mesenchymal Stem Cells on Three-dimensional Type I Collagen versus Plga Scaffolds: A Comparative Analysis, Plastic and Reconstructive Surgery 127(6) (2011) 2301-2311.
[40] Z.S.P. Simon Young, James D. Kretlow, Matthew B. Murphy, Paschalia M. Mountziaris, L. Scott Baggett, Hiroki Ueda, Yasuhiko Tabata, John A. Jansen, Mark Wong, Antonios G. Mikos, Dose Effect of Dual Delivery of Vascular Endothelial Growth Factor and Bone Morphogenetic Protein-2 on Bone Regeneration in a Rat

Critical-Size Defect Model, Tissue Engineering Part A 15(9) (2009) 2347–2362.
[41] Z.S. Patel, S. Young, Y. Tabata, J.A. Jansen, M.E.K. Wong, A.G. Mikos, Dual delivery of an angiogenic and an osteogenic growth factor for bone regeneration in a critical size defect model, Bone 43(5) (2008) 931-940.
[42] D.H. Kempen, L. Lu, A. Heijink, T.E. Hefferan, L.B. Creemers, A. Maran, M.J. Yaszemski, W.J. Dhert, Effect of local sequential VEGF and BMP-2 delivery on ectopic and orthotopic bone regeneration, Biomaterials 30(14) (2009) 2816-25.
[43] Z. Patel, H. Ueda, M. Yamamoto, Y. Tabata, A. Mikos, In Vitro and In Vivo Release of Vascular Endothelial Growth Factor from Gelatin Microparticles and Biodegradable Composite Scaffolds, Pharmaceutical Research 25(10) (2008) 2370-2378.
[44] Z.S. Patel, M. Yamamoto, H. Ueda, Y. Tabata, A.G. Mikos, Biodegradable gelatin microparticles as delivery systems for the controlled release of bone morphogenetic protein-2, Acta Biomaterialia 4(5) (2008) 1126-1138.
[45] M.D. Scott, K.L. Murad, Cellular camouflage: fooling the immune system with polymers, Current pharmaceutical design 4(6) (1998) 423-438.
[46] G. Csucs, R. Michel, J.W. Lussi, M. Textor, G. Danuser, Microcontact printing of novel co-polymers in combination with proteins for cell-biological applications, Biomaterials 24(10) (2003) 1713-1720.
[47] T. Miao, K.S. Rao, J.L. Spees, R.A. Oldinski, Osteogenic differentiation of human mesenchymal stem cells through alginate-graft-poly(ethylene glycol) microsphere-mediated intracellular growth factor delivery, Journal of Controlled Release 192 (2014) 57-66.
[48] J.S. Park, H.N. Yang, S.Y. Jeon, D.G. Woo, K. Na, K.-H. Park, Osteogenic differentiation of human mesenchymal stem cells using RGD-modified BMP-2 coated microspheres, Biomaterials 31(24) (2010) 6239-6248.
[49] O. Jeon, C. Powell, L.D. Solorio, M.D. Krebs, E. Alsberg, Affinity-based growth factor delivery using biodegradable, photocrosslinked heparin-alginate hydrogels, Journal of Controlled Release 154(3) (2011) 258-266.
[50] J. Li, X. Ni, K.W. Leong, Injectable drug-delivery systems based on supramolecular hydrogels formed by poly(ethylene oxide)s and Î±-cyclodextrin, Journal of Biomedical Materials Research, Part A 65A(2) (2003) 196-202.
[51] S.E. Sakiyama-Elbert, J.A. Hubbell, Controlled release of nerve growth factor from a heparin-containing fibrin-based cell ingrowth matrix, Journal of controlled release : official journal of the Controlled Release Society 69(1) (2000) 149-158.
[52] R. Ruppert, E. Hoffmann, W. Sebald, Human bone morphogenetic protein 2 contains a heparin-binding site which modifies its biological activity, Eur J Biochem 237(1) (1996) 295-302.
[53] G. Bhakta, B. Rai, Z.X. Lim, J.H. Hui, G.S. Stein, A.J. van Wijnen, V. Nurcombe, G.D. Prestwich, S.M. Cool, Hyaluronic acid-based hydrogels functionalized with

heparin that support controlled release of bioactive BMP-2, Biomaterials 33(26) (2012) 6113-22.
[54] Y.M. Kolambkar, K.M. Dupont, J.D. Boerckel, N. Huebsch, D.J. Mooney, D.W. Hutmacher, R.E. Guldberg, An alginate-based hybrid system for growth factor delivery in the functional repair of large bone defects, Biomaterials 32(1) (2011) 65-74.
[55] O. Jeon, K.H. Bouhadir, J.M. Mansour, E. Alsberg, Photocrosslinked alginate hydrogels with tunable biodegradation rates and mechanical properties, Biomaterials 30(14) (2009) 2724-2734.
[56] S. Sofia, M.B. McCarthy, G. Gronowicz, D.L. Kaplan, Functionalized silk-based biomaterials for bone formation, Journal of Biomedical Materials Research 54(1) (2001) 139-148.
[57] N. Chattopadhyay, Z. Cai, J.-P. Pignol, B. Keller, E. Lechtman, R. Bendayan, R.M. Reilly, Design and characterization of HER-2-targeted gold nanoparticles for enhanced X-radiation treatment of locally advanced breast cancer, Molecular pharmaceutics 7(6) (2010) 2194-2206.
[58] X. Sun, G. Zhang, D. Patel, D. Stephens, A.M. Gobin, Targeted cancer therapy by immunoconjugated gold-gold sulfide nanoparticles using Protein G as a cofactor, Annals of Biomedical Engineering 40(10) (2012) 2131-2139.
[59] P.R. Kuhl, L.G. Griffith-Cima, Tethered epidermal growth factor as a paradigm for growth factor-induced stimulation from the solid phase, Nature medicine 2(9) (1996) 1022-7.
[60] J.E. Leslie-Barbick, C. Shen, C. Chen, J.L. West, Micron-Scale Spatially Patterned, Covalently Immobilized Vascular Endothelial Growth Factor on Hydrogels Accelerates Endothelial Tubulogenesis and Increases Cellular Angiogenic Responses, Tissue Engineering, Part A 17(1-2) (2011) 221-229.
[61] O.F. Zouani, C. Chollet, B. Guillotin, M.-C. Durrieu, Differentiation of pre-osteoblast cells on poly(ethylene terephthalate) grafted with RGD and/or BMPs mimetic peptides, Biomaterials 31(32) (2010) 8245-8253.
[62] C.-C. Lin, K.S. Anseth, PEG Hydrogels for the Controlled Release of Biomolecules in Regenerative Medicine, Pharmaceutical research 26(3) (2009) 631-643.
[63] S.M. Shiels, K.D. Solomon, M. Pilia, M.R. Appleford, J.L. Ong, BMP-2 tethered hydroxyapatite for bone tissue regeneration: Coating chemistry and osteoblast attachment, Journal of Biomedical Materials Research, Part A 100A(11) (2012) 3117-3123.
[64] H.-W. Liu, C.-H. Chen, C.-L. Tsai, I.H. Lin, G.-H. Hsiue, Heterobifunctional poly(ethylene glycol)-tethered bone morphogenetic protein-2-stimulated bone marrow mesenchymal stromal cell differentiation and osteogenesis, Tissue engineering 13(5) (2007) 1113-1124.

[65] Y. Suzuki, M. Tanihara, K. Suzuki, A. Saitou, W. Sufan, Y. Nishimura, Alginate hydrogel linked with synthetic oligopeptide derived from BMP-2 allows ectopic osteoinduction in vivo, Journal of Biomedical Materials Research 50(3) (2000) 405-409.
[66] M. Peeters, S.E.L. Detiger, L.S. Karfeld-Sulzer, T.H. Smit, A. Yayon, F.E. Weber, M.N. Helder, BMP-2 and BMP-2/7 Heterodimers Conjugated to a Fibrin/Hyaluronic Acid Hydrogel in a Large Animal Model of Mild Intervertebral Disc Degeneration, BioResearch Open Access 4(1) (2015) 398-406.
[67] L. Karfeld-Sulzer, B. Siegenthaler, C. Ghayor, F. Weber, Fibrin Hydrogel Based Bone Substitute Tethered with BMP-2 and BMP-2/7 Heterodimers, 8(3) (2015) 977.
[68] Y. Qian, L. Yang, R. Xue, G. Yao, L. Li, Y. Sun, Polycaprolactone nanofiber scaffold enhances the osteogenic differentiation potency of various human tissue-derived mesenchymal stem cells, Stem Cell Research & Therapy 8(1) (2017).
[69] S. Lin-Gibson, K. Chatterjee, J.A. Cooper, W.E. Wallace, M.L. Becker, C.G. Simon, Jr., F. Horkay, PEG-hydrogels: synthesis, characterization, and cell encapsulation, Polymer Preprints (American Chemical Society, Division of Polymer Chemistry) 50(2) (2009) 108-109.
[70] R.M. Olabisi, Z.W. Lazard, C.L. Franco, M.A. Hall, S.K. Kwon, E.M. Sevick-Muraca, J.A. Hipp, A.R. Davis, E.A. Olmsted-Davis, J.L. West, Hydrogel Microsphere Encapsulation of a Cell-Based Gene Therapy System Increases Cell Survival of Injected Cells, Transgene Expression, and Bone Volume in a Model of Heterotopic Ossification, Tissue Engineering. Part A 16(12) (2010) 3727-3736.
[71] S.K. Perikamana, J. Lee, T. Ahmad, Y. Jeong, D.G. Kim, K. Kim, H. Shin, Effects of Immobilized BMP-2 and Nanofiber Morphology on In Vitro Osteogenic Differentiation of hMSCs and In Vivo Collagen Assembly of Regenerated Bone, ACS applied materials & interfaces 7(16) (2015) 8798-808.
[72] H.J. Cho, S.K. Perikamana, J.H. Lee, J. Lee, K.M. Lee, C.S. Shin, H. Shin, Effective immobilization of BMP-2 mediated by polydopamine coating on biodegradable nanofibers for enhanced in vivo bone formation, ACS applied materials & interfaces 6(14) (2014) 11225-35.
[73] G.M. Cooper, E.D. Miller, G.E. De Cesare, A. Usas, E.L. Lensie, M.R. Bykowski, J. Huard, L.E. Weiss, J.E. Losee, P.G. Campbell, Inkjet-Based Biopatterning of Bone Morphogenetic Protein-2 to Spatially Control Calvarial Bone Formation, Tissue Engineering, Part A 16(5) (2010) 1749-1759.
[74] S. Herberg, G. Kondrikova, S. Periyasamy-Thandavan, R.N. Howie, M.E. Elsalanty, L. Weiss, P. Campbell, W.D. Hill, J.J. Cray, Inkjet-based biopatterning of SDF-1Î² augments BMP-2-induced repair of critical size calvarial bone defects in mice, Bone (New York, NY, United States) 67 (2014) 95-103.
[75] J. Almodovar, R. Guillot, C. Monge, J. Vollaire, S. Selimovic, J.-L. Coll, A. Khademhosseini, C. Picart, Spatial patterning of BMP-2 and BMP-7 on

biopolymeric films and the guidance of muscle cell fate, Biomaterials 35(13) (2014) 3975-3985.
[76] W. Liu, J. Lipner, J. Xie, C.N. Manning, S. Thomopoulos, Y. Xia, Nanofiber scaffolds with gradients in mineral content for spatial control of osteogenesis, ACS applied materials & interfaces 6(4) (2014) 2842-9.
[77] A. Di Luca, B. Ostrowska, I. Lorenzo-Moldero, A. Lepedda, W. Swieszkowski, C. Van Blitterswijk, L. Moroni, Gradients in pore size enhance the osteogenic differentiation of human mesenchymal stromal cells in three-dimensional scaffolds, Sci Rep 6 (2016) 22898.
[78] Y. Yu, L. Wang, J. Yu, G. Lei, M. Yan, G. Smith, P.R. Cooper, C. Tang, G. Zhang, A.J. Smith, Dentin matrix proteins (DMPs) enhance differentiation of BMMSCs via ERK and P38 MAPK pathways, Cell & Tissue Research 356(1) (2014) 171-182.
[79] G. He, T. Dahl, A. Veis, A. George, Nucleation of apatite crystals in vitro by self-assembled dentin matrix protein 1, Nature Materials 2(8) (2003) 552-558.
[80] G. He, T. Dahl, A. Veis, A. George, Dentin Matrix Protein 1 Initiates Hydroxyapatite Formation In Vitro, Connective tissue research 44(Suppl. 1) (2003) 240-245.
[81] F. Nudelman, K. Pieterse, A. George, P.H.H. Bomans, H. Friedrich, L.J. Brylka, P.A.J. Hilbers, G. de With, N.A.J.M. Sommerdijk, The role of collagen in bone apatite formation in the presence of hydroxyapatite nucleation inhibitors, Nature Materials 9(12) (2010) 1004-1009.
[82] S. Lin, L. Cao, Q. Wang, J. Du, D. Jiao, S. Duan, J. Wu, Q. Gan, X. Jiang, Tailored biomimetic hydrogel based on a photopolymerised DMP1/MCF/gelatin hybrid system for calvarial bone regeneration, Journal of Materials Chemistry B 6(3) (2018) 414-427.
[83] S. Wang, J. Mu, Z. Fan, Y. Yu, M. Yan, G. Lei, C. Tang, Z. Wang, Y. Zheng, J. Yu, G. Zhang, Insulin-like growth factor 1 can promote the osteogenic differentiation and osteogenesis of stem cells from apical papilla, Stem Cell Res 8(3) (2012) 346-56.
[84] B. Reible, G. Schmidmaier, A. Moghaddam, F. Westhauser, Insulin-Like Growth Factor-1 as a Possible Alternative to Bone Morphogenetic Protein-7 to Induce Osteogenic Differentiation of Human Mesenchymal Stem Cells in Vitro, Int J Mol Sci 19(6) (2018).
[85] H. Ochiai, S. Okada, A. Saito, K. Hoshi, H. Yamashita, T. Takato, T. Azuma, Inhibition of insulin-like growth factor-1 (IGF-1) expression by prolonged transforming growth factor-beta1 (TGF-beta1) administration suppresses osteoblast differentiation, J Biol Chem 287(27) (2012) 22654-61.
[86] M. Rodrigues, H. Blair, L. Stockdale, L. Griffith, A. Wells, Surface tethered epidermal growth factor protects proliferating and differentiating multipotential stromal cells from FasL-induced apoptosis, Stem Cells (Dayton, Ohio) 31(1) (2013)

104-116.
[87] H. Bentz, J.A. Schroeder, T.D. Estridge, Improved local delivery of TGF-β2 by binding to injectable fibrillar collagen via difunctional polyethylene glycol, Journal of Biomedical Materials Research 39(4) (1998) 539-548.
[88] C.T. Laurencin, K.M. Ashe, N. Henry, H.M. Kan, K.W. Lo, Delivery of small molecules for bone regenerative engineering: preclinical studies and potential clinical applications, Drug Discov Today 19(6) (2014) 794-800.
[89] G. Blaich, B. Janssen, G. Roth, J. Salfeld, Overview: differentiating issues in the development of macromolecules compared with small molecules, Pharmaceutical Sciences Encyclopedia: Drug Discovery, Development, and Manufacturing (2010) 1-35.
[90] K.W. Lo, K.M. Ashe, H.M. Kan, C.T. Laurencin, The role of small molecules in musculoskeletal regeneration, Regen Med 7(4) (2012) 535-49.
[91] K.W. Lo, B.D. Ulery, M. Deng, K.M. Ashe, C.T. Laurencin, Current patents on osteoinductive molecules for bone tissue engineering, Recent Patents on Biomedical Engineering 4(3) (2011) 153-167.
[92] K.A. Wieghaus, S.M. Capitosti, C.R. Anderson, R.J. Price, B.R. Blackman, M.L. Brown, E.A. Botchwey, Small molecule inducers of angiogenesis for tissue engineering, Tissue Eng 12(7) (2006) 1903-13.
[93] V.A. Stadelmann, O. Gauthier, A. Terrier, J.M. Bouler, D.P. Pioletti, Implants delivering bisphosphonate locally increase periprosthetic bone density in an osteoporotic sheep model. A pilot study, Eur Cell Mater 16 (2008) 10-6.
[94] C.E. Petrie Aronin, S.J. Shin, K.B. Naden, P.D. Rios, L.S. Sefcik, S.R. Zawodny, N.D. Bagayoko, Q. Cui, Y. Khan, E.A. Botchwey, The enhancement of bone allograft incorporation by the local delivery of the sphingosine 1-phosphate receptor targeted drug FTY720, Biomaterials 31(25) (2010) 6417-6424.
[95] M. Yamada, N. Tsukimura, T. Ikeda, Y. Sugita, W. Att, N. Kojima, K. Kubo, T. Ueno, K. Sakurai, T. Ogawa, N-acetyl cysteine as an osteogenesis-enhancing molecule for bone regeneration, Biomaterials 34(26) (2013) 6147-56.
[96] A. Oryan, A. Kamali, A. Moshiri, Potential mechanisms and applications of statins on osteogenesis: Current modalities, conflicts and future directions, J Control Release 215 (2015) 12-24.
[97] M.S. Bae, D.H. Yang, J.B. Lee, D.N. Heo, Y.D. Kwon, I.C. Youn, K. Choi, J.H. Hong, G.T. Kim, Y.S. Choi, E.H. Hwang, I.K. Kwon, Photo-cured hyaluronic acid-based hydrogels containing simvastatin as a bone tissue regeneration scaffold, Biomaterials 32(32) (2011) 8161-71.
[98] S. Gao, M. Shiota, M. Fujii, K. Chen, M. Shimogishi, M. Sato, S. Kasugai, Combination of simvastatin and hydroxyapatite fiber induces bone augmentation, Open Journal of Regenerative Medicine 02(03) (2013) 53-60.
[99] A.E.H. Toshitaka Yoshii, Jeffry S. Nyman, Javier M. Esparza, Kenichi

Shinomiya, Dan M. Spengler, Gregory R. Mundy, Gloria E. Gutierrez, Scott A. Guelcher, A Sustained Release of Lovastatin from Biodegradable, Elastomeric Polyurethane Scaffolds for Enhanced Bone Regeneration, Tissue Engineering Part A 16(7) (2010) 2369–2379.
[100] K. Tanabe, H. Nomoto, N. Okumori, T. Miura, M. Yoshinari, Osteogenic effect of fluvastatin combined with biodegradable gelatin-hydrogel, Dental Materials Journal 31(3) (2012) 489-493.
[101] M. Monjo, M. Rubert, J.C. Wohlfahrt, H.J. Ronold, J.E. Ellingsen, S.P. Lyngstadaas, In vivo performance of absorbable collagen sponges with rosuvastatin in critical-size cortical bone defects, Acta Biomater 6(4) (2010) 1405-12.
[102] T. Fukui, M. Ii, T. Shoji, T. Matsumoto, Y. Mifune, Y. Kawakami, H. Akimaru, A. Kawamoto, T. Kuroda, T. Saito, Y. Tabata, R. Kuroda, M. Kurosaka, T. Asahara, Therapeutic effect of local administration of low-dose simvastatin-conjugated gelatin hydrogel for fracture healing, J Bone Miner Res 27(5) (2012) 1118-31.
[103] X. Huang, Z. Huang, W. Li, Highly efficient release of simvastatin from simvastatin-loaded calcium sulphate scaffolds enhances segmental bone regeneration in rabbits, Mol Med Rep 9(6) (2014) 2152-8.
[104] Y. Moriyama, Y. Ayukawa, Y. Ogino, I. Atsuta, K. Koyano, Topical application of statin affects bone healing around implants, Clin Oral Implants Res 19(6) (2008) 600-5.
[105] S. Pauly, D.A. Back, K. Kaeppler, N.P. Haas, G. Schmidmaier, B. Wildemann, Influence of statins locally applied from orthopedic implants on osseous integration, BMC Musculoskelet Disord 13 (2012) 208.
[106] S. Pauly, F. Luttosch, M. Morawski, N.P. Haas, G. Schmidmaier, B. Wildemann, Simvastatin locally applied from a biodegradable coating of osteosynthetic implants improves fracture healing comparable to BMP-2 application, Bone 45(3) (2009) 505-11.
[107] M.R. Thylin, J.C. McConnell, M.J. Schmid, R.R. Reckling, J. Ojha, I. Bhattacharyya, D.B. Marx, R.A. Reinhardt, Effects of simvastatin gels on murine calvarial bone, J Periodontol 73(10) (2002) 1141-8.
[108] R.W. Wong, A.B. Rabie, Statin collagen grafts used to repair defects in the parietal bone of rabbits, Br J Oral Maxillofac Surg 41(4) (2003) 244-8.
[109] R.W. Wong, A.B. Rabie, Histologic and ultrastructural study on statin graft in rabbit skulls, J Oral Maxillofac Surg 63(10) (2005) 1515-21.
[110] T. Yoshii, A.E. Hafeman, J.S. Nyman, J.M. Esparza, K. Shinomiya, D.M. Spengler, G.R. Mundy, G.E. Gutierrez, S.A. Guelcher, A sustained release of lovastatin from biodegradable, elastomeric polyurethane scaffolds for enhanced bone regeneration, Tissue Eng Part A 16(7) (2010) 2369-79.
[111] G. Chen, Y. Lv, Decellularized Bone Matrix Scaffold for Bone Regeneration,

Methods Mol Biol (2017).
[112] D.J. Lee, S. Diachina, Y.T. Lee, L. Zhao, R. Zou, N. Tang, H. Han, X. Chen, C.C. Ko, Decellularized bone matrix grafts for calvaria regeneration, J Tissue Eng 7 (2016) 2041731416680306.
[113] C.A. Smith, T.N. Board, P. Rooney, M.J. Eagle, S.M. Richardson, J.A. Hoyland, Human decellularized bone scaffolds from aged donors show improved osteoinductive capacity compared to young donor bone, PLoS One 12(5) (2017) e0177416.
[114] M.R. Urist, Bone: formation by autoinduction, Science (New York, N.Y.) 150(3698) (1965) 893-899.
[115] E. Gruskin, B.A. Doll, F.W. Futrell, J.P. Schmitz, J.O. Hollinger, Demineralized bone matrix in bone repair: History and use, Advanced Drug Delivery Reviews 64(12) (2012) 1063-1077.
[116] J.M. Katz, C. Nataraj, R. Jaw, E. Deigl, P. Bursac, Demineralized bone matrix as an osteoinductive biomaterial and in vitro predictors of its biological potential, Journal of Biomedical Materials Research Part B: Applied Biomaterials 89B(1) (2009) 127-134.
[117] W.S. Pietrzak, J. Woodell-may, N. McDonald, Assay of Bone Morphogenetic Protein-2, -4, and -7 in Human Demineralized Bone Matrix, Journal of Craniofacial Surgery 17(1) (2006) 84-90.
[118] C.S. Francis, S.S.N. Mobin, M.A. Lypka, E. Rommer, S. Yen, M.M. Urata, J.A. Hammoudeh, rhBMP-2 with a Demineralized Bone Matrix Scaffold versus Autologous Iliac Crest Bone Graft for Alveolar Cleft Reconstruction, Plastic and Reconstructive Surgery 131(5) (2013) 1107–1115.
[119] C. Demers, C.R. Hamdy, K. Corsi, F. Chellat, M. Tabrizian, L. Yahia, Natural coral exoskeleton as a bone graft substitute: a review, Biomed Mater Eng 12(1) (2002) 15-35.
[120] F.X. Roux, D. Brasnu, B. Loty, B. George, G. Guillemin, Madreporic coral: a new bone graft substitute for cranial surgery, J Neurosurg 69(4) (1988) 510-3.
[121] F.X. Roux, D. Brasnu, M. Menard, B. Devaux, G. Nohra, B. Loty, Madreporic coral for cranial base reconstruction. 8 years experience, Acta Neurochir (Wien) 133(3-4) (1995) 201-5.
[122] F. Souyris, C. Pellequer, C. Payrot, C. Servera, Coral, a new biomedical material. Experimental and first clinical investigations on Madreporaria, J Maxillofac Surg 13(2) (1985) 64-9.
[123] G. Guillemin, J.L. Patat, J. Fournie, M. Chetail, The use of coral as a bone graft substitute, J Biomed Mater Res 21(5) (1987) 557-67.
[124] N. Naaman Bou-Abboud, J.L. Patat, G. Guillemin, S. Issahakian, N. Forest, J.P. Ouhayoun, Evaluation of the osteogenic potential of biomaterials implanted in the palatal connective tissue of miniature pigs using undecalcified sections,

Biomaterials 15(3) (1994) 201-7.
[125] C.T. Begley, M.J. Doherty, R.A. Mollan, D.J. Wilson, Comparative study of the osteoinductive properties of bioceramic, coral and processed bone graft substitutes, Biomaterials 16(15) (1995) 1181-5.
[126] J.L. Irigaray, H. Oudadesse, G. Blondiaux, Quantitative study of the coral transformations 'in vivo' by several physical analytical methods, Biomaterials 11 (1990) 73-4.
[127] J. Irigaray, H. Oudadesse, G. Blondiaux, D.J.J.o.r. Collangettes, n. chemistry, Kinetics of the diffusion of some elements evaluated by neutron activation in a coral implanted in vivo, 169(2) (1993) 339-346.
[128] H. Ohgushi, M. Okumura, T. Yoshikawa, K. Inoue, N. Senpuku, S. Tamai, E.C. Shors, Bone formation process in porous calcium carbonate and hydroxyapatite, J Biomed Mater Res 26(7) (1992) 885-95.
[129] B. Du, W. Liu, Y. Deng, S. Li, X. Liu, Y. Gao, L. Zhou, Angiogenesis and bone regeneration of porous nano-hydroxyapatite/coralline blocks coated with rhVEGF165 in critical-size alveolar bone defects in vivo, Int J Nanomedicine 10 (2015) 2555-65.
[130] P. Westbroek, F. Marin, A marriage of bone and nacre, Nature (London) 392(6679) (1998) 861-862.
[131] E. Lopez, B. Vidal, S. Berland, S. Camprasse, G. Camprasse, C. Silve, Demonstration of the capacity of nacre to induce bone formation by human osteoblasts maintained in vitro, Tissue Cell 24(5) (1992) 667-79.
[132] G. Atlan, O. Delattre, S. Berland, A. LeFaou, G. Nabias, D. Cot, E. Lopez, Interface between bone and nacre implants in sheep, Biomaterials 20(11) (1999) 1017-1022.
[133] S. Berland, O. Delattre, S. Borzeix, Y. Catonne, E. Lopez, Nacre/bone interface changes in durable nacre endosseous implants in sheep, Biomaterials 26(15) (2005) 2767-2773.
[134] F. Pascaretti-Grizon, H. Libouban, G. Camprasse, S. Camprasse, R. Mallet, D. Chappard, The interface between nacre and bone after implantation in the sheep: a nanotomographic and Raman study, Journal of Raman Spectroscopy 45(7) (2014) 558-564.
[135] D. Duplat, A. Chabadel, M. Gallet, S. Berland, L. Bédouet, M. Rousseau, S. Kamel, C. Milet, P. Jurdic, M. Brazier, E. Lopez, The in vitro osteoclastic degradation of nacre, Biomaterials 28(12) (2007) 2155-2162.
[136] G. Atlan, N. Balmain, S. Berland, B. Vidal, E. Lopez, Reconstruction of human maxillary defects with nacre powder: histological evidence for bone regeneration, Comptes rendus de l'Academie des sciences.Serie III, Sciences de la vie 320(3) (1997) 253-258.
[137] M. Lamghari, M.J. Almeida, S. Berland, H. Huet, A. Laurent, C. Milet, E.

Lopez, Stimulation of bone marrow cells and bone formation by nacre: in vivo and in vitro studies, Bone 25(2 Suppl) (1999) 94S.
[138] A. Flausse, C. Henrionnet, M. Dossot, D. Dumas, S. Hupont, A. Pinzano, D. Mainard, L. Galois, J. Magdalou, E. Lopez, P. Gillet, M. Rousseau, Osteogenic differentiation of human bone marrow mesenchymal stem cells in hydrogel containing nacre powder, J Biomed Mater Res A 101(11) (2013) 3211-8.
[139] Y.L. Yang, C.H. Chang, C.C. Huang, W.M. Kao, W.C. Liu, H.W. Liu, Osteogenic activity of nanonized pearl powder/poly (lactide-co-glycolide) composite scaffolds for bone tissue engineering, Biomed Mater Eng 24(1) (2014) 979-85.
[140] M. Xu, Y. Li, H. Suo, Y. Yan, L. Liu, Q. Wang, Y. Ge, Y. Xu, Fabricating a pearl/PLGA composite scaffold by the low-temperature deposition manufacturing technique for bone tissue engineering, Biofabrication 2(2) (2010) 025002.
[141] R.Z. Wang, Z. Suo, A.G. Evans, N. Yao, I.A. Aksay, Deformation mechanisms in nacre, Journal of Materials Research 16(9) (2001) 2485-2493.
[142] R.A. Metzler, M. Abrecht, R.M. Olabisi, D. Ariosa, C.J. Johnson, B.H. Frazer, S.N. Coppersmith, P.U.P.A. Gilbert, Architecture of columnar nacre, and implications for its formation mechanism, Physical Review Letters 98(26) (2007) 268102/4.
[143] F. Marin, G. Luquet, Molluscan biomineralization: The proteinaceous shell constituents of Pinna nobilis L, Materials Science & Engineering, C: Biomimetic and Supramolecular Systems C25(2) (2005) 105-111.
[144] M. Rousseau, E. Lopez, P. Stempfle, M. Brendle, L. Franke, A. Guette, R. Naslain, X. Bourrat, Multiscale structure of sheet nacre, Biomaterials 26(31) (2005) 6254-6262.
[145] M. Rousseau, L. Pereira-Mouries, M.-J. Almeida, C. Milet, E. Lopez, The water-soluble matrix fraction from the nacre of Pinctada maxima produces earlier mineralization of MC3T3-E1 mouse pre-osteoblasts, Comparative Biochemistry and Physiology, Part B: Biochemistry & Molecular Biology 135B(1) (2003) 1-7.
[146] M. Rousseau, H. Boulzaguet, J. Biagianti, D. Duplat, C. Milet, E. Lopez, L. Bedouet, Low molecular weight molecules of oyster nacre induce mineralization of the MC3T3-E1 cells, Journal of Biomedical Materials Research, Part A 85A(2) (2008) 487-497.
[147] Y. Lao, X. Zhang, J. Zhou, W. Su, R. Chen, Y. Wang, W. Zhou, Z.-F. Xu, Characterization and in vitro mineralization function of a soluble protein complex P60 from the nacre of Pinctada fucata, Comparative Biochemistry and Physiology, Part B: Biochemistry & Molecular Biology 148B(2) (2007) 201-208.
[148] X. Wang, S. Liu, L. Xie, R. Zhang, Z. Wang, Pinctada fucata mantle gene 3 (PFMG3) promotes differentiation in mouse osteoblasts (MC3T3-E1), Comparative Biochemistry and Physiology Part B: Biochemistry and Molecular Biology 158(2)

(2011) 173-180.
[149] C. Zhang, R. Zhang, Matrix proteins in the outer shells of molluscs, Marine Biotechnology 8(6) (2006) 572-586.
[150] L.L. Hench, Bioceramics: From Concept to Clinic, Journal of the American Ceramic Society 74(7) (1991) 1487-1510.
[151] L.T. Kuhn, M.D. Grynpas, C.C. Rey, Y. Wu, J.L. Ackerman, M.J. Glimcher, A comparison of the physical and chemical differences between cancellous and cortical bovine bone mineral at two ages, Calcif Tissue Int 83(2) (2008) 146-54.
[152] G. Alper, S. Bernick, M. Yazdi, M.E. Nimni, Osteogenesis in Bone Defects in Rats: The Effects of Hydroxyapatite and Demineralized Bone Matrix, The American Journal of the Medical Sciences 298(6) (1989) 371-376.
[153] J.W. Frame, P.G.J. Rout, R.M. Browne, Human tissue response to porous hydroxyapatite implants. A case report, International Journal of Oral and Maxillofacial Surgery 18(3) (1989) 142-144.
[154] A. Piattelli, G.P. Cordioli, P. Trisi, P. Passi, G.A. Favero, R.M. Meffert, Light and confocal laser scanning microscopic evaluation of hydroxyapatite resorption patterns in medullary and cortical bone, International Journal of Oral & Maxillofacial Implants 8(3) (1993).
[155] J.R. Woodard, A.J. Hilldore, S.K. Lan, C.J. Park, A.W. Morgan, J.A.C. Eurell, S.G. Clark, M.B. Wheeler, R.D. Jamison, A.J. Wagoner Johnson, The mechanical properties and osteoconductivity of hydroxyapatite bone scaffolds with multi-scale porosity, Biomaterials 28(1) (2007) 45-54.
[156] N. Ikeda, K. Kawanabe, T. Nakamura, Quantitative comparison of osteoconduction of porous, dense A–W glass–ceramic and hydroxyapatite granules (effects of granule and pore sizes), Biomaterials 20(12) (1999) 1087-1095.
[157] M. Okumura, H. Ohgushi, S. Tamai, Bonding osteogenesis in coralline hydroxyapatite combined with bone marrow cells, Biomaterials 12(4) (1991) 411-416.
[158] P. Fratzl, R.J.P.i.M.S. Weinkamer, Nature's hierarchical materials, 52(8) (2007) 1263-1334.
[159] J. Hu, Y. Zhou, L. Huang, J. Liu, H. Lu, Effect of nano-hydroxyapatite coating on the osteoinductivity of porous biphasic calcium phosphate ceramics, BMC Musculoskelet Disord 15 (2014) 114.
[160] B. Li, X. Liao, L. Zheng, X. Zhu, Z. Wang, H. Fan, X. Zhang, Effect of nanostructure on osteoinduction of porous biphasic calcium phosphate ceramics, Acta Biomater 8(10) (2012) 3794-804.
[161] F. Chen, W.M. Lam, C.J. Lin, G.X. Qiu, Z.H. Wu, K.D. Luk, W.W. Lu, Biocompatibility of electrophoretical deposition of nanostructured hydroxyapatite coating on roughen titanium surface: in vitro evaluation using mesenchymal stem cells, J Biomed Mater Res B Appl Biomater 82(1) (2007) 183-91.

[162] X. Guo, J.E. Gough, P. Xiao, J. Liu, Z. Shen, Fabrication of nanostructured hydroxyapatite and analysis of human osteoblastic cellular response, J Biomed Mater Res A 82(4) (2007) 1022-32.
[163] Z. Shi, X. Huang, Y. Cai, R. Tang, D. Yang, Size effect of hydroxyapatite nanoparticles on proliferation and apoptosis of osteoblast-like cells, Acta Biomater 5(1) (2009) 338-45.
[164] T.J. Webster, C. Ergun, R.H. Doremus, R.W. Siegel, R. Bizios, Enhanced functions of osteoblasts on nanophase ceramics, Biomaterials 21(17) (2000) 1803-10.
[165] T.J. Webster, C. Ergun, R.H. Doremus, R.W. Siegel, R. Bizios, Enhanced osteoclast-like cell functions on nanophase ceramics, Biomaterials 22(11) (2001) 1327-33.
[166] M. Zandi, H. Mirzadeh, C. Mayer, H. Urch, M.B. Eslaminejad, F. Bagheri, H. Mivehchi, Biocompatibility evaluation of nano-rod hydroxyapatite/gelatin coated with nano-HAp as a novel scaffold using mesenchymal stem cells, J Biomed Mater Res A 92(4) (2010) 1244-55.
[167] H. Wang, Y. Li, Y. Zuo, J. Li, S. Ma, L. Cheng, Biocompatibility and osteogenesis of biomimetic nano-hydroxyapatite/polyamide composite scaffolds for bone tissue engineering, Biomaterials 28(22) (2007) 3338-48.
[168] O. Brown, M. McAfee, S. Clarke, F. Buchanan, Sintering of biphasic calcium phosphates, J Mater Sci Mater Med 21(8) (2010) 2271-9.
[169] J.W. Jang, J.H. Yun, K.I. Lee, J.W. Jang, U.W. Jung, C.S. Kim, S.H. Choi, K.S. Cho, Osteoinductive activity of biphasic calcium phosphate with different rhBMP-2 doses in rats, Oral Surg Oral Med Oral Pathol Oral Radiol 113(4) (2012) 480-7.
[170] G. Spence, N. Patel, R. Brooks, N. Rushton, Carbonate substituted hydroxyapatite: resorption by osteoclasts modifies the osteoblastic response, Journal of biomedical materials research. Part A 90(1) (2009) 217-224.
[171] J. Vuola, H. Göransson, T. Böhling, S. Asko-Seljavaara, Bone marrow induced osteogenesis in hydroxyapatite and calcium carbonate implants, Biomaterials 17(18) (1996) 1761-1766.
[172] M. Ainola, Pannus invasion into cartilage and bone in rheumatoid arthritis, 2018.
[173] M. Hasegawa, Y. Doi, A. Uchida, Cell-mediated bioresorption of sintered carbonate apatite in rabbits, The Journal of bone and joint surgery: British volume 85(1) (2003) 142-147.

CHAPTER 2 : PEGYLATED OSTEOGENIC GROWTH FACTORS INITIATE MINERALIZATION IN ACELLULAR ENVIRONMENTS

2.1 Introduction

The formation of bone is a complex sequence of events involving both cell- and protein-mediated processes. In general, it involves the cell-guided development of a protein-based organic matrix followed by cellular deposition of osteoid, which crystallizes on the matrix in a manner controlled by the comprising proteins. Many proteins and growth factors play a role in bone formation. Some of these proteins stimulate cellular activity while others provide a template for the nucleation of bone mineral crystals. BMP-2, for instance, is known to induce differentiation in precursor cells toward the osteoblast lineage but has not been shown to nucleate calcium from solution.[1] BSP, on the other hand, has been shown to readily nucleate and self-assemble apatite (calcium phosphate) crystals in solution.[2] The water-soluble matrix (WSM) of nacre has been shown to nucleate and self-assemble aragonite (calcium carbonate) crystals in solution as well as to play a significant role in osteogenic response.[3, 4] The nacre-derived peptide, n16N, has also been shown to nucleate calcium from solution, but does not appear to induce osteogenesis.[5] Thus, although headway has been made in determining which proteins are “osteonucleators” and which are osteoinductors, little data exists to

elucidate any relationship between acellular mineralization and osteogenic activity, and few studies have directly compared the two processes. This relationship between cell- and protein-mediated processes may hold significance in the understanding of microspatial control of bone tissue formation.

Approaches to harness microspatial control involve incorporating osteogenic and/or osteonucleating proteins into biomaterials. Poly(ethylene glycol) (PEG) is a hydrophilic, bioinert polymer (Figure 2.1) that is easily modified to fit numerous biomedical engineering applications in both tissue engineering and drug delivery. In particular, PEG can be covalently attached to proteins, peptides, and other small molecules, and these in turn can be incorporated into a larger PEG hydrogel, thus "functionalizing" an otherwise inert hydrogel.[6, 7] Such functionalized PEG hydrogel networks have been shown to exhibit high affinities for therapeutics, which enables control of the presentation and release of the therapeutics, both *in vitro* and *in vivo*.[6, 8] PEG has also been used to covalently modify and completely immobilize growth factors and therapeutics on and within various substrates ranging from PEG and other hydrogel networks to glass surfaces.[7, 9] Although moieties covalently bound to PEG have been used to guide angiogenesis and cell-mediated biomaterial degradation, spatial control over mineralization using PEGylated molecules has been accomplished by restricting osteoprogenitor cell

access to attachment sites like RGDS rather than by PEGylating osteogenic proteins in specified patterns.[10-13] In short, attachment sites were patterned, not mineralization sites. This work aims to demonstrate that PEGylated growth factors are capable of organizing mineral formation when immobilized onto substrates.

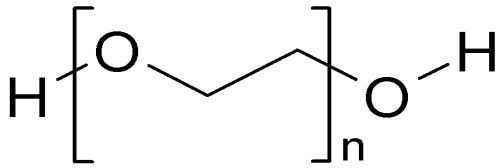

Figure 2.1: Poly(ethylene glycol) (PEG) chemical structure

2.2 Materials and Methods

2.2.1 Extraction of Nacre Water-soluble Matrix

The shells of the giant oyster Pinctada maxima were obtained from the Phillipines. The inner nacreous layer of the shells was stripped from the outer calcite layer using a tungsten carbide drill bit. The resulting powder (50 g) was sterilized via dry heat (170^{o}C, 1 h) to eliminate contamination. The sterile powder was then immediately placed into a sterile container with 100 mL cold ultrapure water (~18 MΩ-cm) and stirred under refrigeration for four days. Afterward, the slurry was transferred into 50 mL conical centrifuge tubes and centrifuged at 3700 g for 20 minutes. The supernatant was then transferred into clean conical tubes and

lyophilized until dry and stored at -20ºC. The resulting material was then weighed and used as-is, designated as nacre WSM (water soluble matrix).

2.2.2 Synthesis of PEGylated proteins and peptides

Nacre proteins were extracted as described above. BMP-2 (Life Technologies Cat# PHC7141), BSP, DMP-1 (Life Technologies, 11929H08H50), and the synthetic cell adherent peptide RGDS (MedChemExpress, HY12290) were purchased and used as received. The synthesis of the aragonite-nucleating nacre-derived peptide, n16N[5] (Biomatik, custom order), was outsourced and used as received. Proteins were PEGylated by combining them with Acrylate-PEG-succinimidyl valerate (SVA) in HEPES buffered saline (HBS, pH 8.5) at a 20:1 PEG-SVA:protein molar ratio for BMP-2, a 16:1 molar ratio for BSP, a 21:1 molar ratio for DMP-1, a 5:1 molar ratio for n16N, and a 100:1 PEG-SVA:nacre WSM weight ratio. The molar stoichiometric amounts are relative to the number of primary amine residues in the protein sequence. The ratios for WSM and n16N were selected to ensure excess PEG-SVA would be present for the reaction.

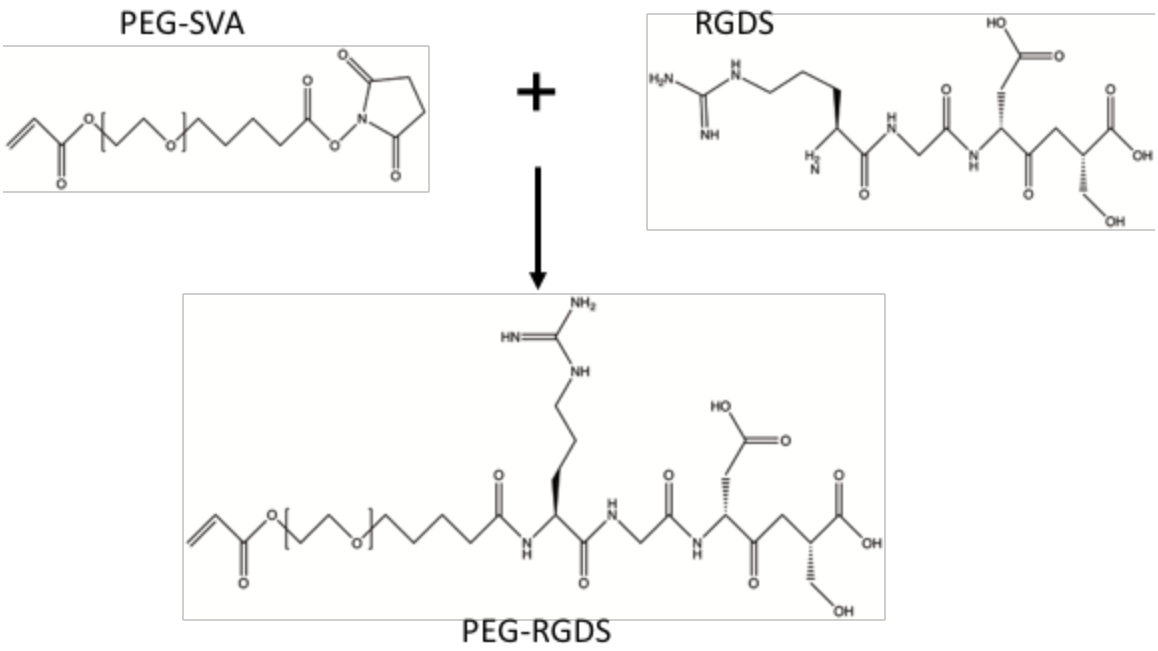

Figure 2.2: Schematic of reaction between Acrylate-PEG-SVA and RGDS.

2.2.3 Confirmation of Protein Conjugation

Protein-PEG conjugation was confirmed using the ninhydrin assay for free amines. Ninhydrin reacts with free amines to form a purple dye called Ruhemann's purple. This purple reaction product is used in a colorimetric assay to measure the total available free amines in a given peptide or protein sample. After reacting the proteins and peptides with acrylate-PEG-SVA, samples were lyophilized to dryness and reconstituted in 100 µL phosphate buffered saline (PBS, pH 7.4). The solutions were then separately added to 100 µL sodium citrate buffer (pH 5.0) and 200 µL ninhydrin solution (2%) in low protein binding microcentrifuge tubes. The tubes were heated to >95^{O}C for 15 minutes to facilitate

the reaction. The absorbance was then read at 570 nm. Standard curves for all proteins and peptides were prepared using known concentrations of each. The conjugation efficiency was reported as the quotient of occupied amines post conjugation to available amines pre-conjugation.

2.2.4 Synthesis of Surface-immobilized Protein Substrate

Nucleation capacity was tested on glass slides coated with proteins. The nucleation protocol was adapted from He et al.[14, 15] The glass slides were cleaned in an acidic mixture of concentrated hydrochloric acid (HCl, 22.5%) and nitric acid (HNO_3, 7.5%) to remove any residual biological contaminates and to condition the slides for subsequent adsorption steps. The slides were placed into the acid mixture and subjected to sonication (50 kHz) for 1 hour at 60°C. The slides were then washed in ultrapure water five times. Each wash lasted 1 minute under sonication. The washed slides were placed into a HEPA-filtered incubator overnight to dry. The slides were then coated with proteins by placing 50 μL protein solution (0.2 mg/mL in ultrapure water) onto the surface of the glass slides. The slides were again allowed to dry overnight for protein deposition, after which they were washed twice in cold ultrapure water to remove excess and unadsorbed proteins.

PEGylated proteins were immobilized on the glass slides via photoconjugation reaction. Slides were cleaned in concentrated HCl/HNO_3 as described above. The clean slides were then acrylated using 3-(trimethoxysilyl)propyl acrylate to permit conjugation of PEGylated proteins. 3-(trimethoxysilyl)propyl acrylate was dissolved in chloroform at 0.1% by volume. The slides were coated with 50 μL of the acrylate solution pipetted onto the surface of the glass slide. Care was taken to completely cover the surface. The slides were then dried overnight in a HEPA-filtered environment. Once dry, a thin acrylate film could be seen on the surface of the slide. The slides were washed twice in cold ultrapure water to remove excess acrylate. Once washed and dried, no film was visible to the naked eye on the glass surface. Further, the absence of film was confirmed via light and electron microscopy, indicating that only adsorbed acrylate groups were present and that a poly acrylated surface did not form. After the acrylated slides were dry, they were coated with 50 μL PEGylated protein solution (2 mg protein equivalent per mL ultrapure water), taking care to cover the entire slide to facilitate homogenous distribution of protein. The slides were exposed to white light for 1 minute to facilitate surface conjugation via photo-initiated acrylate coupling between the PEGylated proteins and the acrylated slide surface. The protein-conjugated slides were then washed twice with cold ultrapure water to remove unbound proteins.

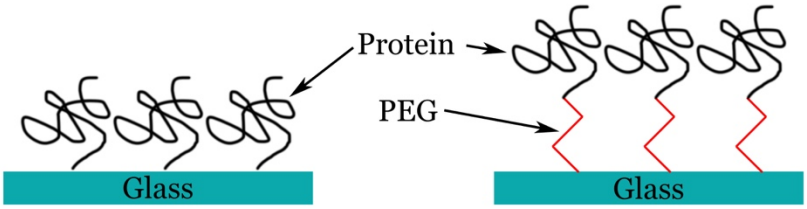

Figure 2.3: Schematic of protein-adsorbed vs. PEGylated protein glass slides. Proteins were directly adsorbed to clean glass slides or immobilized to acrylated slides via a PEG linker.

2.2.5 Acellular Mineralization

The slides containing surface-adsorbed and surface-conjugated proteins were placed into the center of a modified horizontal electrophoresis chamber such that a thin film of buffer would form over the slides once the chamber was filled (Figure 2.4). The anode chamber was filled with a calcium buffer (165 mM NaCl, 10 mM HEPES, 2.5 mM $CaCl_2$, pH 7.4) and the cathode chamber was filled with phosphate buffer (165 mM NaCl, 10 mM HEPES, 1 mM KH_2PO_4, pH 7.4). The thin film of buffer allowed the ions to move freely across the surface of the slides, where the proteins could facilitate Ca/P binding. An external 10 mA current was applied to prevent non-specific mineral nucleation. The buffer was changed twice per day to maintain pH and ion concentration. After 3 days, the slides were removed from the buffer and washed once in cold water to remove any residual buffer. The slides were then dried under vacuum and sputter coated with gold (10 nm) before

imaging on a Zeiss Sigma Field Emission SEM equipped with an Oxford INCA PentaFETx3 EDS system.

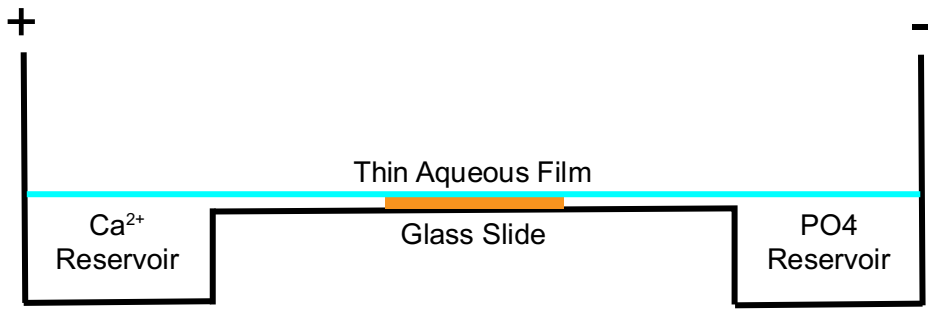

Figure 2.4: Illustration of electrophoresis chamber for mineral nucleation over glass slides.

2.2.6 Characterization of Acellular Mineralization

The resulting FE-SEM images were analyzed via ImageJ software. The images were first thresholded to remove the background and converted to black and white. The images were then analyzed for particle sizes >1 μm. The resulting particle analysis was then used to calculate the total mineralized area of each slide and the average particle size.

2.2.7 Statistical Analysis

Conjugation efficiency, total area of mineralization, nodule size, submicron particle counts, and total area of submicron particles, were compared between the different protein or peptide groups using an analysis of variance (ANOVA). Following ANOVA,

pairwise comparisons between groups was performed using a Tukey-Kramer HSD (honestly significant difference) post-hoc analysis. *p* Values less than 0.05 were considered significant and analyses were conducted using Microsoft Excel. Statistical significance is indicated by asterisks in the figures or figure legends, which are reported as graphs of mean ± standard deviation.

2.3 Results

2.3.1 Nacre Protein Extraction

After lyophilization, 0.072 g nacre WSM was collected from 50 g powdered nacre. The dry protein was white in color and readily dissolved when reconstituted in aqueous medium.

2.3.2 Confirmation of PEGylation

The ninhydrin assay indicated that between 10 and 20 percent conjugation of free amines were achieved for all protein samples. The conjugation efficiencies were observed to be 18.3 ± 5.1 percent, 15.4 ± 7.0 percent, 17.2 ± 7.7 percent, and 12.4 ± 9.7 percent for BMP-2, BSP, DMP1, and WSM, respectively (Figure 2.3). The conjugation efficiencies of the peptides were higher than that of the proteins. The conjugation efficiency of free amines in n16N was greater at 30.9 ± 2.9 percent. This is likely due to less steric interference as the molecular weight of n16N is significantly lower than that of the full proteins. The conjugation efficiency of free

amines in RGDS was observed to be 90.1 ± 4.1 percent. As RGDS only constitutes four amino acid residues, steric interference of the reaction site is expected to be much lower than that of any of the other proteins or peptide, thus resulting in a much higher reaction efficiency. Additionally, RGDS has only one primary amine at the N-terminal, resulting in a much more predictable reaction with comparable efficiencies reported in the literature.[16]

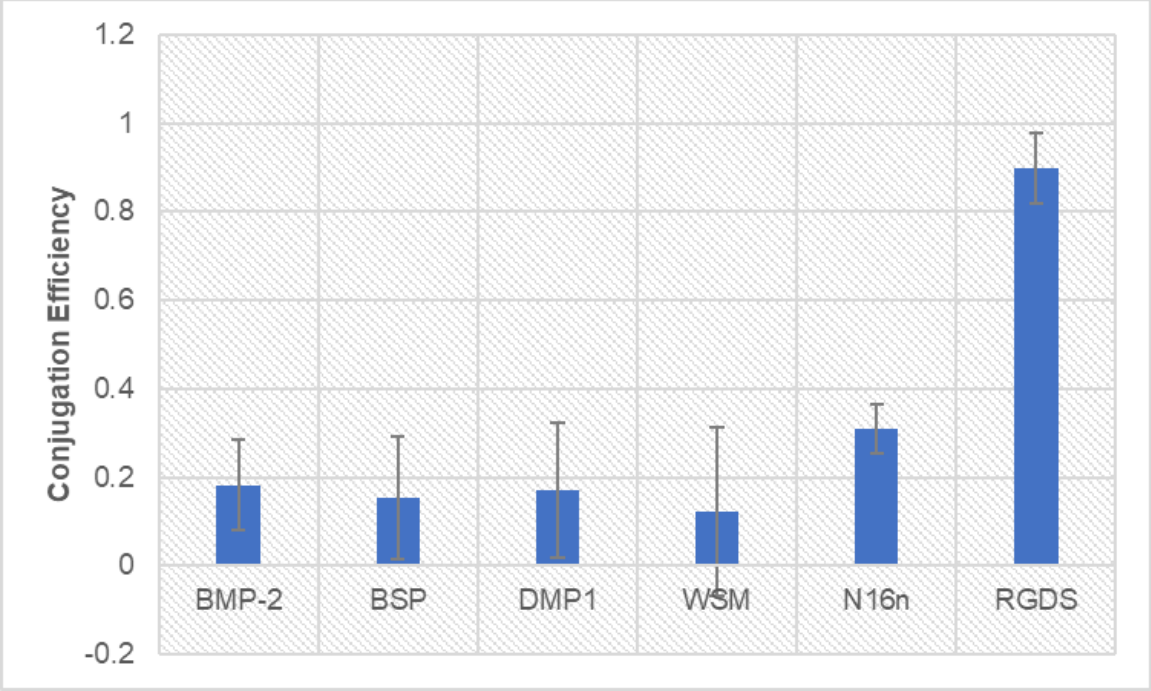

Figure 2.5: Conjugation efficiency of PEG-SVA to free amines in each protein/peptide. Error bars represent standard deviation in triplicate samples.

2.3.3 FE-SEM Visualization of Acellular Mineralization

FE-SEM images of the protein-adsorbed slides post-nucleation showed surface features consistent with calcium phosphate mineralization (Figure 2.6). Additionally, increased mineralization was observed for all proteins compared to negative control slides. PEGylated BMP-2, BSP, and WSM also appeared to induce acellular mineralization. In contrast, no mineralization occurred in any PEGylated DMP1 samples. FE-SEM images of PEG-WSM taken before mineralization assays indicated that acrylation and protein conjugation caused no change in surface features on the glass slides, suggesting that any changes were due to mineralization.

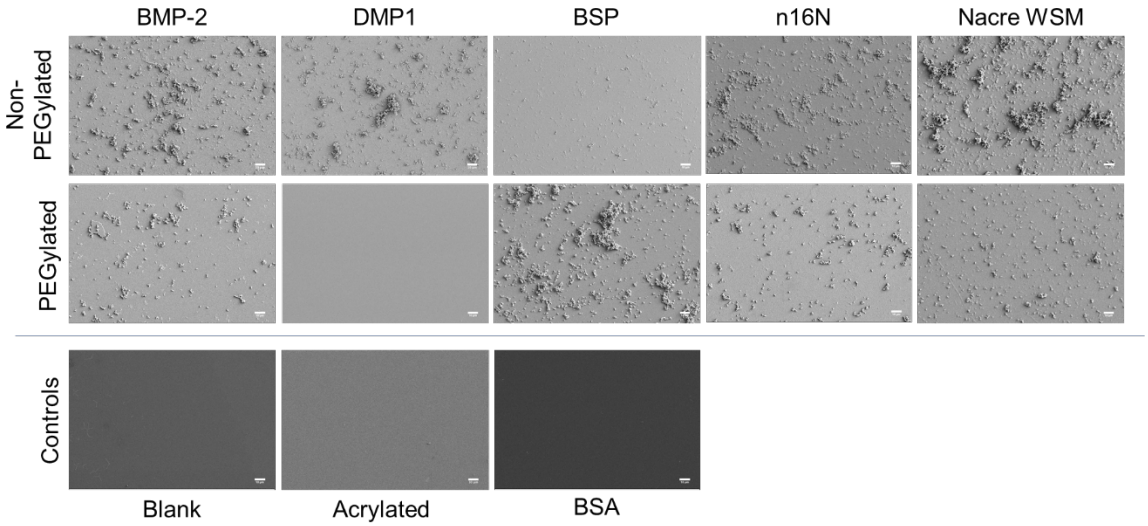

Figure 2.6: FE-SEM images of glass slides coated in PEGylated and non-PEGylated proteins or peptides. Scale bars are 10 μm.

Particle analysis was performed using ImageJ software (Figure 2.7). The PEGylated BSP slides showed the highest average total mineralization area, but all non-PEGylated samples were comparable to one another (Figure 2.8). PEGylated samples, however, showed greater variance. No mineralization was observed in PEGylated DMP1 samples. Conjugation of BMP-2 and n16N showed decreased mineralization compared to their non-PEGylated counterparts. Both PEGylated BSP and WSM samples showed similar or slightly increased mineralization area compared to non-PEGylated BSP and WSM, respectively. PEGylation and immobilization appeared to increase nodule size in BMP-2 and BSP samples but decreased average nodule size in WSM and n16N samples with the PEGylation of n16N resulting in significantly decreased average size compared to non-Pegylated n16N (Figure 2.9).

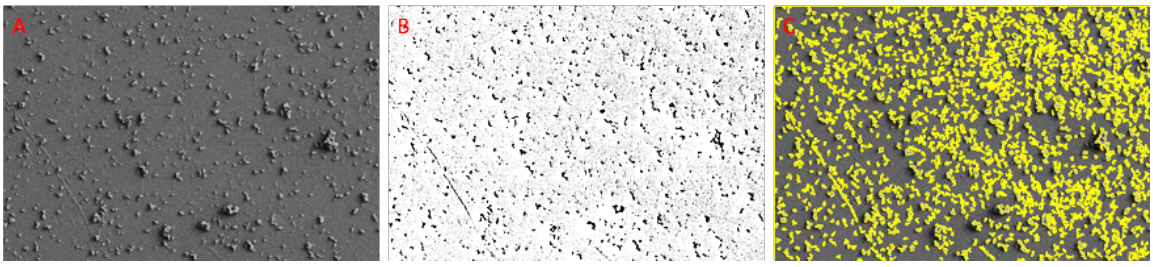

Figure 2.7: ImageJ particle analysis on slides coated with PEG-WSM. The raw FE-SEM images (A) were first thresholded to remove background features and color (B). Particles were then highlighted, counted, and characterized using the software's particle analysis tool (C).

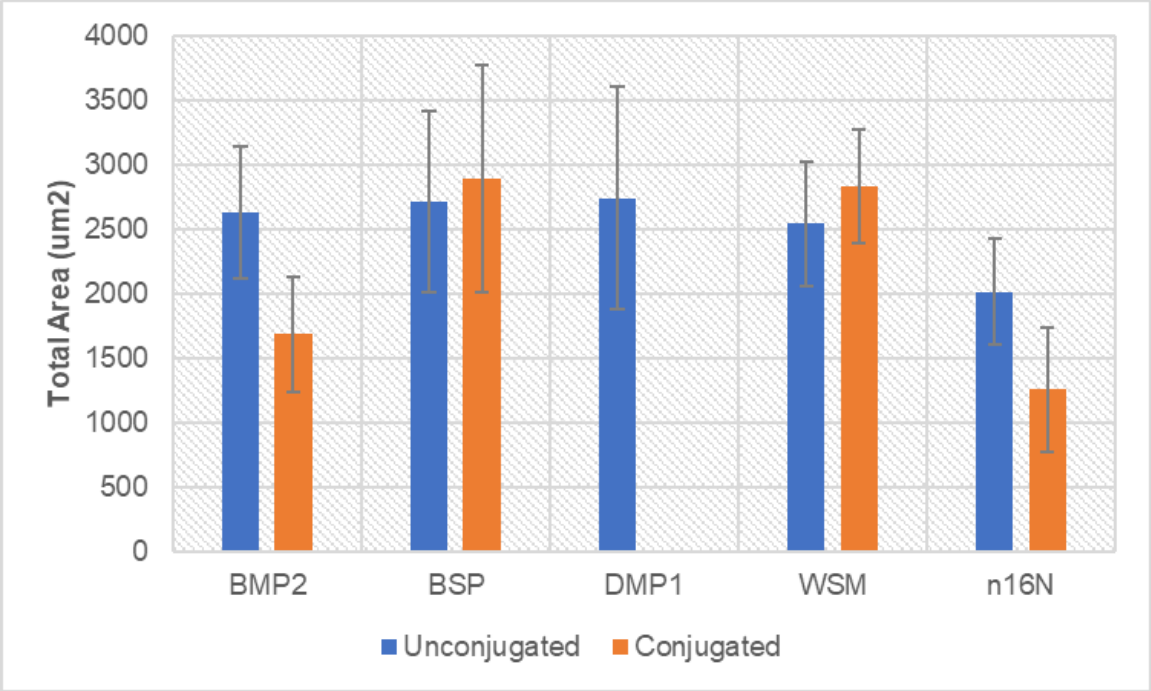

Figure 2.8: Average total area of mineralization calculated from FE-SEM images. Error bars represent the standard deviation. Note: No mineralization observed in PEGylated DMP1 samples.

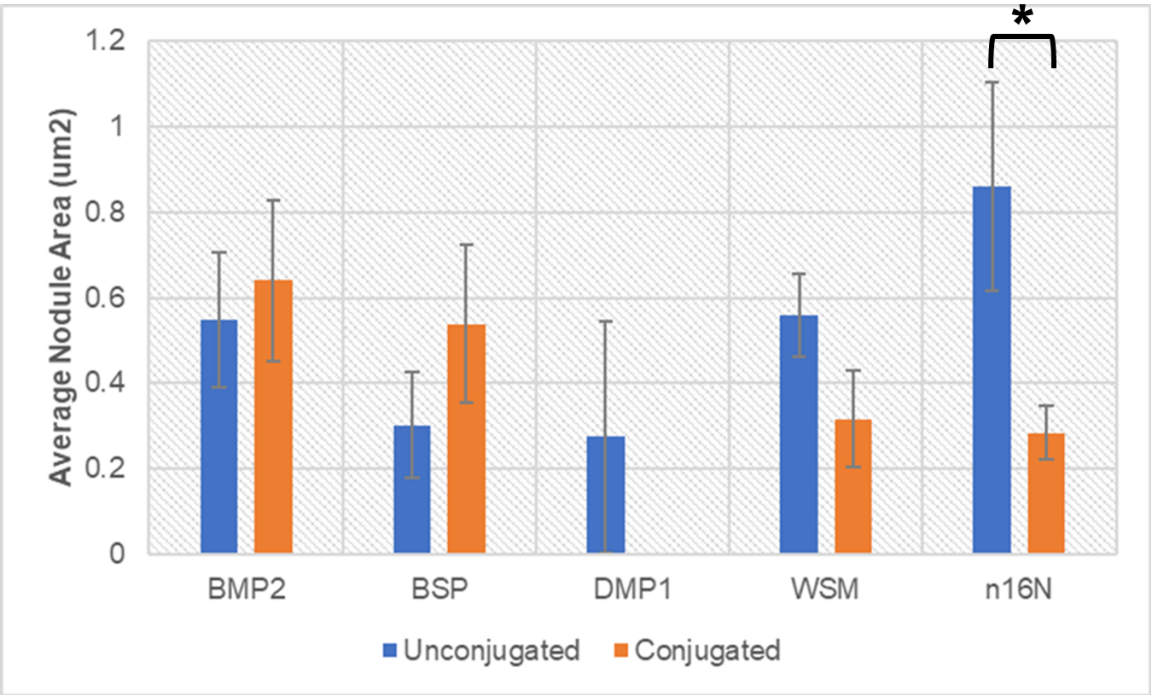

Figure 2.9: Average nodule size for PEGylated and non-PEGylated proteins. Error bars show standard deviation. Asterisks denote significant difference between indicated samples ($p < 0.05$). Note: No mineralization observed in PEGylated DMP1 samples.

Higher magnification revealed submicron features on the PEGylated WSM slides (Figure 2.10). No such features were present on the PEGylated BMP-2 slides (Figure 2.10D). When thresholding was bound at a maximum particle size of 1 μm^2, a particle count confirmed this observation (Figure 2.11), as did an assessment of the total area of submicron particles observed (Figure 2.12). Further analysis reveals that PEGylation of WSM and n16N, a peptide derived from WSM,

increases the occurrence of sub-micron features whereas PEGylation of the other proteins tested resulted in the decreased presence of these features relative to their non-PEGylated counterparts.

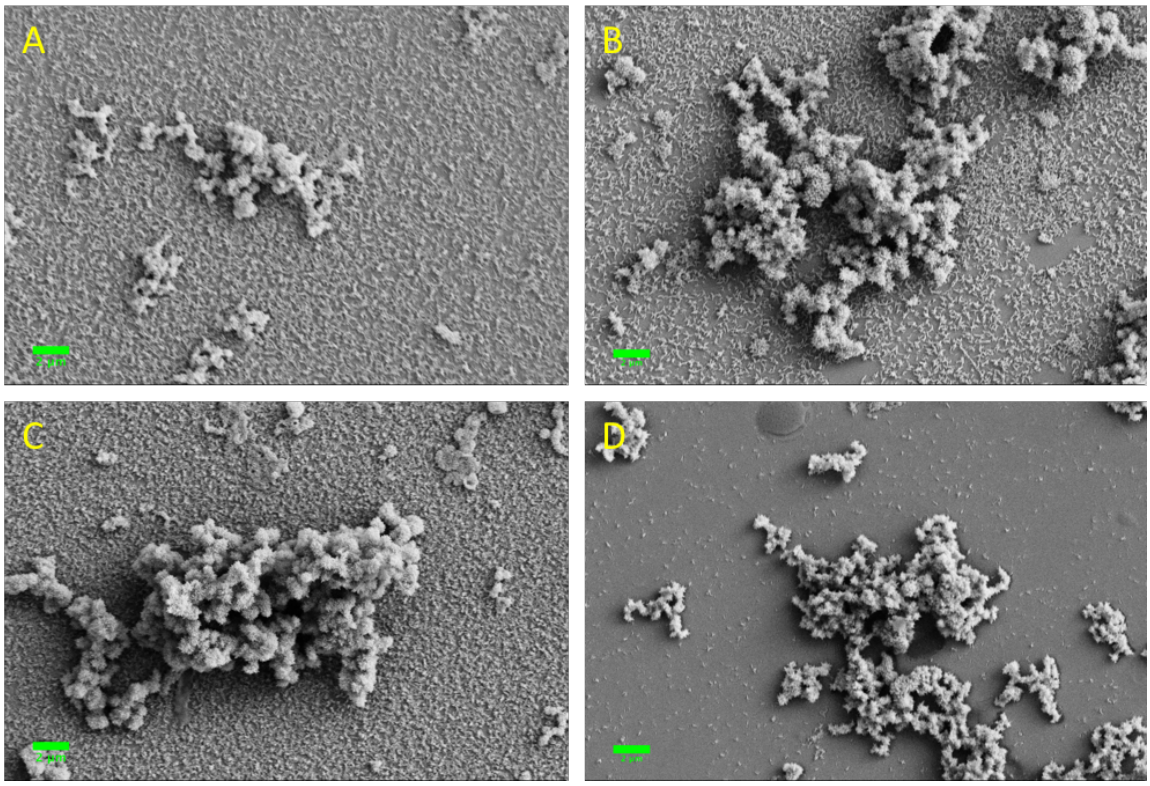

Figure 2.10: FE-SEM images at 10,000X magnification of slides coated with A) WSM, B) PEG-WSM, C) BMP-2, AND D) PEG-BMP-2. Mineralization features below 1 μm can be seen as a "dusting of snow" in both non-PEGylated proteins BMP-2 and WSM. PEGylation inhibits this type of mineralization in BMP-2 but not in WSM as they are present in the PEG-WSM slide but not on the PEG-BMP-2 slide.

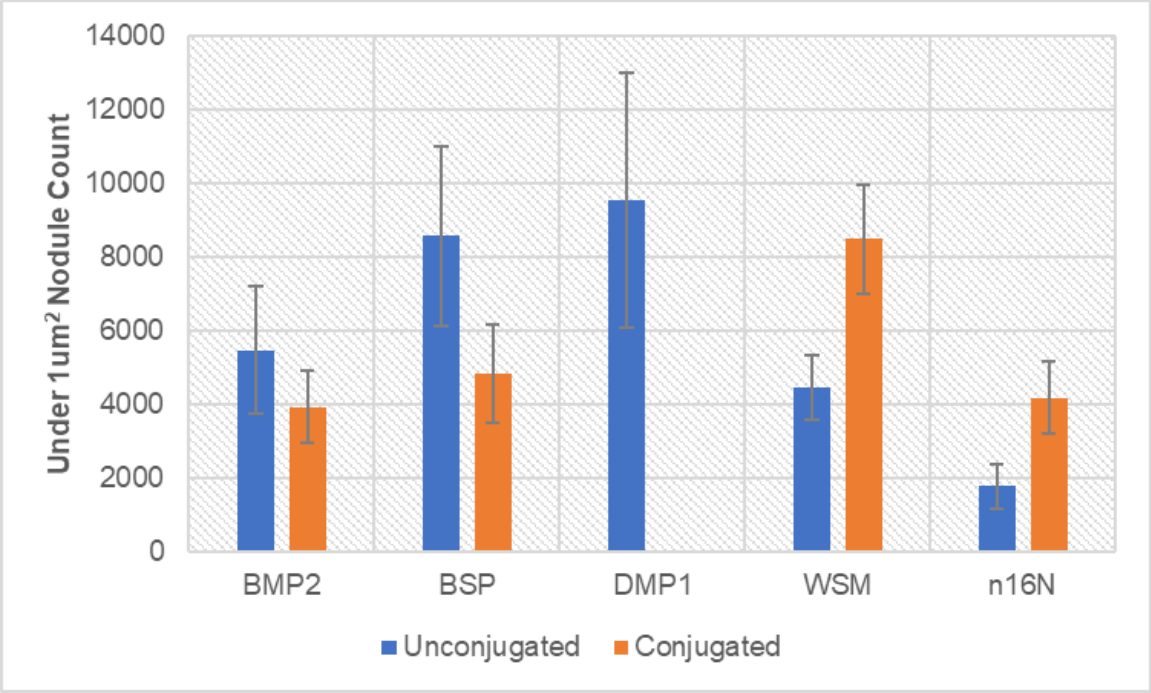

Figure 2.11: Number of sub-1µm particles counted in FE-SEM images. Error bars represent the standard deviation. Note: No mineralization observed in PEGylated DMP1 samples.

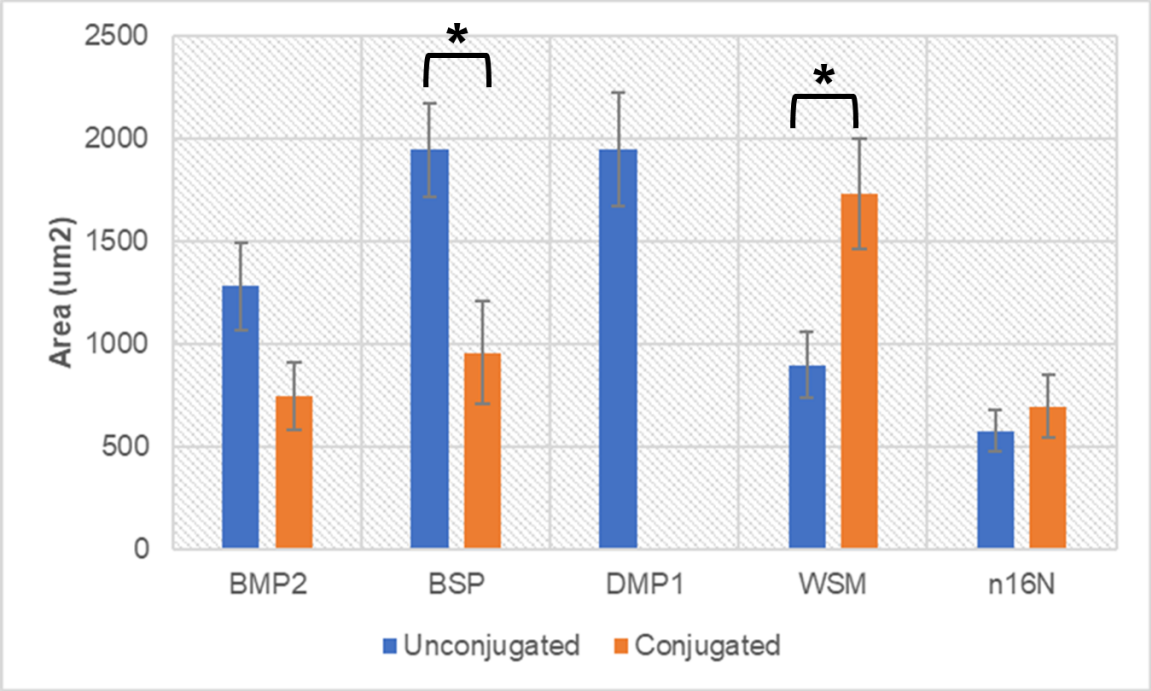

Figure 2.12: Total area of submicron particles in FE-SEM images of acellular mineralization. Error bars represent the standard deviation. Asterisks denote significant difference between indicated samples ($p < 0.05$). Note: No mineralization observed in PEGylated DMP1 samples.

2.4 Discussion

The lack of acellular mineralization altogether in the PEG-DMP1 samples may be the result of excessive modification to the protein structure or via steric hindrance due to the presence of PEG. This method of PEGylation binds PEG to free primary and secondary amines. The presence of multiple amine-containing residues means that any number of these sites may be PEGylated and used to bind the protein to

the substrate in multiple orientations relative to one another. Some PEG binding sites may also interfere with calcium binding sites due to a reorganization of the protein structure during PEG conjugation.[17]

The elevated presence of submicron features in acellular mineralization of PEG-WSM is particularly interesting, especially when compared to the other commonly studied osteogenic growth factors. For instance, BMP-2 is known to be a powerful osteogenic agent, and our results show that it is capable of nucleating an abundance of submicron minerals. The fact that PEGylated BMP-2 loses this ability may explain the decreased osteogenic activity that has been reported for PEGylated BMP-2,[18] thus diminishing its potential use within biomaterials. Conversely, PEGylated WSM does not suffer a loss in its capacity to form submicron minerals. If nothing else, these features offer an abundance of nucleation sites, which should translate to more mineralization in PEG-WSM groups than in other PEGylated osteogenic proteins. This was indeed the case, as PEGylated WSM showed comparable mineralization to both non-PEGylated BMP-2 and WSM. Since PEGylation can interfere with protein function, the ubiquitous nature of these features coupled with a lower average nodule size than other PEGylated growth factors suggests that PEGylated WSM may be able to act on a more therapeutically relevant spatial scale than the other PEGylated proteins. If

coupled with a sufficient targeting motif, PEG-WSM may be a promising therapeutic candidate for bone tissue engineering, fracture repair, or perhaps even the treatment of chronic bone diseases such osteoporosis via targeted micro remodeling.

2.5 References

[1] J. Almodovar, R. Guillot, C. Monge, J. Vollaire, S. Selimovic, J.-L. Coll, A. Khademhosseini, C. Picart, Spatial patterning of BMP-2 and BMP-7 on biopolymeric films and the guidance of muscle cell fate, Biomaterials 35(13) (2014) 3975-3985.
[2] G.K. Hunter, H.A. Goldberg, Nucleation of hydroxyapatite by bone sialoprotein, Proceedings of the National Academy of Sciences of the United States of America 90(18) (1993) 8562-8565.
[3] M. Rousseau, L. Pereira-Mouries, M.-J. Almeida, C. Milet, E. Lopez, The water-soluble matrix fraction from the nacre of Pinctada maxima produces earlier mineralization of MC3T3-E1 mouse pre-osteoblasts, Comparative Biochemistry and Physiology, Part B: Biochemistry & Molecular Biology 135B(1) (2003) 1-7.
[4] J.-j. Wang, J.-t. Chen, C.-l. Yang, Effects of soluble matrix of nacre on bone morphogenetic protein-2 and Cbfa1 gene expressions in rabbit marrow mesenchymal stem cells, Nanfang Yike Daxue Xuebao 27(12) (2007) 1838-1840.
[5] R.A. Metzler, J.S. Evans, C.E. Killian, D. Zhou, T.H. Churchill, N.P. Appathurai, S.N. Coppersmith, P.U.P.A. Gilbert, Nacre Protein Fragment Templates Lamellar Aragonite Growth, Journal of the American Chemical Society 132(18) (2010) 6329-6334.
[6] A. Kolate, D. Baradia, S. Patil, I. Vhora, G. Kore, A. Misra, PEG - A versatile conjugating ligand for drugs and drug delivery systems, Journal of Controlled Release 192 (2014) 67-81.
[7] H.-W. Liu, C.-H. Chen, C.-L. Tsai, I.H. Lin, G.-H. Hsiue, Heterobifunctional poly(ethylene glycol)-tethered bone morphogenetic protein-2-stimulated bone marrow mesenchymal stromal cell differentiation and osteogenesis, Tissue engineering 13(5) (2007) 1113-1124.
[8] M.O. Ronke, W.L. ZaWaunyka, L.F. Christy, A.H. Mary, K. Sun Kuk, M.S.-M. Eva, A.H. John, R.D. Alan, A.O.-D. Elizabeth, L.W. Jennifer, Hydrogel

Microsphere Encapsulation of a Cell-Based Gene Therapy System Increases Cell Survival of Injected Cells, Transgene Expression, and Bone Volume in a Model of Heterotopic Ossification, Tissue Engineering Part A 16(12) (2010) 3727-3736.
[9] X. He, J. Ma, E. Jabbari, Effect of Grafting RGD and BMP-2 Protein-Derived Peptides to a Hydrogel Substrate on Osteogenic Differentiation of Marrow Stromal Cells, Langmuir 24(21) (2008) 12508-12516.
[10] J.E. Leslie-Barbick, C. Shen, C. Chen, J.L. West, Micron-Scale Spatially Patterned, Covalently Immobilized Vascular Endothelial Growth Factor on Hydrogels Accelerates Endothelial Tubulogenesis and Increases Cellular Angiogenic Responses, Tissue Engineering, Part A 17(1-2) (2011) 221-229.
[11] G.M. Cooper, E.D. Miller, G.E. De Cesare, A. Usas, E.L. Lensie, M.R. Bykowski, J. Huard, L.E. Weiss, J.E. Losee, P.G. Campbell, Inkjet-Based Biopatterning of Bone Morphogenetic Protein-2 to Spatially Control Calvarial Bone Formation, Tissue Engineering, Part A 16(5) (2010) 1749-1759.
[12] S. Herberg, G. Kondrikova, S. Periyasamy-Thandavan, R.N. Howie, M.E. Elsalanty, L. Weiss, P. Campbell, W.D. Hill, J.J. Cray, Inkjet-based biopatterning of SDF-1Î² augments BMP-2-induced repair of critical size calvarial bone defects in mice, Bone (New York, NY, United States) 67 (2014) 95-103.
[13] O.F. Zouani, C. Chollet, B. Guillotin, M.-C. Durrieu, Differentiation of pre-osteoblast cells on poly(ethylene terephthalate) grafted with RGD and/or BMPs mimetic peptides, Biomaterials 31(32) (2010) 8245-8253.
[14] G. He, T. Dahl, A. Veis, A. George, Nucleation of apatite crystals in vitro by self-assembled dentin matrix protein 1, Nature Materials 2(8) (2003) 552-558.
[15] G. He, T. Dahl, A. Veis, A. George, Dentin Matrix Protein 1 Initiates Hydroxyapatite Formation In Vitro, Connective tissue research 44(Suppl. 1) (2003) 240-245.
[16] C. Nazli, T.I. Ergenc, Y. Yar, H.Y. Acar, S. Kizilel, RGDS-functionalized polyethylene glycol hydrogel-coated magnetic iron oxide nanoparticles enhance specific intracellular uptake by HeLa cells, International journal of nanomedicine 7 (2012) 1903-1920.
[17] A. Gericke, C. Qin, Y. Sun, R. Redfern, D. Redfern, Y. Fujimoto, H. Taleb, W.T. Butler, A.L. Boskey, Different forms of DMP1 play distinct roles in mineralization, Journal of dental research 89(4) (2010) 355-359.
[18] H. Uludag, D. D'Augusta, J. Golden, J. Li, G. Timony, R. Riedel, J.M. Wozney, Implantation of recombinant human bone morphogenetic proteins with biomaterial carriers: A correlation between protein pharmacokinetics and osteoinduction in the rat ectopic model, 50(2) (2000) 227-238.

CHAPTER 3 : PEGYLATED OSTEOGENIC GROWTH FACTORS INDUCE OSTEOGENIC RESPONSE IN TWO- AND THREE-DIMENSIONAL CELL CULTURE

3.1 Introduction

In order to probe the relationship between mineral nucleation and osteoinduction, the ability of proteins and/or peptides to induce both must be examined. Thus, the mineralization experiments that characterized the nucleation capacity of the proteins must be adapted for cell-mediated biomineralization to determine the osteogenic capacity of the proteins. Therefore, the ultimate goal of this chapter is to assess cellular osteogenesis induced by PEG-conjugated proteins when they are immobilized on (2D) and within (3D) biocompatible substrates.

Many diseases and conditions disrupt bone tissue formation by altering one or more steps in the normal tissue formation process. Additionally, medical interventions and treatments for such diseases may have the side effect of impeding certain steps in this process. For instance, bisphosphonates, which are used in the treatment of osteoporosis, slow osteoclast activity to prevent the formation of pits and pores within bone that characterize the disease.[1, 2] However, this has the unintentional side effect of interrupting the natural

remodeling process entirely, as bone remodeling is cyclical, and osteoblast activity requires signaling factors left by osteoclasts to identify remodeling sites.[3] This side effect has resulted in a new class of mid-femur fractures that had not been previously encountered.[4-6] Thus, there is a need for anabolic therapeutics and materials that promote osteogenesis rather than impede bone remodeling as a whole, either to be used alone or administered concurrently with existing bisphosphonate treatments.[7]

Currently, the only FDA-approved anabolic treatment is a synthetic parathyroid hormone (PTH) marketed under the trade name Teriparatide™.[8] PTH has been shown to stimulate osteoblast mineralization *in vitro* and *in vivo* and has improved bone density in clinical trials.[9-12] However, this treatment is limited to intermittent systemic application for the treatment of the osteoporosis itself and thus is not suitable for localized bone tissue engineering applications.[13, 14] Additionally, Teriparatide™ has been linked to the development of osteosarcoma.[15] Aside from the obvious contraindication in patients at risk for cancer, this limits the approved treatment period to two years.

As the physiological processes that produce bone *in vivo* involves and indeed requires the presence of cellular processes in order to produce mature bone tissue

(Figure 3.1), the PEG-conjugated osteogenic factors presented in Chapter 2 must be assessed for their ability to induce osteogenesis in the presence of cells. BMP-2, BSP, and DMP1 have been shown to induce osteogenic differentiation in bone mesenchymal stem cells.[16-18] The experiments described in this chapter are designed to determine whether these proteins, once PEGylated, are still capable of osteoinduction in 2D and 3D environments.

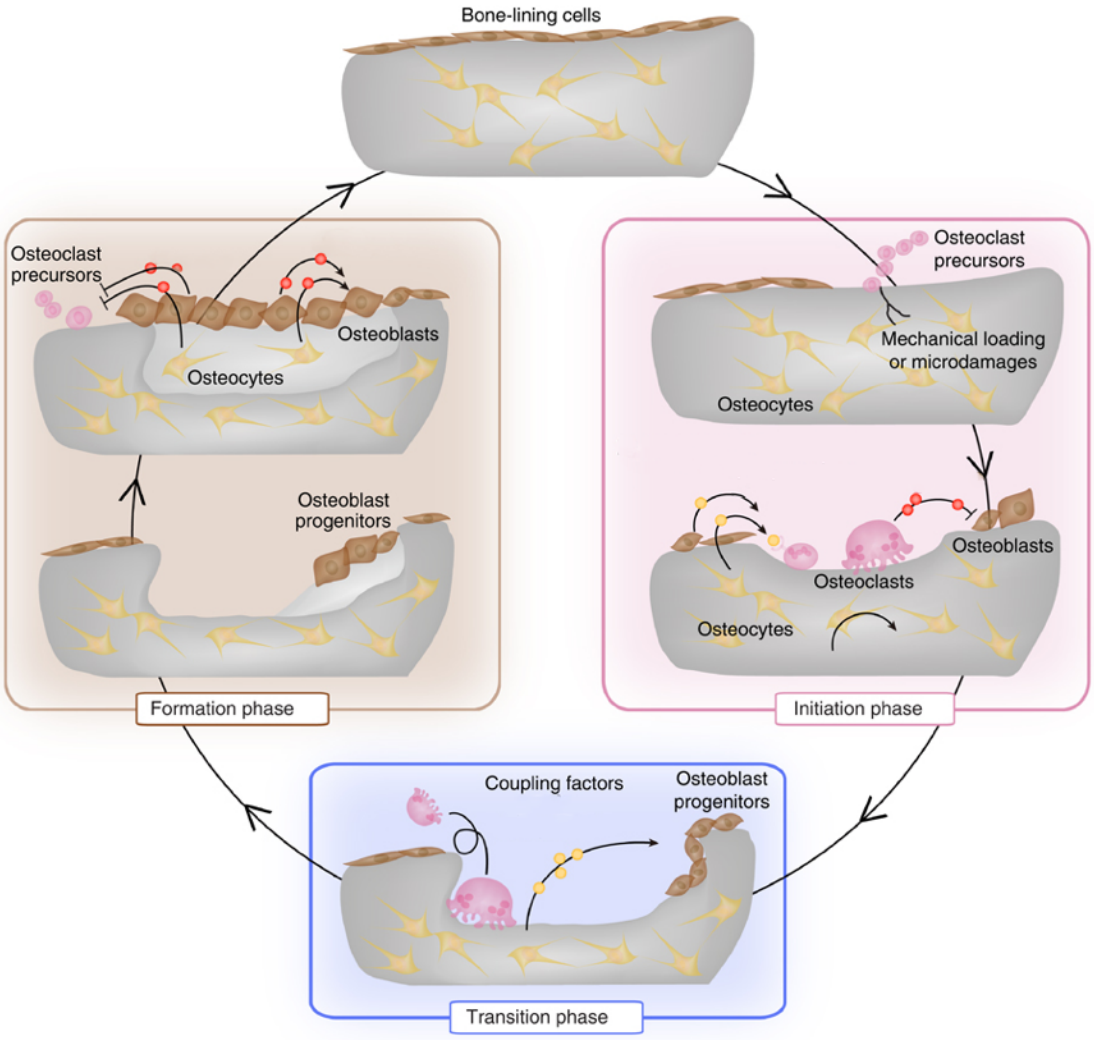

Figure 3.1: The bone remodeling process begins in the initiation phase with the identification of defects and recruitment of preosteoblasts. The transition phase occurs as differentiated osteoblasts vacate the resulting pit and leave signaling proteins and coupling factors that help with the recruitment of osteoblast progenitors. During the Formation phase, Osteoblasts differentiate and lay down new bone tissue, filling the pit and completing the remodeling cycle.

3.2 Materials and Methods

3.2.1 PEGDA Hydrogel Formation and Protein Incorporation

Nacre WSM, BMP-2, DMP1, BSP, and n16N were acquired and processed as described in section 2.2.1. The proteins and peptides were PEGylated as described in section 2.2.2. Hydrogel disks (1-cm diameter) were formed via photopolymerization in glass and silicon molds. Prepolymer solutions were prepared by combining 0.1 g/mL 10 kDa PEGDA (10% w/v) with 10 mM PEG-RGDS, 1 ml HBS and 10 μL/mL photoinitiator solution (2,2-dimoxy-2-phenyl-acetophenone 300 mg/mL in N-vinyl-pyrrolidone; acetophenone/NVP). Separate solutions were supplemented with 200ng/mL of one PEGylated or non PEGylated protein or peptide. The disks were formed by injecting the solution into 1 cm-diameter silicon molds clamped between glass slides and exposing the prepolymer molds to long-wavelength UV light (365 nm, 10 mW/cm2) for 1 min.

The resulting gels were then washed in PBS to remove excess photoinitiator and allowed to swell in growth medium at 4°C for 24 h before use.

3.2.2 Cell Culture

3.2.2.1 W-20-17 Cell Culture

W-20-17 mouse bone marrow stromal cells (ATCC, Manassas, VA, USA) were seeded on PEGDA scaffolds at 10,000 cells/cm^2. Cells were cultured in DMEM supplemented with 10% fetal bovine serum and 1% penicillin/streptomycin solution (10,000 Units penicillin and 10 mg streptomycin per mL). Seeded scaffolds were placed in 6 well transwells (Sigma Aldrich, St. Louis, MO, USA) and moved to new wells 12 hours after seeding to retain only cells that attached to the surface. Media was replaced daily until differentiation analysis was conducted.

3.2.2.2 MC3T3-E1 Cell Culture on 2D Scaffold

MC3T3-E1 mouse preosteoblast cells (ATCC, Manassas, VA, USA) were seeded on PEGDA scaffolds at 10,000 cells/cm^2. Cells were cultured in MEM-α supplemented with 10% fetal bovine serum and 1% penicillin/streptomycin solution (10,000 Units penicillin and 10 mg streptomycin per mL). Seeded scaffolds were placed in 6 well transwells (Sigma Aldrich, St. Louis, MO, USA) and moved to new wells 12 hours

after seeding to retain only cells that attached to the surface. Media was replaced every other day until mineralization analysis was conducted.

3.2.2.3 MC3T3-E1 Cell Culture in Microspheres

MC3T3-E1 Subclone 4 cells were encapsulated in PEGDA microspheres via water-in-oil emulsification followed by photopolymerization. A bulk prepolymer solution was prepared by dissolving 0.2 g poly(ethylene glycol) diacrylate, 0.30 μL triethanolamine, 0.20 μL eosin Y solution (1.0mM), 0.2 μL pluronic acid, 7.5 μL photoinitiator solution (300 mg 2,2-dimethoxy-2-phenyl acetophenone in 1 mL 1 - vinyl-2-pyrrolidinone) in 1 mL HBS (25 mM). The bulk prepolymer solution was then aliquoted into 10 separate vials. One growth factor was added to each vial to a final concentration of 200 ng/mL protein or PEG-protein equivalent. The prepolymer solutions were combined with an equal volume of cell suspension such that the final cell concentration was $5x10^6$ cells/mL. A separate mineral oil solution was prepared by adding 3 μL photoinitiator solution to 1 mL mineral oil. 100 μL of the cell/prepolymer solution was then added to 1 mL of the mineral oil solution in a borosilicate test tube and briefly vortexed to create and water-in-oil emulsion where the cells remained in the aqueous phase. The emulsion was then exposed to white light for 20 seconds with intermittent vortexing and rotation to

maintain the integrity of the emulsion while evenly applying light to the entire tube (Figure 3.2).

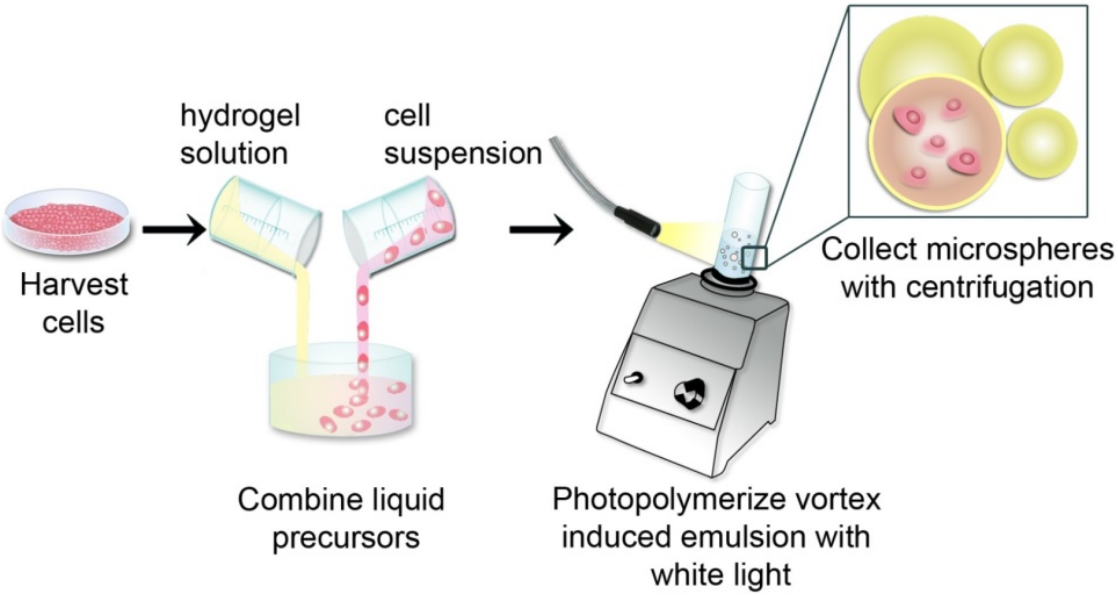

Figure 3.2. Cell microencapsulation technique. Cells are harvested, combined with a 10 kDa PEGDA containing photoinitiator, subjected to vortex to induce a water-in-oil emulsion, and exposed to white light to polymerize the resulting droplets.

The microsphere-encapsulated MC3T3-E1 cells were cultured in 12-well transwells (Sigma Aldrich, St. Louis, MO, USA) containing MEM-α supplemented with 10% fetal bovine serum and 1% penicillin/streptomycin solution (10,000 Units penicillin and 10 mg streptomycin per mL). Media was replaced every other day until mineralization analysis was conducted.

3.2.3 Cell Analysis

3.2.3.1 Osteogenic Response of W-20-17 Cells in 2D Culture

W-20-17 bone marrow stromal cells were cultured on PEGDA hydrogels in the presence of PEGylated and non PEGylated osteogenic proteins. After 4 days, the growth medium was aspirated from the wells. The gels were washed with PBS to remove any media residue. The cells were then stained for ALP activity using a Stemgent AP II staining kit, and the stain was visualized via light microscopy. The images were processed for stain intensity via imageJ.

3.2.3.2 Mineralization of MC3T3-E1 Cells in 2D Culture

MC3T3-E1 mouse preosteoblast cells were cultured on PEGDA hydrogels in the presence of PEGylated and non PEGylated osteogenic proteins. After 12 days, the growth medium was aspirated from the wells. The gels were washed with PBS to remove any media residue. The cells were fixed in 10% paraformaldehyde for 15 minutes, then stained for calcium mineralization via Alizarin red S (40mM, pH 4.1). After removal of excess Alizarin red S solution and washing with ultrapure water, the cells were imaged using light microscopy. The images were processed for stain intensity via imageJ.

3.2.4 Mineralization of Encapsulated MC3T3-E1 Cells

After 21 days, the microspheres were removed from the media, washed with ultrapure water, and fixed in 10% paraformaldehyde for 15 minutes. Each sample was then stained with Alizarin red S (40 mM, pH 4.1) for 15 minutes. After removal of excess Alizarin red S solution and washing with ultrapure water, the cells were imaged using light microscopy.

Mineralization was quantified within each image by assigning numeric value to the stain intensity of each microsphere within an image, adding up the values, and then dividing by the total number of microspheres within the image. Unstained microspheres were assigned a value of zero, partially-stained microspheres were assigned a value of 1, and fully stained microspheres were assigned a value of 2. So the normalized mineralization value of an image ranges between 0 and 2.

3.2.5 Statistical Analysis

Samples were compared using a one-way ANOVA followed by a Tukey-Kramer HSD post-hoc test. Unless otherwise indicated, p-Values less than 0.05 were considered significant and analyses were conducted using Microsoft Excel. Statistical significance is indicated with asterisks in the figures or figure legends, which are depicted as bar graphs reporting mean ± standard deviation.

3.3 Results

3.3.1 Osteogenic Differentiation of 2D Cell Cultures

W-20-17 cells were stained for ALP expression after 4 days of growth on PEGDA hydrogels incorporating PEGylated and non-PEGylated proteins (Figure 3.3). ALP expression appeared to be highest in BMP-2 and WSM samples. All samples appeared to retain the ability to induce osteodifferentiation in W-20-17 cell monolayers when PEGylated. When samples were thresholded for pigmentation, the quantified data also supports these observations. When all images were thresholded against a standard background, the highest area percentage of pigmentation was present in the WSM images followed by BMP-2 (Figure 3.4). However, PEGylation did not significantly affect osteodifferentiation across all protein and peptide samples. All samples showed significant bioactivity compared to control gels without protein incorporation.

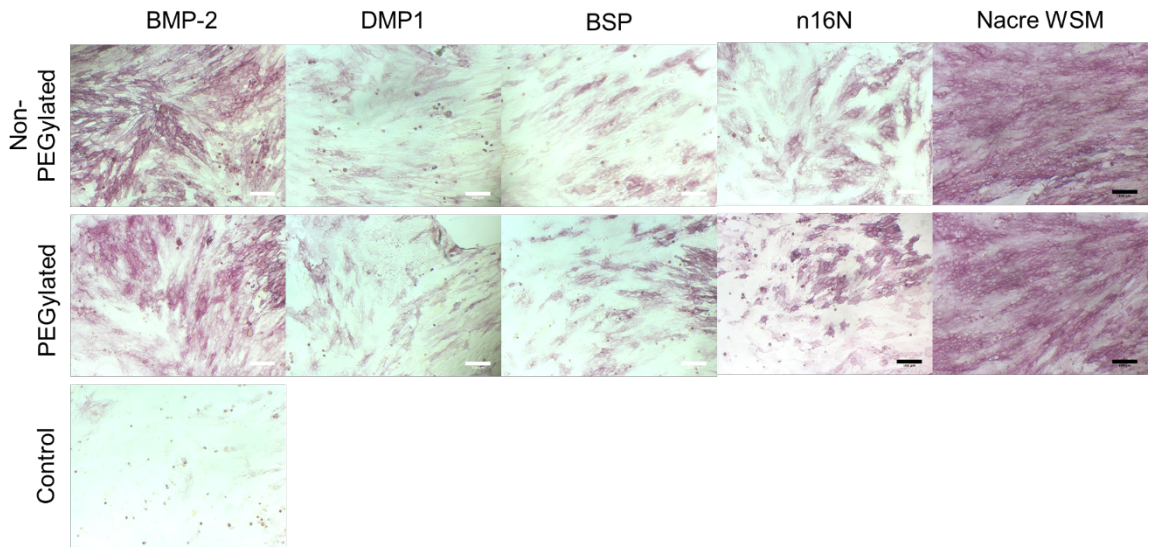

Figure 3.3: W-20-17 cells seeded onto PEGDA hydrogels incorporating PEGylated and non-PEGylated osteogenic proteins and peptides. Cells stained for ALP.

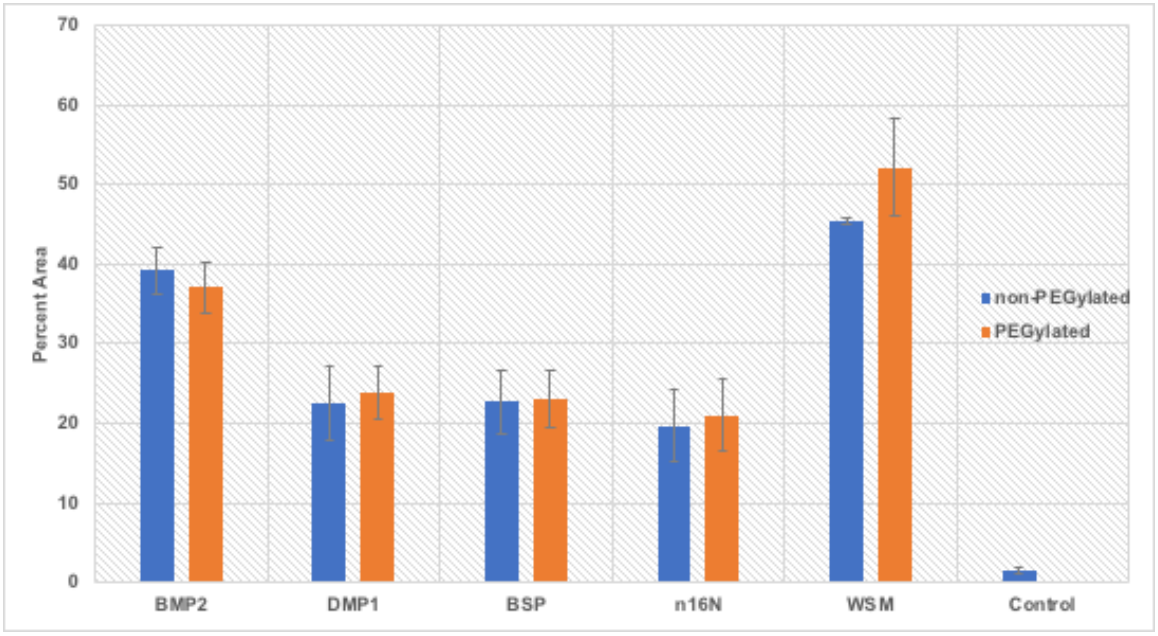

Figure 3.4: ALP expression in W-20-17 cells quantified as percent area covered. Error bars show standard deviation.

3.3.2 Alizarin Red S Visualization of Cellular Mineralization in 2D Cell Culture

MC3T3-E1 cells were stained for calcium mineralization after 12 days of growth on PEGDA hydrogels incorporating PEGylated and non-PEGylated proteins (Figure 3.5). PEGylation appeared to negatively impact mineralization in BMP-2 and n16N. However, statistical analysis did not reveal a significant change due to PEGylation. Though PEGylation did not significantly alter mineralization, PEGylated WSM is the only covalently incorporated protein sample to show significantly increased mineralization compared to protein-negative controls. Among non-PEGylated proteins, only BMP-2 and n16N showed significantly increased mineralization compared to negative controls (Figure 3.6).

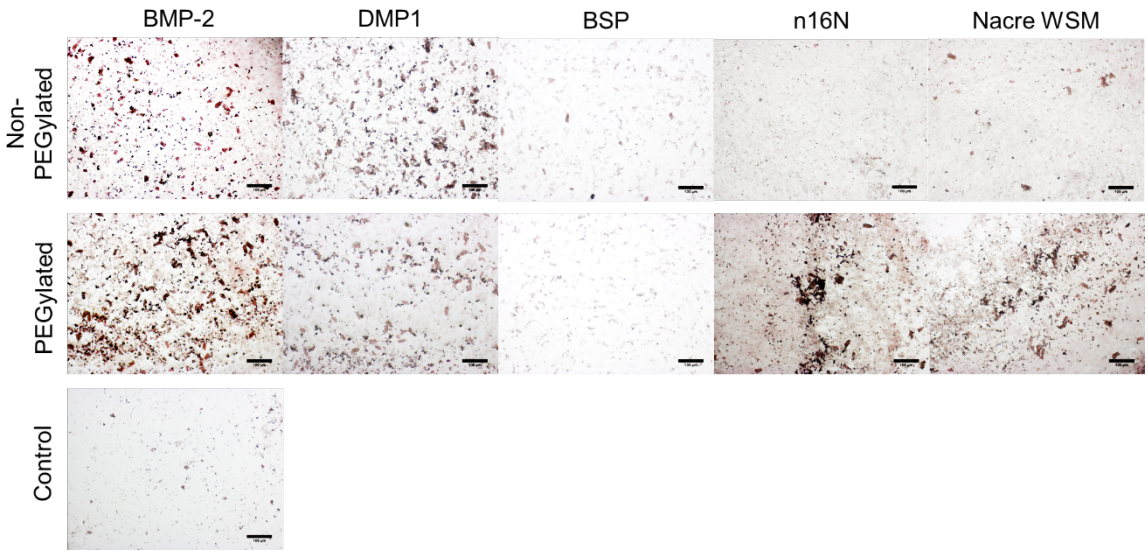

Figure 3.5: MC3T3-E1 cells on PEGDA hydrogels incorporating PEGylated and non-PEGylated proteins. Cells stained with Alizarin red S to visualize calcium.

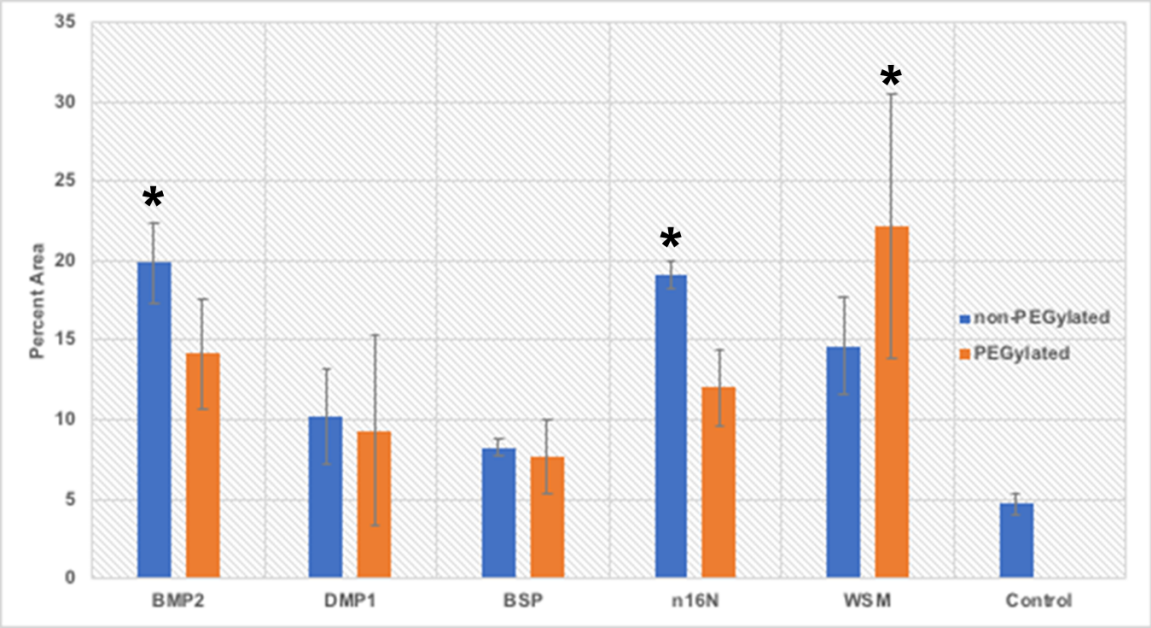

Figure 3.6: Quantification of calcium mineralization in MC3T3-E1 cells on PEGDA hydrogels incorporating PEGylated and non-PEGylated osteogenic proteins. Error bars represent standard deviation. Asterisks denote significant difference between sample and protein negative control ($p < 0.05$).

3.3.3 Mineralization in 3D Cultures

MC3T3-E1 cells were encapsulated in hydrogel microspheres containing PEGylated and non-PEGylated osteogenic proteins and peptides. After 21 days, Alizarin red S staining of encapsulated MC3T3-E1 cells in the presence of growth factors showed elevated mineralization when compared to hydrogels prepared without growth factors (Figure 3.7). Cellular mineralization appeared to increase

with immobilization for all proteins. However, no significant difference due to PEGylation was observed. PEGylated BMP-2 and n16N showed significant difference in mineralization compared to the negative control.

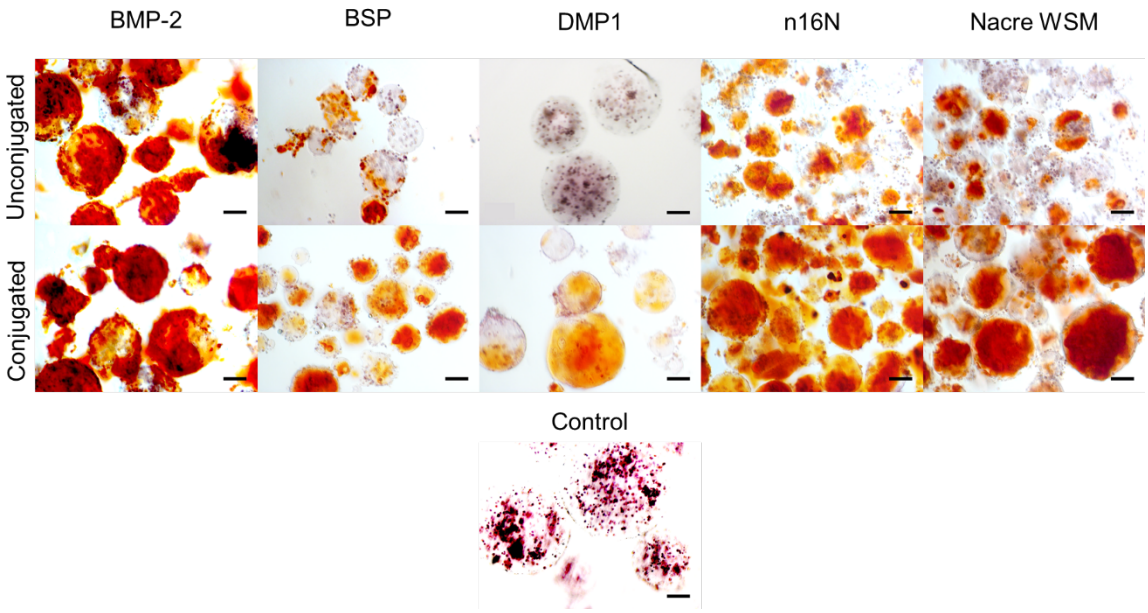

Figure 3.7: Encapsulated MC3T3-E1 cells stained with ARS. Scale bars are 100 μm.

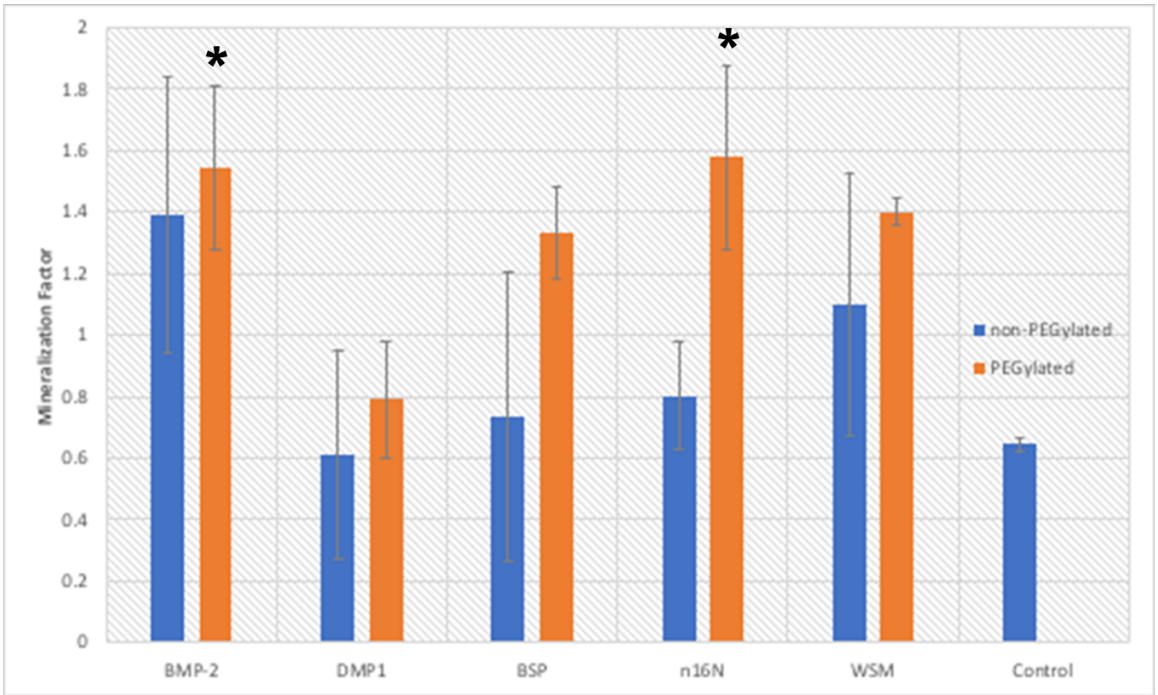

Figure 3.8: Quantification of mineralization in MC3T3-E1 cells encapsulated in microspheres incorporating PEGylated and non-PEGylated growth factors. Each image was quantified by coding fully mineralized microspheres as 2, partially mineralized microspheres as 1, and unmineralized microspheres as 0. The total coded values were summed for each image and then divided by the total number of microspheres in the respective image to normalize the mineralization on a per microsphere basis, reported as the Mineralization Factor. Error bars represent standard deviation. Asterisks denote significant difference compared to protein-negative controls ($p < 0.05$).

3.4 Discussion

The results of this study indicate that induction of osteogenic mineralization can be enhanced by covalently immobilizing growth factors within PEG hydrogel substrates and thus preventing the factors from migrating away from the desired area of action. In particular, covalently incorporating nacre WSM and n16N into a hydrogel substrate appears to offer increased bioactivity. Additionally, the increased mineralization observed in these samples may correlate to the observed increase in sub-micron particles observed in their acellular counterparts. Taken together, this indicates that immobilizing these proteins may increase their availability to osteoblasts. This may hold promise in the field of orthopaedics when systemic drug delivery is undesirable or where mineralization needs to occur on the microscale such as the treatment of osteoporosis.

The lower mineralization observed in PEGylated DMP1 samples is consistent with the lack of mineralization observed in acellular PEGylated DMP1 samples, indicating that modification with PEG may detrimentally alter the osteoinductive properties of DMP1.

3.5 References

[1] R. Eastell, J.S. Walsh, N.B. Watts, E. Siris, Bisphosphonates for postmenopausal osteoporosis, Bone 49(1) (2011) 82-88.
[2] M.J. Rogers, J.C. Crockett, F.P. Coxon, J. Mönkkönen, Biochemical and molecular mechanisms of action of bisphosphonates, Bone 49(1) (2011) 34-41.
[3] M.R. Allen, D.B. Burr, Bisphosphonate effects on bone turnover, microdamage, and mechanical properties: What we think we know and what we know that we don't know, Bone 49(1) (2011) 56-65.
[4] R.M. Dell, A.L. Adams, D.F. Greene, T.T. Funahashi, S.L. Silverman, E.O. Eisemon, H. Zhou, R.J. Burchette, S.M. Ott, Incidence of atypical nontraumatic diaphyseal fractures of the femur, Journal of bone and mineral research : the official journal of the American Society for Bone and Mineral Research 27(12) (2012) 2544-2550.
[5] P. Franceschetti, M. Bondanelli, G. Caruso, M.R. Ambrosio, V. Lorusso, M.C. Zatelli, L. Massari, E.C. degli Uberti, Risk factors for development of atypical femoral fractures in patients on long-term oral bisphosphonate therapy, Bone (New York, NY, United States) 56(2) (2013) 426-431.
[6] L. Gedmintas, D.H. Solomon, S.C. Kim, Bisphosphonates and risk of subtrochanteric, femoral shaft, and atypical femur fracture: A systematic review and meta-analysis, Journal of Bone and Mineral Research 28(8) (2013) 1729-1737.
[7] R. Baron, E. Hesse, Update on bone anabolics in osteoporosis treatment: rationale, current status, and perspectives, Journal of Clinical Endocrinology and Metabolism 97(2) (2012) 311-325.
[8] E. Quattrocchi, H. Kourlas, Teriparatide: A review, Clinical Therapeutics 26(6) (2004) 841-854.
[9] D. Aslan, M.D. Andersen, L.B. Gede, T.K. de Franca, S.R. Jorgensen, P. Schwarz, N.R. Jorgensen, Mechanisms for the bone anabolic effect of parathyroid hormone treatment in humans, Scandinavian journal of clinical and laboratory investigation 72(1) (2012) 14-22.
[10] P. Morley, J.F. Whitfield, G.E. Willick, Parathyroid hormone: an anabolic treatment for osteoporosis, Curr Pharm Des 7(8) (2001) 671-87.
[11] R.M. Neer, C.D. Arnaud, J.R. Zanchetta, R. Prince, G.A. Gaich, J.Y. Reginster, A.B. Hodsman, E.F. Eriksen, S. Ish-Shalom, H.K. Genant, O. Wang, B.H. Mitlak, Effect of parathyroid hormone (1-34) on fractures and bone mineral density in postmenopausal women with osteoporosis, The New England journal of medicine 344(19) (2001) 1434-41.
[12] L. Osagie-Clouard, A. Sanghani, M. Coathup, T. Briggs, M. Bostrom, G. Blunn, Parathyroid hormone 1-34 and skeletal anabolic action: The use of parathyroid hormone in bone formation, Bone & joint research 6(1) (2017) 14-21.

[13] S.W. Kuo, M.G. Rimando, Y.S. Liu, O.K. Lee, Intermittent Administration of Parathyroid Hormone 1-34 Enhances Osteogenesis of Human Mesenchymal Stem Cells by Regulating Protein Kinase Cδ, Int J Mol Sci 18(10) (2017).
[14] Q. Liu, Q. Wan, R. Yang, H. Zhou, Z. Li, Effects of intermittent versus continuous parathyroid hormone administration on condylar chondrocyte proliferation and differentiation, Biochem Biophys Res Commun 424(1) (2012) 182-8.
[15] V. Subbiah, V.S. Madsen, A.K. Raymond, R.S. Benjamin, J.A.J.O.I. Ludwig, Of mice and men: divergent risks of teriparatide-induced osteosarcoma, 21(6) (2010) 1041-1045.
[16] J. Sun, J. Li, C. Li, Y. Yu, Role of bone morphogenetic protein-2 in osteogenic differentiation of mesenchymal stem cells, Molecular Medicine Reports 12(3) (2015) 4230-4237.
[17] S. Lin, L. Cao, Q. Wang, J. Du, D. Jiao, S. Duan, J. Wu, Q. Gan, X. Jiang, Tailored biomimetic hydrogel based on a photopolymerised DMP1/MCF/gelatin hybrid system for calvarial bone regeneration, Journal of Materials Chemistry B 6(3) (2018) 414-427.
[18] J.A.R. Gordon, C.E. Tye, A.V. Sampaio, T.M. Underhill, G.K. Hunter, H.A. Goldberg, Bone sialoprotein expression enhances osteoblast differentiation and matrix mineralization in vitro, Bone (San Diego, CA, United States) 41(3) (2007) 462-473.

CHAPTER 4 : MICROSPATIAL PATTERNING OF CELLULAR OSTEOGENIC RESPONSE

4.1 Introduction

As nacre is spatially directed and assembled via protein-mediated processes, its soluble matrices may hold the potential to spatially direct and control osteogenic processes as well. Indeed, the WSM of nacre has been shown to facilitate mineralization in mouse preosteoblast cells.[1] Fractionated and individual components of nacre's protein matrix have also been shown to induce and promote mineralization within preosteoblast cells.[2, 3] A protein fragment, n16N, derived from *P. fucata*, commonly referred to as the Japanese Pearl Oyster, has been shown to facilitate the ordered nucleation of calcium carbonate when in solution and when adsorbed to chitin substrates.[4, 5] When attached to ordered silk fibroins, chitin-n16N complexes have also been shown to spatially direct calcium carbonate mineralization along the fibroin direction, indicating the potential to microspatially direct mineralization along predefined geometries.[6]

Though mineral-nucleating proteins have the capability to spatially direct nucleation from solution, they have not yet been shown to pattern cell-mediated mineralization in a microspatially relevant context. However, some work has been

done in the field of patterned bone tissue engineering. BMP-2 and BMP-7 have been patterned into poly(L-lysine) and hyaluronan substrates via microfluidic diffusion.[7] These substrates demonstrated the graduated control of C2C12 differentiation along a continuous protein gradient. BMP-2 has also been patterned onto commercial scaffolds and evaluated *in vivo* to facilitate increased healing in critical sized rat calvarial defects.[8, 9] Micro CT scans showed preferential bone formation in the printed areas of the scaffolds. Alkaline phosphatase (ALP) staining *in vitro* also showed preferential differentiation of C2C12 cells in printed areas. Moreover, these studies indicate that spatial presentation of osteogenic growth factors can spatially control osteogenic differentiation and mineralization without simultaneous restrictions to cell binding geometries. This is an important distinction that demonstrates the ability of a substrate to control cell-mediated biomineralization, which is more challenging than preventing biomineralization by preventing cell attachment. However, these studies do not indicate microspatial control and the printing process does not permanently or semipermanently bind the proteins to the substrate. Rather they are allowed to diffuse out of the scaffold over time.

Micron-scale control has been demonstrated in angiogenic studies, however. Vascular Endothelial Growth Factor (VEGF) has been covalently bound to PEG

hydrogels in prescribed patterns, resulting in increased angiogenic response and tubule formation *in vitro*.[10] However, these studies also patterned cell-binding sites along with the bioactive protein, limiting the direction that endothelial cells were allowed to grow. Because of this growth restriction, this model does not strictly isolate the influence of VEGF. The objective of the following experiments is to demonstrate microspatial control over osteogenic differentiation and cell-mediated mineralization via patterned osteogenic proteins within an environment that does not spatially restrict cell growth or attachment.

Pilot studies indicated that nacre WSM may have the ability to microspatially control osteoblast mineralization *in* vivo (Figure 4.1). MC3T3-E1 mouse preosteoblast cells were seeded onto hydrogels patterned with PEGylated nacre WSM proteins and cultured in growth media. After 12 days, the cultures were stained with von Kossa silver nitrate solution. When both the von Kossa stained image and the fluorescent pattern were thresholded and overlayed with one another, a particle analysis suggested that 90.20 ± 8.90 percent of the mineralized nodules were associated with the pattern.

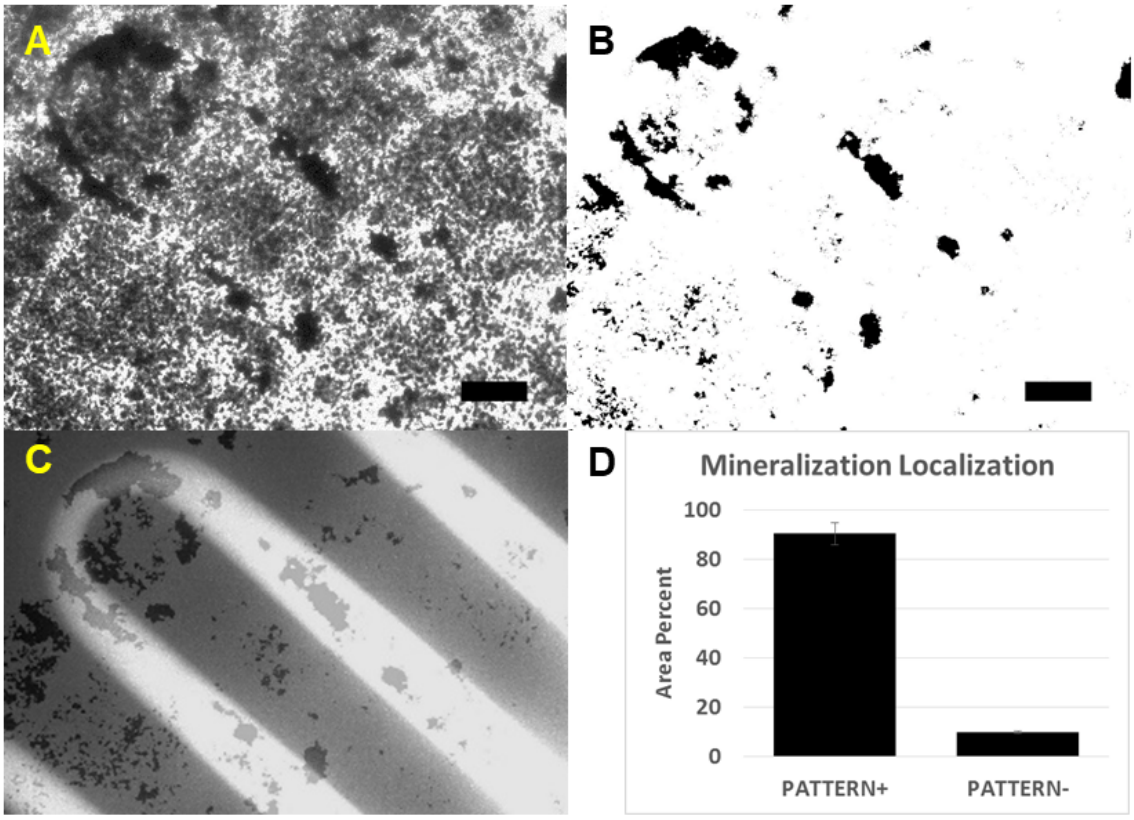

Figure 4.1: MC3T3-E1 cells seeded onto PEG hydrogel patterned with nacre WSM proteins. Mineralization is visualized via von Kossa stain (A), thresholded via ImageJ to remove background noise (B), overlayed with thresholded fluorescent pattern image (C), and analyzed for particle association with patterned proteins (D). Scale bars are 200 μm.

4.2 Materials and Methods

4.2.1 Protein Patterning

Hydrogel disks (1-cm diameter) were formed via photopolymerization in glass and silicon molds. Prepolymer solutions were prepared by combining 0.1 g 10 kDa

PEGDA (10% w/v) with 10 mM mg PEG-RGDS, 1 ml HBS and 10 μl photoinitiator solution (2,2-dimoxy-2-phenyl-acetophenone 300 mg/ml in N-vinyl-pyrrolidone; acetophenone/NVP), injecting the solution into 1 cm-diameter silicon molds clamped between glass slides, and exposing the prepolymer molds to long-wavelength UV light (365 nm, 10 mW/cm2) for 1 min. The gels were then washed in PBS to remove excess photoinitiator and allowed to swell in sterile PBS at 4°C for 24 h.

Fluorescein o-acrylate solution (50 μL) was then pipetted onto the surface of the hydrogels and covered with a photomask transparency printed with a prescribed microscale pattern. The hydrogels were exposed to intense, white light from a Metal Halide Illuminator (Edmonds Optics) passing through a focusing lens for 1 minute to conjugate the acrylate groups in the fluorescent compound to the acrylate groups on the hydrogel surface within the boundaries of the prescribed photomask pattern. After extensive washing in PBS, protein conjugation was confirmed using fluorescent microscopy to visualize the resulting pattern.

4.2.2 Acellular Patterning of Mineralization

Nacre WSM, BMP-2, DMP1, BSP, and n16N were acquired and processed as described in section 2.2.1. The proteins and peptides were PEGylated as described

in section 2.2.2. Acrylated glass slides were prepared as described in section 2.2.3. The PEGylated proteins were patterned onto the surface of acrylated slides via photolithography. As previously described, after the acrylated slides were dry, they were coated with 50 μL PEGylated protein solution (2 mg protein equivalent per mL ultrapure water), taking care to cover the entire slide to facilitate homogenous distribution of protein. A crosshatched nylon photomask was then placed over the top of the solution such that only openings in the mesh were exposed to focused white light for 1 minute. For acellular patterning, the nylon meshes offered higher resolution than the photomasks used for hydrogel patterning, permitting visualization of mineralization with electron microscopy. The slides were then washed twice with cold ultrapure water to remove unbound proteins. Mineralization was then initiated and assessed as described in section 2.2.5.

4.2.3 Patterning Cellular Osteogenic Response

A 50 μL droplet of PEGylated protein solution (0.2 mg/mL) containing photoinitiator was pipetted onto the surface of each hydrogel and covered with a photomask transparency printed with a prescribed microscale pattern. The hydrogels were exposed to intense, white light passing through a focusing lens for 1 minute to conjugate the PEGylated proteins to the hydrogel within the

boundaries of the prescribed photomask pattern. Fluorescent patterns were confirmed as described in section 4.2.1.

W-20-17 and MC3T3-E1 cells were cultured on the patterned hydrogel substrates as described 3.2.2.1 and 3.2.2.2, respectively. ALP activity in W-20-17 cells were visualized on day 4 via ALP staining using a Stemgent AP Staining Kit II. MC3T3-E1 cell monolayers were assayed for calcium mineralization after 12 days via Alizarin red S staining as described in section 3.2.3.2 and imaged via brightfield color microscopy.

4.2.4 Statistical Analysis

Mineralization associated with patterns or not associated were compared using a student's T test. Unless otherwise indicated, *p*-Values less than 0.05 were considered significant and analyses were conducted using Microsoft Excel. Statistical significance is indicated with asterisks in the figures or figure legends, which are depicted as bar graphs reporting mean ± standard deviation.

4.3 Results

4.3.1 Visualizing Pattern Transfer

Patterned substrates were visualized via fluorescent microscopy. The bright green areas present in Figure 4.2 shows conjugation patterns transferred via several different geometries. Microscale features were also clearly visible within the edges of the pattern consistent with the micron scale features present in the edges of the photomask.

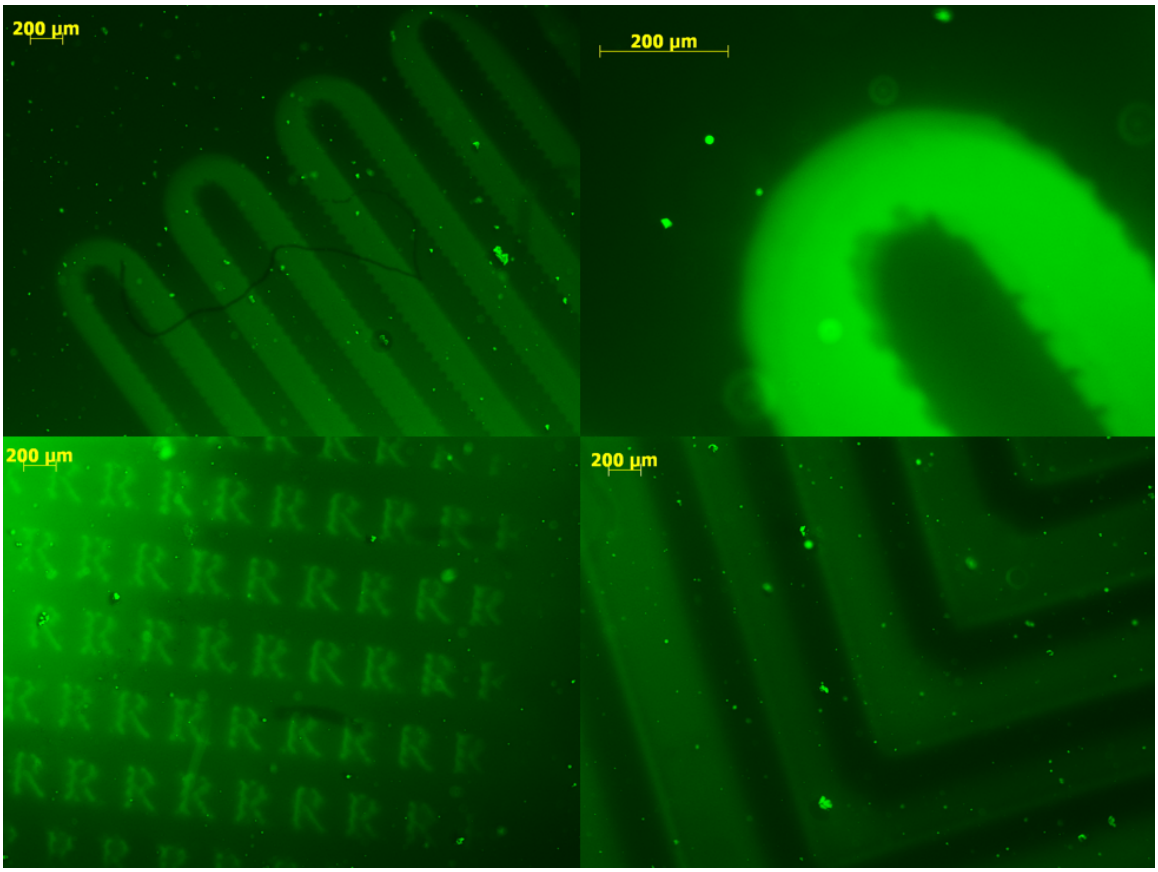

Figure 4.2: Fluorescein o-acrylate patterns on hydrogels visualized via fluorescent microscopy. Scale bars are 200 μm.

4.3.2 Patterned Acellular Mineralization

Quantification of mineralization directly associated to the pattern could not be readily conducted as direct transfer of the pattern onto the glass substrate could not be observed. However, Patterned WSM resulted in the development of crosshatched areas of mineralization under acellular conditions (Figure 4.3). The photomask, however, did not readily align with the observed mineralization. When the photomask was enlarged 2.69 times and rotated, alignment could be approximated (Figure 4.4). This suggests that the photomask may be elevated above the surface of the glass rather than making contact, creating an enlarged projection of the mask onto the substrate. From optics, this can be characterized and tested if a few parameters are known (Figure 4.5). The hypothetical distance between the mask and the surface of the slide, L, was calculated at 1.3 mm. The actual distance between the mask and the surface of the slide was measured to be 1.1 mm, meaning the calculated value of 1.3 mm showed an 18 percent deviation from the measured value. Mineralization associated with the photomask pattern was determined to be 97.87 percent. In contrast to the PEGylated WSM, patterned

mineralization consistent with the photomask was not observed in any of the other protein samples.

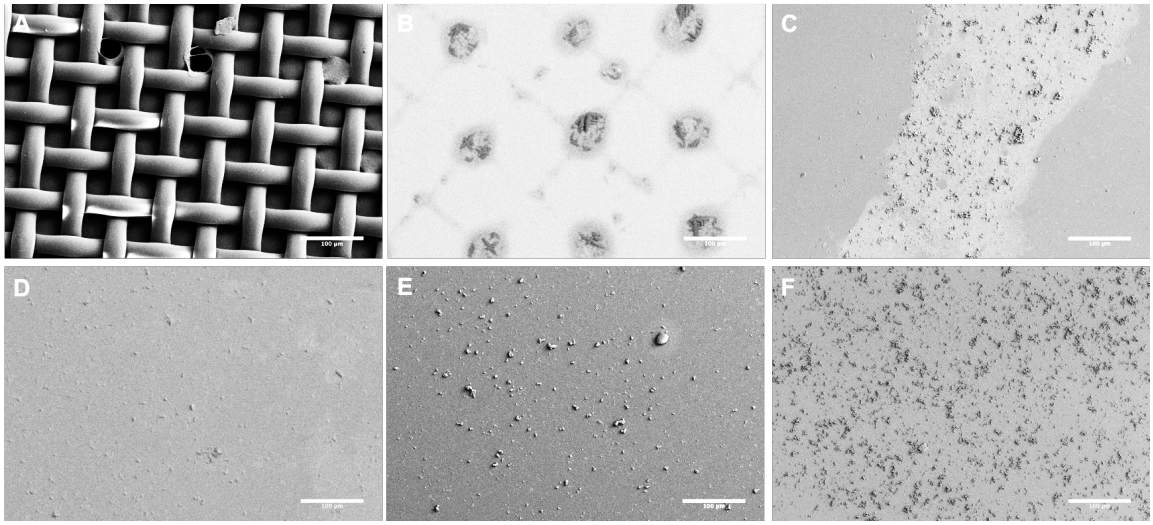

Figure 4.3: FE-SEM micrographs of mineralization on glass slides patterned with PEGylated proteins. PEGylated Nacre WSM (B), BMP-2 (C), DMP-1 (D), BSP (E), and n16N (F) were patterned using a nylon mesh photomask (A). Scale bars are 100 μm.

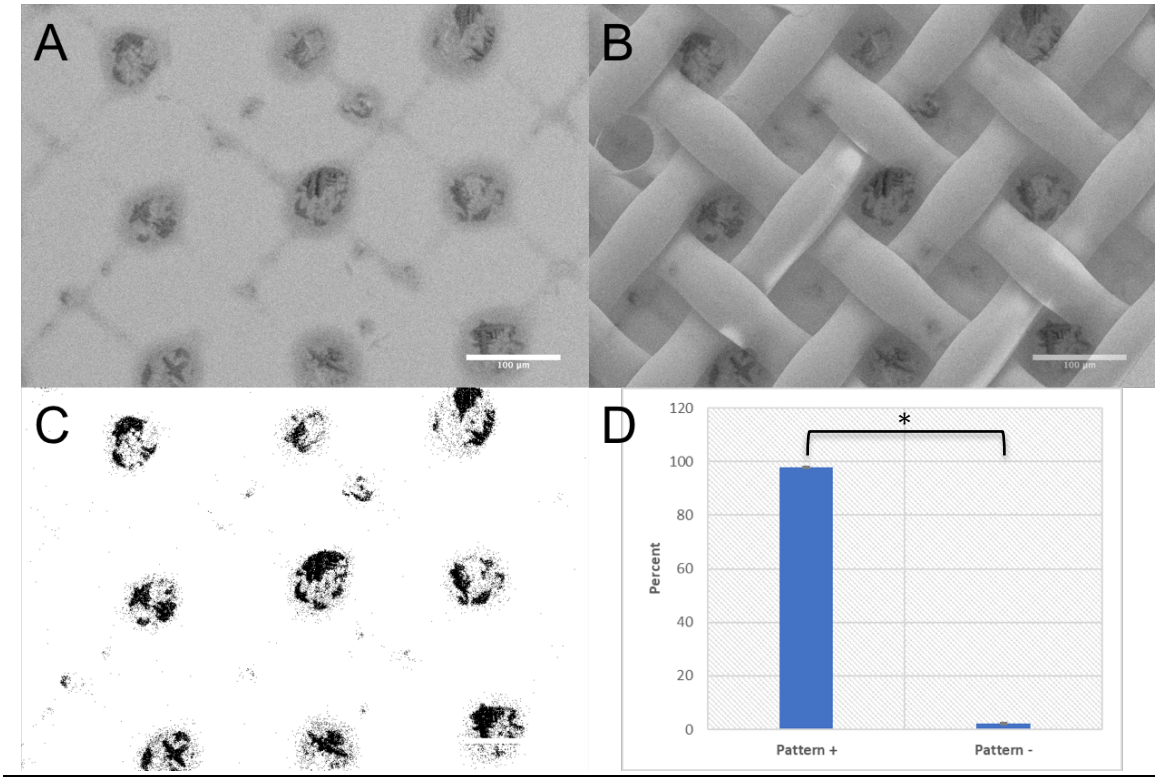

Figure 4.4: Quantifying patterned acellular mineralization. (A) FE-SEM image of patterned mineralization over patterned PEGylated WSM, (B) patterned mineralization overlayed with enlarged and rotated photomask image, (C) thresholded patterned mineralization image, (D) quantified mineral nodules associated with photomask pattern. Error bars indicate standard deviation. Asterisk shows statistical significance.

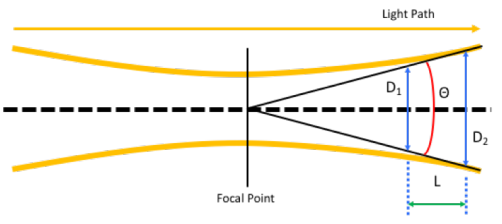

Θ = beam divergence
D_2 = diameter of projection
D_1 = diameter of beam at mask
L = distance between mask and surface of slide

$$\Theta = 2\arctan\left(\frac{D_2 - D_1}{2L}\right)$$

Figure 4.5: Schematic of diagram illustrating photomask projections. Beam divergence and both diameters are known, allowing for the calculation of a hypothetical distance between the mask and the surface of the slide.

4.3.3 Patterned Cellular Osteogenic Response

PEG hydrogels patterned with covalently bound osteogenic proteins were seeded with either W-20-17 cells (Figure 4.6) or MC3T3-E1 cells (Figure 4.6). PEGylated WSM and BMP-2 show patterned differentiation (Figure 4.7). ALP expression correlated to the pattern was determined to be 83.17 percent and 93.48 percent in hydrogels patterned with PEGylated WSM and BMP-2, respectively. Mineralization patterns were observed in MC3T3 cells after 12 days when cultured on hydrogels patterned with nacre WSM (Figure 4.8 B). The association of the mineralization with the pattern is apparent when the pattern is rotated and digitally overlaid onto the stained image (Figure 4.9). Mineralization associated with the PEGylated WSM pattern was calculated to be 63.37 percent from the thresholded image. Though the pattern transfer could be observed on the hydrogels directly following the photomask step, the pattern could not be viewed concurrently with mineralization or ALP staining due to differences in camera specifications and orientation, preventing a direct pixel-to-pixel overlay. Thus, representative scale patterns were used for illustration purposes.

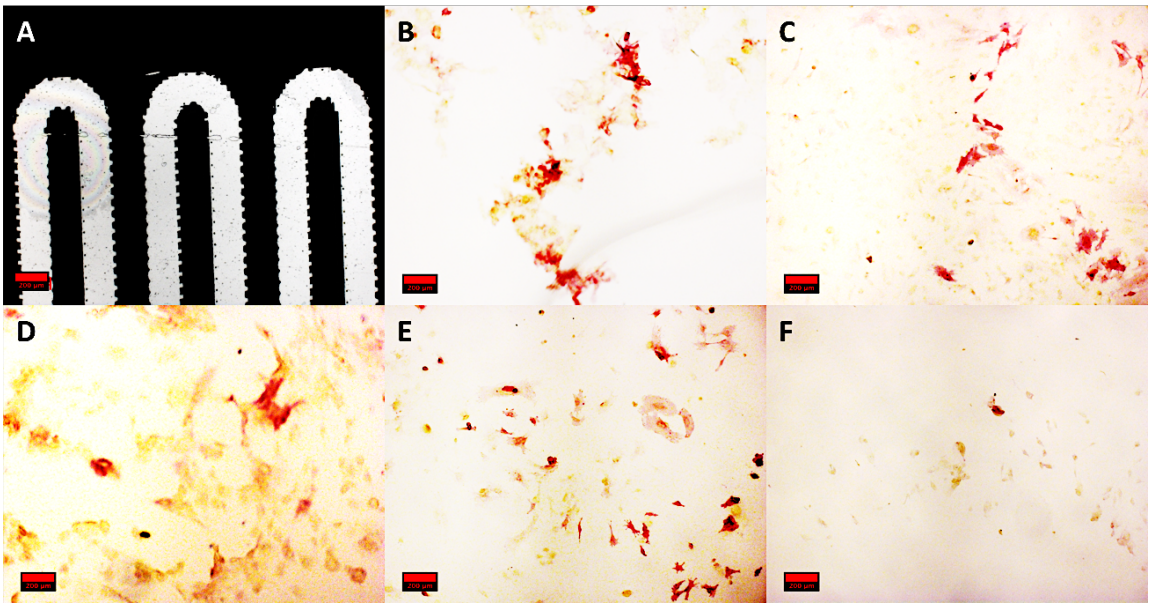

Figure 4.6: Alkaline phosphatase (ALP) staining of Day 4 W-20-17 cells seeded on PEG hydrogels patterned with PEGylated proteins. Red color indicates ALP activity. Hydrogels were patterned via photlithography through a transparency photomask pattern (A) with PEGylated nacre WSM proteins (B), BMP-2 (C), DMP-1 (D), BSP (E), and n16N (F). ALP activity did not appear to be associated with patterns. Scale bars are 200 μm.

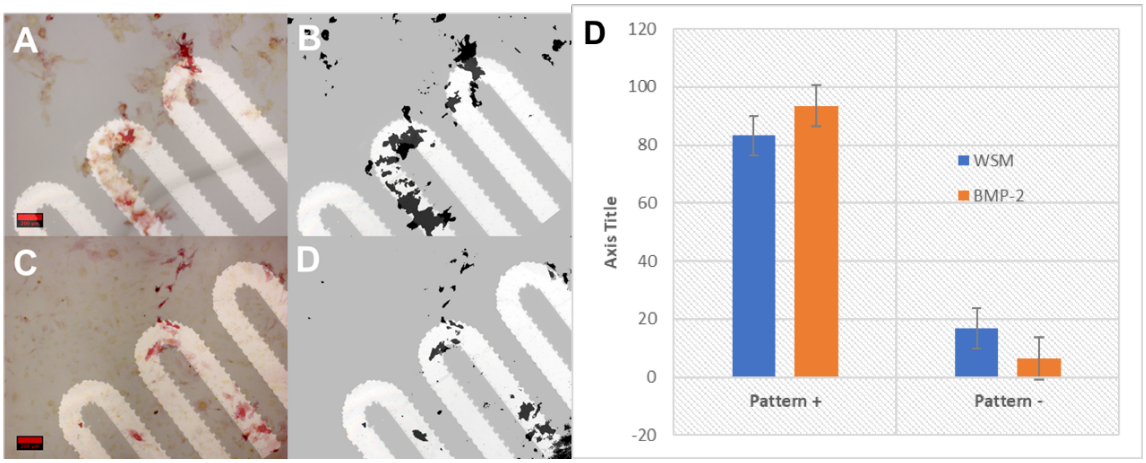

Figure 4.7: ALP-stained images of PEGDA hydrogels incorporating patterned PEGylated WSM (A) and BMP-2 (C) were thresholded for intensity and overlayed with pattern (B, D). Mineralization associated with the overlayed patterns were quantified (D). ALP expression appears red. Patterns are illustrative.

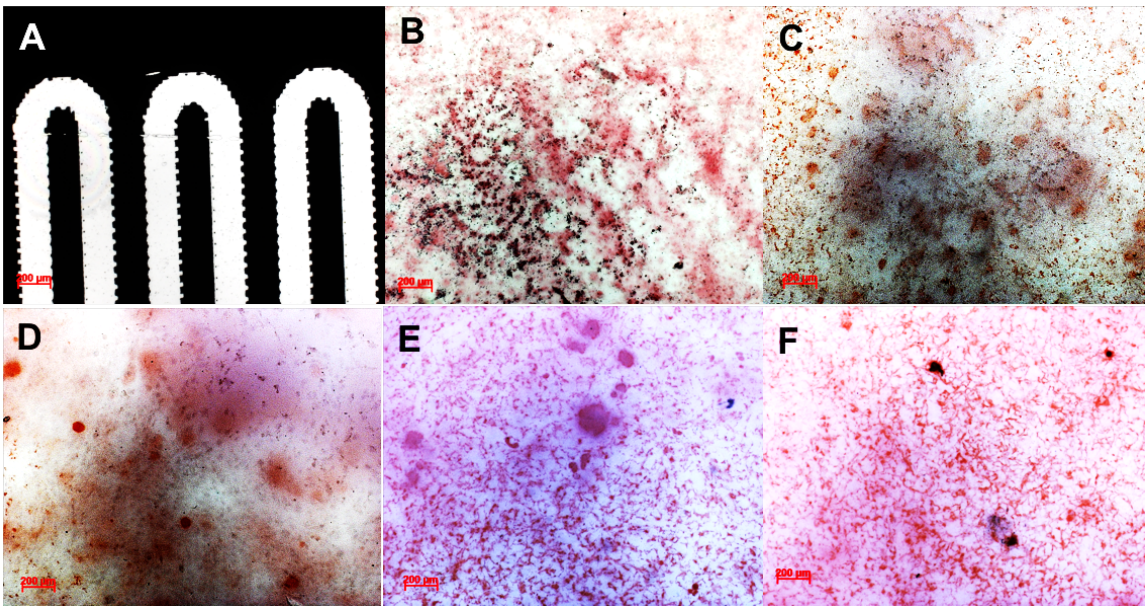

Figure 4.8: Alizarin red S stain of Day 12 MC3T3-E1 cells on patterned PEGDA hydrogels. Hydrogels were patterned via photolithography through a

transparency photomask pattern (A) with nacre WSM proteins (B), BMP-2 (C), DMP-1 (D), BSP (E), and n16N (F). Red stain is indicative of calcium mineralization. B-F show red stain, while only B shows red stain following a pattern. Scale bars are 200 μm.

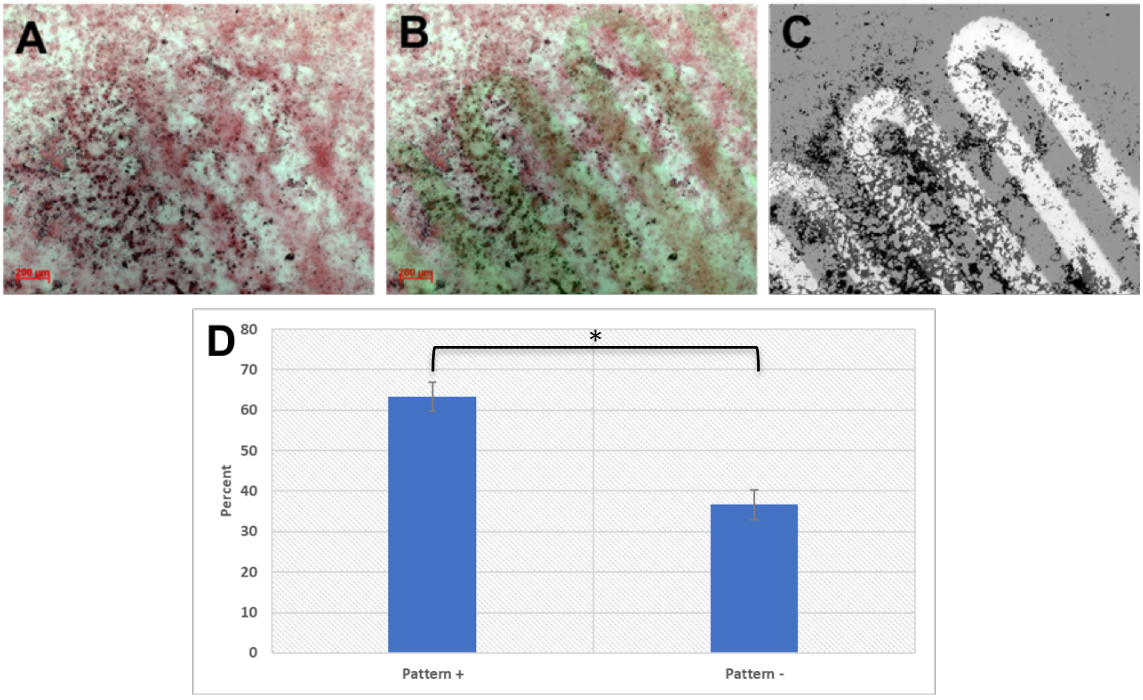

Figure 4.9: Day 12 MC3T3-E1 cells seeded onto PEG hydrogels patterned with PEG-WSM proteins and stained with Alizarin red S (A). Mineralization overlaid with fluorescent pattern (B). Thresholded binary image of mineralization overlaid with photomask pattern (C). Mineralization associated with the overlayed pattern was quantified (D). Calcium mineralization appears red and is collocated with the

fluorescent pattern. Patterns are illustrative. Scale bars are 200 μm. Error bars show standard deviation. Asterisk indicates significance.

4.4 Discussion

In both acellular and cellular patterning experiments, patterned PEG-WSM demonstrated an ability to exert spatial control over the resulting mineralization. Mineralization was concentrated within the patterns only in the PEG-WSM groups. The other PEGylated proteins exhibited no such control. All other groups showed diffuse mineralization not associated with any patterns. This was particularly unexpected for the acellular case since the proteins offered the only mineralization sites. In control samples with no proteins, no mineralization occurred. This was expected in the focal areas of the mesh pattern without PEGylated proteins; it was not expected that mineralization would extend beyond the pattern. This may be explained in several ways. While the close association of the mineralization in the nacre WSM samples with the nylon mesh grid is encouraging, the non-specific mineralization observed in the other protein samples may indicate artifact introduced by the grid. The non-specific mineralization may be a result of the physical contact of the mesh to the glass surface. The mesh may have physically altered the surface, creating additional nucleation sites. The mesh was used because the transparency pattern used for the

hydrogel patterning was not appropriate for glass slide patterning. The transparency would adhere to the glass slide during the patterning process, impacting the resolution of any resulting patterns. Another possibility for the nonspecific patterning observed lies in the presentation of acrylate groups. In the hydrogels, acrylate groups are ubiquitous within the gel structure. However, these groups may be more disperse on the glass surface, providing fewer acrylate groups per unit area for covalent conjugation in general. Another curiosity is the presence, albeit comparatively low, of mineralization observed in PEG-DMP1 patterned glass slides as there was no such mineralization observed in non-patterned PEG-DMP1 samples in Chapter 2. Again, this may have been caused by physical alteration to the acrylated surface caused by the nylon mesh.

A one-to-one comparison between acellular and cellular mineralization patterns is not possible for several reasons. Since the cells are capable of migrating, it is possible that they come into contact with the PEGylated protein, receive an osteogenic signal, migrate, and lay down osteoid outside of the pattern. Further, as aforementioned, the presence of acrylate groups in hydrogels and on the glass slides are different, and thus the presentation of the PEGylated proteins are different. Although a direct comparison is not possible, it is possible to determine correlation. In this study, PEGylated proteins capable of restricting acellular

mineralization to patterns are also capable of restricting cellular mineralization to patterns.

Patterned ALP expression was observed in W-20-17 cells cultured over PEGylated WSM and BMP-2 patterns, indicating that these proteins are capable of patterning early osteogenic differentiation. As expected, the presence of nacre WSM, BMP-2, DMP1, BSP, and n16N induced ALP production, indicating that these proteins are capable of inducing osteoblastic differentiation in progenitor cells. The protein fragment n16N is derived from the full protein isolated from the nacre of *P. fucata*. This larger protein has been shown to inhibit osteoclast differentiation and promote osteodifferentiation and biomineralization in MC3T3-E1 cells.[11] The protein fragment appears to retain this activity, possibly to a lesser extent. Both the peptide and protein, as well as WSM proteins have demonstrated the ability to nucleate aragonite. This study is the first to demonstrate that aragonite nucleators can be used to pattern both acellular and cellular mineralization.

Patterned mineralization was observed only in the nacre WSM patterned hydrogels. This is consistent with the patterned mineralization observed in the pilot study. However, none of the other proteins resulted in patterned mineralization on their own, with the BMP-2, DMP1, and BSP samples resulting

in a high degree of non-specific mineralization deposited onto the hydrogel surfaces. Very few individual constituents of the nacre protein matrix have been identified. The mechanism through which microscale control occurs remains unclear. It is possible that a yet unidentified protein within the nacre matrix is responsible for microscale control by inducing local mineralization without inducing large scale cell-cell signaling. The production of BMP-2 and other factors by osteoblasts during osteogenesis should induce osteogenesis in neighboring cells. It is possible that the WSM acts as both a stimulator and a substrate upon which osteoblasts mineralize. For instance, locations for calcium mineralization within collagen have been identified.[12] These calcium binding sites are responsible for assembling collagen minerals appropriately within bone. It is possible that proteins within the WSM behave similarly when organizing mineralization during patterning. It is also possible that multiple proteins are necessary to achieve spatial control, and that these proteins act synergistically to control biomineralization within the patterns. The WSM is a collection of proteins while all other groups were single proteins (or a peptide). Regardless of the ultimate reasons, these studies demonstrate that WSM can be PEGylated, that following PEGylation it can be covalently attached to a substrate, and finally, once there it retains its ability to induce osteogenesis and nucleate mineralization. Further study to elucidate these compounds is needed.

4.5 References

[1] M. Rousseau, L. Pereira-Mouries, M.-J. Almeida, C. Milet, E. Lopez, The water-soluble matrix fraction from the nacre of Pinctada maxima produces earlier mineralization of MC3T3-E1 mouse pre-osteoblasts, Comparative Biochemistry and Physiology, Part B: Biochemistry & Molecular Biology 135B(1) (2003) 1-7.
[2] Y. Lao, X. Zhang, J. Zhou, W. Su, R. Chen, Y. Wang, W. Zhou, Z.-F. Xu, Characterization and in vitro mineralization function of a soluble protein complex P60 from the nacre of Pinctada fucata, Comparative Biochemistry and Physiology, Part B: Biochemistry & Molecular Biology 148B(2) (2007) 201-208.
[3] M. Rousseau, H. Boulzaguet, J. Biagianti, D. Duplat, C. Milet, E. Lopez, L. Bedouet, Low molecular weight molecules of oyster nacre induce mineralization of the MC3T3-E1 cells, Journal of Biomedical Materials Research, Part A 85A(2) (2008) 487-497.
[4] E.C. Keene, J.S. Evans, L.A. Estroff, Matrix Interactions in Biomineralization: Aragonite Nucleation by an Intrinsically Disordered Nacre Polypeptide, n16N, Associated with a β-Chitin Substrate, Crystal Growth & Design 10(3) (2010) 1383-1389.
[5] R.A. Metzler, J.S. Evans, C.E. Killian, D. Zhou, T.H. Churchill, N.P. Appathurai, S.N. Coppersmith, P.U.P.A. Gilbert, Nacre Protein Fragment Templates Lamellar Aragonite Growth, Journal of the American Chemical Society 132(18) (2010) 6329-6334.
[6] E.C. Keene, J.S. Evans, L.A. Estroff, Silk Fibroin Hydrogels Coupled with the n16N−β-Chitin Complex: An in Vitro Organic Matrix for Controlling Calcium Carbonate Mineralization, Crystal Growth & Design 10(12) (2010) 5169-5175.
[7] J. Almodovar, R. Guillot, C. Monge, J. Vollaire, S. Selimovic, J.-L. Coll, A. Khademhosseini, C. Picart, Spatial patterning of BMP-2 and BMP-7 on biopolymeric films and the guidance of muscle cell fate, Biomaterials 35(13) (2014) 3975-3985.
[8] G.M. Cooper, E.D. Miller, G.E. De Cesare, A. Usas, E.L. Lensie, M.R. Bykowski, J. Huard, L.E. Weiss, J.E. Losee, P.G. Campbell, Inkjet-Based Biopatterning of Bone Morphogenetic Protein-2 to Spatially Control Calvarial Bone Formation, Tissue Engineering, Part A 16(5) (2010) 1749-1759.
[9] S. Herberg, G. Kondrikova, S. Periyasamy-Thandavan, R.N. Howie, M.E. Elsalanty, L. Weiss, P. Campbell, W.D. Hill, J.J. Cray, Inkjet-based biopatterning of SDF-1Î² augments BMP-2-induced repair of critical size calvarial bone defects in mice, Bone (New York, NY, United States) 67 (2014) 95-103.

[10] J.E. Leslie-Barbick, C. Shen, C. Chen, J.L. West, Micron-Scale Spatially Patterned, Covalently Immobilized Vascular Endothelial Growth Factor on Hydrogels Accelerates Endothelial Tubulogenesis and Increases Cellular Angiogenic Responses, Tissue Engineering, Part A 17(1-2) (2011) 221-229.
[11] J.-Y. Ma, K.-L. Wong, Z.-Y. Xu, K.-Y. Au, N.-L. Lee, C. Su, W.-W. Su, P.-B. Li, P.-C. Shaw, N16, a Nacreous Protein, Inhibits Osteoclast Differentiation and Enhances Osteogenesis, Journal of Natural Products 79(1) (2016) 204-212.
[12] G. He, A. George, Dentin Matrix Protein 1 Immobilized on Type I Collagen Fibrils Facilitates Apatite Deposition in Vitro, 279(12) (2004) 11649-11656.

CHAPTER 5 : CONCLUSIONS AND FUTURE DIRECTIONS

5.1 Dissertation Summary

The work presented in this dissertation was directed toward developing a platform capable of exerting microscale control over key osteogenic processes. A significant hurdle in this task is effectively immobilizing therapeutics, preventing their escape from treatment sites. Exciting developments in scaffold technologies hold promise. However, scaffolds must also be optimized and essentially developed independently for each growth factor as the release kinetics ultimately depend on the growth factor's size, shape, and affinity to the varying substrates. For example, VEGF shows a higher affinity and more favorable release profile from acidic gelatin microparticles while BMP-2 performed more favorably in basic gelatin microparticles.[1-3] These studies also demonstrate that *in vivo* efficacy of these systems varies greatly, likely due to the complex interplay between the various components. The authors point out that affinity operates on a relative scale. For example, the protein release profiles from affinity-based delivery systems can be accelerated *in vivo* if they are displaced by other proteins and molecules that show a greater affinity for the delivery substrate. Covalently binding the growth factors to the substrate – this dissertation uses a PEG linker, for instance – can effectively mitigate this consideration.

It has been repeatedly demonstrated that BMP-2 has a short half-life and a poor affinity to the collagen sponges that are typically used as a delivery vehicle.[4] This has necessitated high doses that have in turn resulted in complications such as cancer promotion and ectopic bone formation, which has led to alarming symptoms such as neurologic impairment and airway restriction. These complications have prompted efforts to more efficiently deliver BMP-2. Previous work has demonstrated that covalently immobilizing BMP-2 and/or cell binding sites within a scaffold may be a viable approach.[5, 6] This indicates that other growth factors may also benefit from immobilization. However, BMP-2 remains the only clinically approved growth factor for implants. At this time, nacre and nacre WSM are well established within the field of biomineralization and bone tissue engineering.[7-13] Though whole nacre has been shown to be osteogenic both *in vitro* and *in vivo*, it is not an ideal therapeutic on its own due to irregularities in shape and composition. To mediate some of this, whole nacre has been ground into powder and incorporated into hydrogels, which has shown some success in inducing bone formation.[14] This method, however, does not effectively retain the WSM proteins, which leech out of the powder in aqueous environments. Since the proteins are the agents responsible for organizing biomineralization, extracting and immobilizing the proteins may be a more effective approach. The WSM of

nacre, however, has been shown to organize biomineralization in acellular and cellular environments, marking it as an ideal candidate for incorporation into bone tissue scaffolds.

PEGylated nacre WSM indeed shows the ability to direct cell-mediated mineralization. To a lesser extent, covalently bound BMP-2 may have the capacity to induce osteogenesis in prescribed patterns. As BMP-2 is already FDA-approved, this work may lead to future breakthroughs in drug delivery applications. Some proteins in this study, most notably DMP1, may be particularly sensitive to PEGylation as the process appeared to completely negate its capacity to induce acellular nucleation. However, PEGylation of all the growth factors in this study appears to increase mineralization in cells encapsulated in three-dimensional microsphere environments, indicating the possibility that factor retention within the hydrogel matrix leads to increased cellular exposure in this arrangement. It is also possible that the hydrogels trap cellular products, such as collagen or secreted growth factors during, leading to increased activity within a given microsphere. This increase may not have transferred over to the two-dimensional cell cultures due to the PEGylated growth factors being incorporated within the bulk scaffold, meaning that only the fraction of the proteins near the cell-seeded surface were available to the cells for the duration of the experiment. Additionally, entrapped

non-PEGylated proteins may have become available to the cells as they eventually migrated out to the surfaces of the gels, where the cells were seeded. This gradual replenishment of growth factors may have mitigated any difference between the observed cellular effects. However, it is important to consider potential use cases where this migration and eventual release might introduce the growth factor systemically.

Acellular mineralization studies revealed that PEGylated WSM proteins may increase mineralization on the sub-micron scale compared to other PEGylated proteins. This may indicate a relationship between nacre WSM's ability to organize calcium mineralization and its ability to spatially direct cell-mediated mineralization.

5.2 Contribution to the Field

For the first time, this work demonstrates that patterned nacre WSM is capable of microspatial control over osteogenic differentiation and mineralization. Additionally, this study attempted to compare a wide range of osteogenic growth factors on a highly reproducible PEGDA scaffold, providing a 1-to-1 comparison between each factor.

While n16N, a protein fragment derived from the calcium binding domain of a larger protein within nacre, has been shown to template and direct aragonite formation, this is the first study reporting osteogenic mineralization. This result is promising as the field of bone tissue engineering may be able to expand further by drawing on the broader biomineralization literature in the future.

5.3 Future Directions

This work serves as a foundation for further study in osteogenesis and biomineralization. There are several directions to move into: (1) further work on the potential of nacre WSM in disease treatment and (2) further characterization of nacre WSM proteins.

5.3.1 WSM in the Treatment of Disease

A substance capable of controlling microscale mineralization features may also serve as a therapeutic target to repair non-fracture related damage to bone tissues as a result of osteoporosis and other metabolic bone diseases. A promising systemic delivery vector was recently developed to target the tartrate-resistant acid phosphatase (TRAP) found in osteoclast pits (Figure 4.1).[13] However, no osteogenic compounds have been shown to control bone tissue formation on the

μm scale these pits occupy. Thus, the development of therapeutic systems capable of spatially controlling bone formation has multiple driving factors.

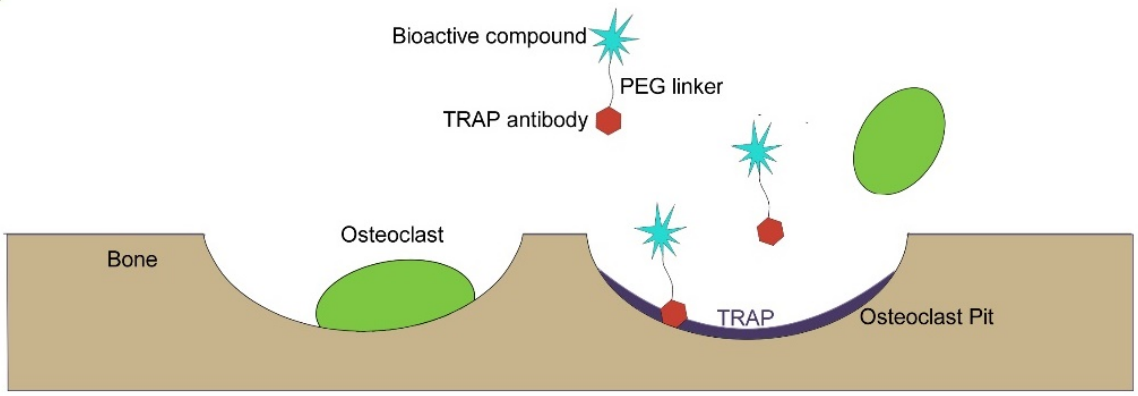

Figure 5.1: Schematic of tartrate-resistant acid phosphatase (TRAP) targeting within osteoclast pits. WSM presents as a possible bioactive compound candidate.

5.3.2 WSM Protein Studies

While nacre WSM proteins show promise in the field of bone tissue engineering, the ultimate goal is to isolate or derive a biofactor that can be reliably reproduced. A body of work already exists in the biomineralization literature as several proteins and peptide derivatives capable of facilitating and directing biomineralization have been identified from nacre.[14-20] This provides a good place to begin exploring potential osteogenic effects as well. The protein from which n16N was derived has shown to both inhibit osteoclast differentiation and

enhance osteogenesis.[17] Additionally, low molecular weight fractions of nacre proteins have been shown to induce mineralization in MC3T3-E1 cells.[21] New avenues of inquiry continue to be opened through these interactions with the broader field of biomineralization. Thus, a targeted approach seems likely to yield even more success.

5.3.3 Characterization of Mineral Composition

Though the observed mineralization is consistent with calcium phosphate mineralization, the thesis presented here would benefit from further characterization. In particular, the use of EDS or X-ray diffraction could be used to quantify the calcium to phosphate ratio in the acellular mineralization studies, indicating the calcium phosphate polymorph nucleated by the PEGylated proteins. Additionally, examining the physical micro and nano structure of the crystals themselves may shed some light on the broader protein-mediated mineralization process.

5.4 References

[1] Z. Patel, H. Ueda, M. Yamamoto, Y. Tabata, A. Mikos, In Vitro and In Vivo Release of Vascular Endothelial Growth Factor from Gelatin Microparticles and Biodegradable Composite Scaffolds, Pharmaceutical Research 25(10) (2008) 2370-2378.

[2] Z.S. Patel, M. Yamamoto, H. Ueda, Y. Tabata, A.G. Mikos, Biodegradable gelatin microparticles as delivery systems for the controlled release of bone morphogenetic protein-2, Acta Biomaterialia 4(5) (2008) 1126-1138.
[3] Z.S. Patel, S. Young, Y. Tabata, J.A. Jansen, M.E.K. Wong, A.G. Mikos, Dual delivery of an angiogenic and an osteogenic growth factor for bone regeneration in a critical size defect model, Bone 43(5) (2008) 931-940.
[4] R.M. Olabisi, Z. Lazard, M.H. Heggeness, K.M. Moran, J.A. Hipp, A.K. Dewan, A.R. Davis, J.L. West, E.A. Olmsted-Davis, An injectable method for noninvasive spine fusion, The Spine Journal 11(6) (2011) 545-556.
[5] O.F. Zouani, C. Chollet, B. Guillotin, M.-C. Durrieu, Differentiation of pre-osteoblast cells on poly(ethylene terephthalate) grafted with RGD and/or BMPs mimetic peptides, Biomaterials 31(32) (2010) 8245-8253.
[6] H. Pan, Q. Zheng, S. Yang, X. Guo, Effects of functionalization of PLGA-[Asp-PEG]n copolymer surfaces with Arg-Gly-Asp peptides, hydroxyapatite nanoparticles, and BMP-2-derived peptides on cell behavior in vitro, Journal of Biomedical Materials Research Part A 102(12) (2014) 4526-4535.
[7] G. Atlan, N. Balmain, S. Berland, B. Vidal, E. Lopez, Reconstruction of human maxillary defects with nacre powder: histological evidence for bone regeneration, Comptes rendus de l'Academie des sciences.Serie III, Sciences de la vie 320(3) (1997) 253-258.
[8] G. Atlan, O. Delattre, S. Berland, A. LeFaou, G. Nabias, D. Cot, E. Lopez, Interface between bone and nacre implants in sheep, Biomaterials 20(11) (1999) 1017-1022.
[9] S. Berland, O. Delattre, S. Borzeix, Y. Catonne, E. Lopez, Nacre/bone interface changes in durable nacre endosseous implants in sheep, Biomaterials 26(15) (2005) 2767-2773.
[10] D.W. Green, H.-J. Kwon, H.-S. Jung, Osteogenic potency of nacre on human mesenchymal stem cells, Molecules and Cells 38(3) (2015) 267-272.
[11] M.J. Almeida, L. Pereira, C. Milet, J. Haigle, M. Barbosa, E. Lopez, Comparative effects of nacre water-soluble matrix and dexamethasone on the alkaline phosphatase activity of MRC-5 fibroblasts, Journal of Biomedical Materials Research 57(2) (2001) 306-312.
[12] M. Rousseau, L. Pereira-Mouries, M.-J. Almeida, C. Milet, E. Lopez, The water-soluble matrix fraction from the nacre of Pinctada maxima produces earlier mineralization of MC3T3-E1 mouse pre-osteoblasts, Comparative Biochemistry and Physiology, Part B: Biochemistry & Molecular Biology 135B(1) (2003) 1-7.
[13] J.-j. Wang, J.-t. Chen, C.-l. Yang, Effects of soluble matrix of nacre on bone morphogenetic protein-2 and Cbfa1 gene expressions in rabbit marrow mesenchymal stem cells, Nanfang Yike Daxue Xuebao 27(12) (2007) 1838-1840.

[14] A. Flausse, C. Henrionnet, M. Dossot, D. Dumas, S. Hupont, A. Pinzano, D. Mainard, L. Galois, J. Magdalou, E. Lopez, P. Gillet, M. Rousseau, Osteogenic differentiation of human bone marrow mesenchymal stem cells in hydrogel containing nacre powder, 2013.